Autonomous robots using artificial potential fields

Autonomous Robots using Artificial Potential Fields

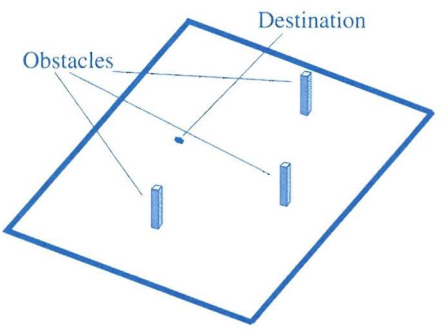

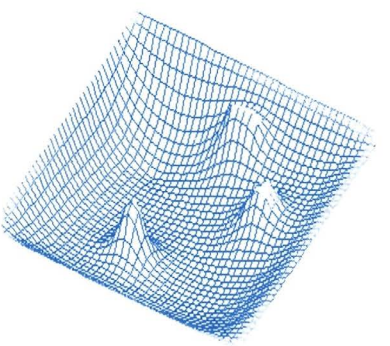

P. Dunias

AUTONOMOUS ROBOTS USING ARTIFICIAL POTENTIAL FIELDS

Paraskevas Dunias

AUTONOMOUS ROBOTS USING ARTIFICIAL POTENTIAL FIELDS

PROEFSCHRIFT

ter verkrijging van de graad van doctor aan de
Technische Universiteit Eindhoven, op gezag
van de Rector Magnificus, prof.dr. M. Rem,
voor een commissie aangewezen door het College
van Dekanen in het openbaar te verdedigen op
maandag 2 december 1996 om 16.00 uur

door

Paraskevas Dunias

geboren te Athene

Dit proefschrift is goedgekeurd door de promotoren:

prof.dr.ir. P.P.J. van den Bosch
en
prof.dr.ir. J.J. Kok

CIP-DATA LIBRARY TECHNISCHE UNIVERSITEIT EINDHOVEN

Dunias, Paraskevas

Autonomous Robots using Artificial Potential Fields / by Paraskevas Dunias. - Eindhoven :
Technische Universiteit Eindhoven, 1996. - VIII, 117 p.
Proefschrift. - ISBN 90-386-0200-6
NUGI 832
Trefw.: robots / numerieke besturing / manipulatiemechanismen.
Subject headings: robots / path planning / planning (artificial intelligence).

Druk: Boek- en Offsetdrukkerij Letru, Helmond, (0492) 53 77 97

To my wife, Monique

Preface

> ... for me there is only the travelling on the paths that have a heart, on any path that may have a heart. There I travel, and the only worthwhile challenge for me is to traverse its full length... looking, looking, looking, breathlessly.
>
> *The Teachings of Don Juan,*
> Carlos Castaneda

The heart of my PhD research is the choice of its scientific subject, *artificial potential fields in robotics.* Thanks to Dan Koditchek who drawn my attention to the philosophical value of artificial potential fields in mechanical systems, I have chosen the topic of this thesis. Mostly, I was looking, looking breathlessly that sometimes even became suffocated. In retrospect, my research topic was in my opinion rather difficult but at the same time giving worthwhile challenge for me to traverse its full length.
During my research everyone in my surrounding has inevitably influence on the course of events, however some persons I would in particular like to thanks for their support and devotion. For the very existence of this thesis, I am especially indebted to my wife, Monique. Without her love, and devotion, I could not have pursed this thesis.

Some colleagues in our group have been of invaluable importance for me from the very first moment. Thanks to Bart Kouwenberg who was functioning as organiser and supervisor, the PhD research has become reality. Working for The ESPRIT project gave me the opportunity to widen my knowledge and to work together with Wil Hendrix and Ton van de Graft. Thanks to them staying at the university it was definitely enjoyable.
Thanks, finally, to my son Marc for helping me discover the *real value* of my PhD research.

Summary

This dissertation discusses the issue of robot motion planning for autonomous robots. Artificial potential fields have been employed by solving the basic motion planning problem stated as: generate a collision-free robot trajectory starting from an initial position towards a given goal position. The goal position is formulated in the work space of the robot or in the configuration space of the robot. The robot motion planning problem is formulated and solved in the configuration space of a robot. A potential field is constructed in the configuration space of a robot which represents a mechanism for control and planning.

The kinematics of a robot including the direct and inverse kinematics are briefly given to understand how we can transform obstacles from the physical space of the robot to the configuration space. This yields the free configuration space which represents that part of the configuration space of the robot where no collisions between robot and obstacles occur.

Based on a general dynamic model of a robot we introduce a control strategy, involving artificial potential fields. Basically, the gradient of the potential field is included in the input torque vector of the robotic system which enforces the robot to asymptotically reach a goal configuration while avoiding collisions.

Following the requirements stated by the control strategy concerning the artificial potential field, the construction of the artificial potential fields has been examined. Harmonic functions are used to construct a potential field which attains its maximal values along the boundary of the obstacles and its global minimal values along the boundary of the goal configurations. The problem of finding a harmonic function under the stated constraints has been analysed and solved. The Boundary Element Method (BEM) has been used which gives an analytic expression of the potential field, extended even for higher dimensions than three.

Thus, the basic motion planning problem can be solved in four steps: (1) transform the arbitrary shaped obstacles in the work space into discretised forbidden configurations in the configuration space; (2) generate the discretised goal con-

figurations; (3) calculate a potential field using the BEM; (4) use the gradient of the obtained potential field in the control strategy.
Two practical problems arising in real-time applications have been indicated and solved. The first problem concerns the upper admissible limit of the input torque vector of the joints of a robot. Second, an iterative algorithm is given to reduce calculation time of the solution of the BEM when obstacles are added or deleted.
According to some experiments done for two- and three-dimensional configuration spaces we conclude that the method can be used for robot motion planning giving in general satisfactory results. The main drawbacks are the large requirements for computer memory and calculation speed.

Contents

List of Figures

Chapter 1

Introduction

Robotics is an interesting and dynamic interdisciplinary field of study, especially when attributed with terms as intelligence and autonomy. Evidently, the main subject of robotics is researching robots either mobile or articulated.

Robots have been already used in the industry for several decades. This is rather evident thinking of the obvious advantages of a robot such as *flexible programmable* and *repeatability*. Until recently, robots were primarily employed for carrying out programmed, repetitious tasks. Much research has been done to develop theories and algorithms needed for robots to process information and to interact with the environment. Aspects of such capabilities include perception, reasoning, planning, and learning. On the one hand these aspects are mostly used when the term intelligence is defined, on the other hand such aspects are a prerequisite when autonomy has to be achieved.

Robot applications concern motion of robots to accomplish a specific task. Robots are widely used for tasks such as material handling, spot and arc welding, spray painting, mechanical and electronic assembly, material removal and water jet cutting. Most of such tasks include a primary problem of getting a robot to move from one position to another without bumping into any obstacles. This problem denoted as the **Robot Motion Planning** (MP) problem has been the subject of a great amount of research. The term *robot* can convey many different meanings in the mind of the reader, depending on the context. In the treatment presented here, a robot will be taken to mean an industrial robot, also called a *robotic manipulator* or a *robot arm*.

Although the fundamentals of robotics and the analysis and control of robots have been satisfactory introduced in several books (Schilling 1990; McKerrow 1991), in the following sections the necessary background is given to minimize

the prerequisites of the reader. Therefore, we start in the next section with a definition and classification of robots, different methods of robot motion planning and modelling techniques of a robot.
We discuss the crucial term of "artificial potential fields" related to the motion planning problem when autonomy has to be achieved. A general introduction is given of the main characteristics of the artificial potential fields in a historical perspective and of the bottlenecks that appear when artificial potential fields are employed in robotics.
According to the given information about robotics and artificial potential fields, a first description of the problem addressed in this thesis is formulated. In addition the proposed solution of the given problem is highlighted.
The chapter concludes with the general outline of this thesis.

1.1 Introduction to Robotics

1.1.1 Defining a Robot

Many definitions of a robot have been proposed with each covering certain aspects of a robot. For the purpose of the material presented here, the following definition is introduced:

Robot. *A robot is a software-controllable mechanical device that uses sensors to guide one or more end-effectors through programmed motion in a work space in order to manipulate physical objects.*

In figure 1.1 an example of an industrial robot is shown. This is an articulated robot which can be seen as a chain of rigid links interconnected by rotational joints.
At the end of the manipulator, a tool (i.e. a welding torch or a gripper) can be attached which in the current analysis is going to be generally indicated as the end-effector. Whether we want to refine the notion of a robotic manipulator, it is usual to classify them according to different criteria such as drive technologies, joint types and motion control methods.
The kind of source power used to drive the joints of a robot forms one of the criteria to classify robots. The two most popular drive technologies are electric and hydraulic. Very often electric drives are used which can be for example DC servomotors or DC stepper motors. However, when high-speed manipulations of substantial loads is required, hydraulic drives are preferred. Both types of robots often use pneumatic driven end-effectors, in particular when the only action to be accomplished is grasping.

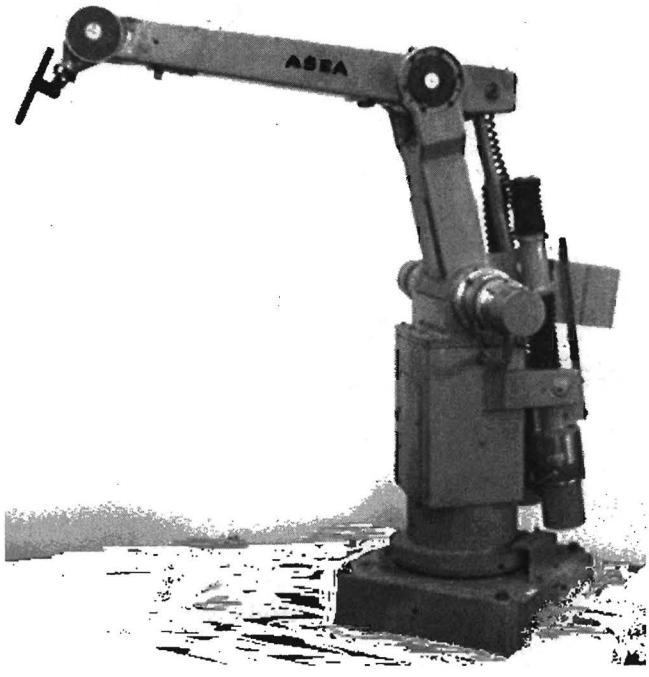

Figure 1.1: The Irb-6 ASEA Robot

Generally, there are two kinds of joint types; the revolute joints (R) which exhibit a rotary motion about an axis and the prismatic joints (P) exhibiting a translational motion along an axis. When the first three joints of a robot, also called the major axes, are revolute then the robot is indicated as a RRR type of robots. Robots can be generally formed by combinations of joint types resulting for instance in RPP type (cylindrical robot), RRP type (SCARA robot) or RRP type (spherical robot) as depicted in figure 1.2 and figure 1.3. Another fundamental classification criterion is the methodology employed to control the movement of the end-effector and more specific the movement of a predefined point at the end-effector the so-called tool centre point (TCP). Two types of movement can be distinguished, referred as the point-to-point motion used for instance by spot welding, pick-and-place applications and the continuous path motion employed for instance by spray painting, arc welding or gluing. By point-to-point motion, the end-effector moves to a sequence of discrete points where the motion between these points is not explicitly controlled

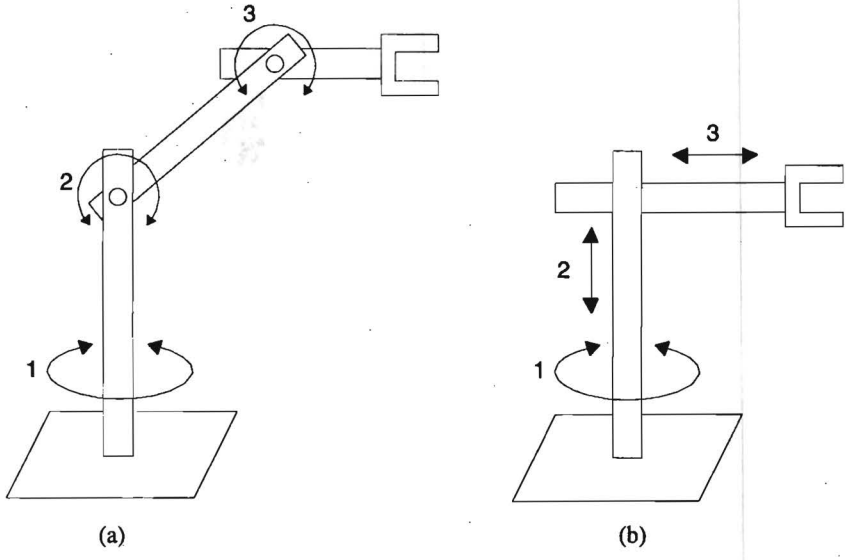

Figure 1.2: (a) an example of a RRR articulated robot, and (b) an example of a RPP cylindrical robot

by the user. On the contrary, by the continuous path motion the end-effector must follow a predefined path where not only positions are taken into account but also time information (e.g. velocity). In that case the TCP has to follow a predefined (time) trajectory.
When a certain task has to be accomplished by a robot, the robot has to be programmed to execute a certain motion according to a predefined plan. Finding an appropriate motion for a certain task is the subject of the so-called *robot motion planning*. Robot motion planning has attract a lot of scientific attention and it will be introduced in the next section.

1.1.2 Robot Motion Planning

A typical approach of solving the motion planning problem concerns separately path planning or trajectory planning which results in a reference path or trajectory that the robot must follow using robot control techniques. Path planning typically refers to the design of only geometric (kinematic) specifications of the positions and orientations of robots, whereas trajectory planning includes the

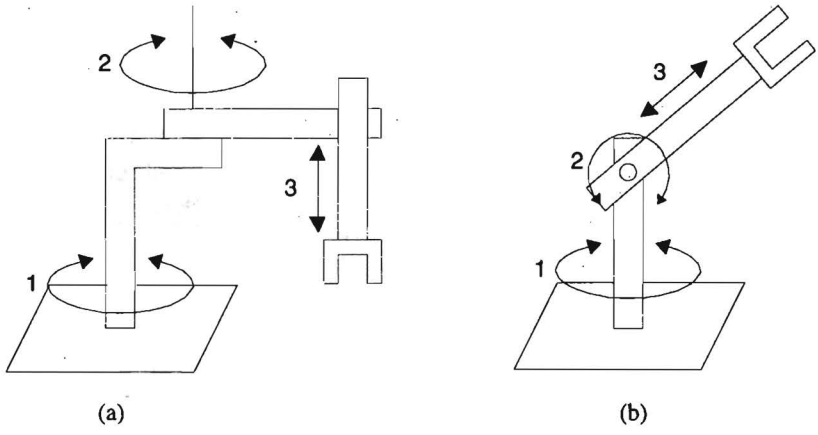

Figure 1.3: (a) an example of a RRP SCARA robot, and (b) an example of a RRP spherical robot

design of the linear and angular velocities as well. Therefore, path planning is a subset of trajectory planning, wherein the dynamics of robots are unimportant or neglected. In addition, the major part of research in robotics has been concentrated in solving the motion planning problem under the assumption of perfectly known environment of the robot. Without this assumption it is really hard to find a solution for high dimensional robots. That's why in these cases we notice that the research areas are merely concerned with mobile robots which merely moves in only two dimensions.

There are several different classes of motion planning methods. Motion planning can be static or dynamic, depending on whether the information on the robot's environment is fixed or updated. In the static case information about the geometry of the obstacles is assumed to be known. According to this information the motion of the robot is designed to reach its goal. In dynamic planning only partial information is available for instance the visible parts of the obstacles. In that case during execution of the motion the information of the geometry of the obstacles is gradually updated. Consequently, the robot motion has to be automatically replanned until its goal is reached. Thinking of a hardly predictable or not perfectly known environment it does not make sense to make very precise plans before moving. Real-time planning of the robot using data from a sensory system becomes then a necessity.

Further categorization of the motion planning is related to the obstacles, which can be stationary or moving resulting in a motion problem denoted respectively

as time invariant or time varying. It is also possible to let the robot to move some objects implying the so-called movable object motion planning problem. Generally, more than one robot is employed for more complicated tasks which leads to another category of motion planning denoted as the multimovers problem.
Finally, motion planning is either constrained or unconstrained, depending on whether there are constraints on a robot's motion other than collisions with obstacles. These constraints include bounds on a robot's velocity and acceleration and constraints on the curvature of a robot's paths. Apparently, motion planning of any physical mechanical system is constrained, since the actuators of the system have a limited input range.
Numerous methods have been developed for motion planning. Some methods are applicable to a wide variety of motion planning problems, whereas others have a limited applicability. These methods are variations of a few general approaches: skeleton (Canny 1987; Canny 1988), cell decomposition (Keil and Sack 1985), and potential field (Koditchek 1989; Khatib 1985; Khatib 1987). Most classes of motion planning problems can be solved by using these approaches. These approaches are not necessarily mutually exclusive, and a combination of them is often used in developing a motion planner. Motion planning methods are based on certain models of the manipulator which describe its static and dynamic behaviour. These models will be introduced in the next section.

1.1.3 Modelling a Robot

Robot motion planning can be carried out in two different spaces in which a robot can be described, the work space and the joint space. The work space refers to the physical space robots and obstacles exist in. Defining an obstacle or a robot in the work space means specifying the position and orientation of the obstacle or robot's TCP with respect to a predefined coordinate system. Another way to represent a robot is by using the set of joint angles. Accordingly the joint space refers to the space of joint angles of a robot. The dimension of the joint space determines the number of parameters representing a configuration of the robot, also called degrees of freedom (DOF). It is noted that joint angles are used to denote both the controllable angles of revolute (R) joints and the controllable translation of a prismatic (P) joint.
The relation between these two spaces is described by the direct and inverse kinematics of a robot. In figure 1.4 a graphical representation of the direct and inverse kinematics of a manipulator is depicted.
Obviously, the kinematics of a robot describe the relation between positions and orientations of the TCP and the corresponding joint angles of the robot

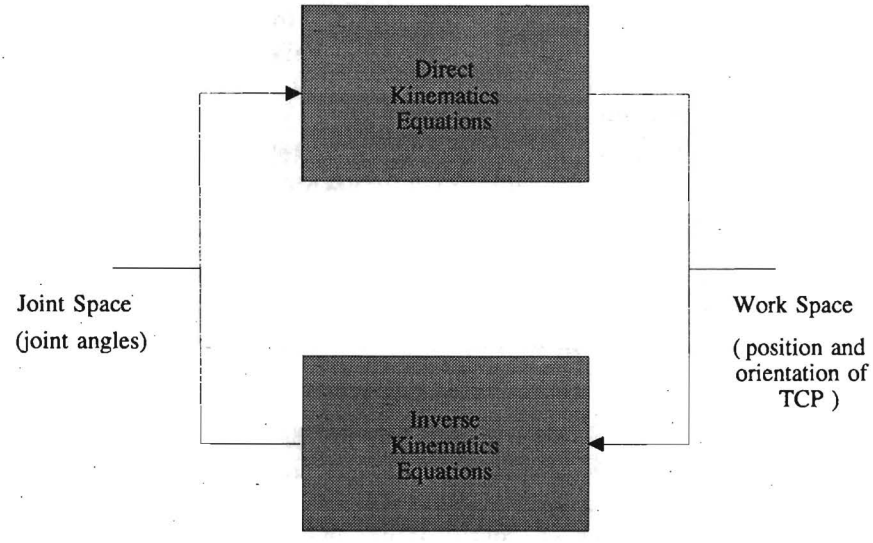

Figure 1.4: The direct and inverse kinematics of a robot in a schematic way

whereby only static properties of the robot are included. The transformation from joint space to the work space appears to be a one-to-one relation, in contrary to the transformation from the work space to the joint space which is not always a one-to-one relation. That means that there are cases where more than one set of joint values can give the same position and orientation of the TCP. That is for instance the case when the dimension of the joint space is higher than the dimension of the work space. In that case the robot arm is said to be kinematically redundant.

In addition to the kinematic model of a robot, a dynamic model of a robot can be formulated which defines in general the relation between torques or forces applied at the actuators of the joints and the joint angle positions, velocities and accelerations. Robot dynamics have been extensively investigated (Paul 1982; and Graig 1986). Different dynamic models can be used representing a manipulator according to the degree of reliability and complexity required and the nature of the specific physical phenomenons involved. In realistic dynamic models, terms as manipulator inertia, Coriolis, centrifugal, gravitation, and friction forces, are included, which give highly complex, non-linear dynamic models.

Dynamic models of a robot are necessary when a certain control strategy has to be designed for either continuous path motion or point-to-point motion.

In case of continuous path motion, the objective is to let the robot faithfully "track" a predefined trajectory. This problem appears to be very difficult due to the complexity of the dynamic model of the robot. A common approach to robot control used in many commercial robots, is the single-axis P(roportional) I(ntegrate) D(erivative) control (Schilling 1990). The term single-axis indicates that each axis of the robot is separately controlled using a PID control scheme. The PID control strategy uses in that case a linearized dynamic model of each axis of the robot.
More sophisticate control strategies like the computed-torque control employ estimations of the non-linear terms of the dynamic model. Using these estimations, again a more reliable linear model is obtained. However, the estimates of the robot parameters are never exact and in addition complex which explains the limited usage of this technique.
In case of the point-to-point motion a more easier control strategy can be employed as the objective is less demanding; to reach a goal position independently of the way to come there. A control strategy denoted as PD-plus-Gravity control has been proven to be able to control a robot in a asymptotic stable fashion. PD-plus-Gravity will be explained in more details in the following chapters as it plays an important role in this thesis.

1.1.4 Perception and the Environment of the Robot

In the physical space in which a robot operates there are mostly objects, either fixed or variable. Inevitably, avoiding collisions with or manipulating objects demands knowledge of the geometry of the objects in the environment of the robot. When no a priori information is available concerning the objects in the environment of the robot, sensory information can be used. Perception capabilities for robots are necessary when dynamic motion planning has to be performed. Generally, only partial information is available, for instance the visible parts of the obstacles which means that during execution of the motion the information concerning the geometry of the obstacles is gradually updated. Sensing can in general classified in two categories:

- Contact sensing: it requires physical contact with an object. Contact sensor signals include force/torque, temperature, position, etc.
- Non-contact sensing: it is based on the signals generated by a transducer which is not in physical contact with the object it senses. Non-contact sensor signals include visual (light intensity), range, acoustic, temperature, chemical, etc.

For robot motion planning, non-contact sensing is mostly utilized. Several technologies have been developed concerning the detection of objects. The most

usable technologies involve stereo vision techniques, laser range finder (Shirai 1989), opto electronic sensoring (using components like LED's, Laser diodes, Photo transistors etc.) (Marszalec and Keranen 1992), optical phase sensoring (optical radar) (Soumekh 1992), acoustic sensoring (ultra-sonic sensors). Ultra-sound sensors are mostly employed in robotics due to their small physical size, and fast measuring capabilities. Unfortunately, ultra-sound sensors are rather sensitive to atmospheric variation and noise disturbances.
However, perception falls beyond the scope of this thesis and only an ultra-sound sensor system has been developed. A simple threshold detection is used for measuring (Kuc 1990; Cai and Regtien 1993), giving sufficient accuracy for experimental purposes. However, more complex techniques can be used to increase accuracy like correlation methods (Barshan and Kuc 1992) and phased-arrays (Macovski 1979; Soumekh 1992).

1.2 Artificial Potential Fields in Robotics

One of the motion planning methods is using artificial potential fields as mentioned previously. The idea of artificial potential fields for robot motion planning has been introduced begin eighties and further exploited by a number of scientists. It appears as one of the few motion planning methods for real-time robot applications. The artificial potential field is a function whose gradient is used to calculate a torque applied to the robot, enforcing it to reach its goal while avoiding obstacles. Apparently this potential field depends on the goal state of the motion planning and the geometry of the environment of the robot. The artificial potential field has to attain its maximum values at the obstacles and its global minimum at the goal state.
The major problem in using artificial potential fields is the occurrence of local minima which could lead the robot to stack there before reaching its goal. The solution of the problem of finding an artificial potential field without local minima includes the employment of the so-called harmonic functions. Harmonic functions have indeed no local minima but are rather difficult to find for arbitrary boundary conditions. Therefore the Boundary Element Method is employed which results in an approximation of an analytic solution of the desired artificial potential field.
Using a potential field to accomplish a certain motion implies that the trajectory of the robot is not known or calculated in advance. That means that the robot "chooses" autonomously its way to reach its goal.

Some attractive characteristics of the usage of artificial potential fields are:

- real-time usage,

- applicable to redundant and non-redundant robots,
- incorporation of the dynamics of the robot.

1.3 Problem Formulation and Solution Proposal

The problem addressed in this thesis is the autonomous motion planning of robots in known environments and with unknown, possible moving, obstacles. Only electrically driven, articulated industrial robots are considered with all their joints of the revolute type. The motion planning itself is of the point-to-point type where the main objective is to reach a given goal pose of the robot without colliding with any obstacles.
The desired goal pose of the robot is given in terms of either a goal configuration of the joints of the robot (in the joint space) or the position and orientation of the TCP (in the work space). In the latter case the set of all configurations, corresponding to the given position and orientation of the TCP, is calculated. The objective of the motion planning is in that case to program the robot to reach a configuration belonging to the set of the goal configurations.
The obstacles have to be detected using appropriate sensors, resulting in a geometrical model of the environment of the robot. Generally, the space where the robot and obstacles exist in, is modelled by a discretized grid. When a cell of this grid is occupied by an obstacle, it is possible to find all these configurations where the robot touches the occupied cell, denoted by the term configuration obstacle. According to the configuration obstacles together with the goal configuration(s), an artificial potential field is calculated which attains its maximum values at the boundaries of the configuration obstacles and its minimum values at the boundaries of the goal configuration(s). Apparently, the obtained artificial potential fields has to be free of local minima. That leads us to the underlying problem of finding an artificial potential field without local minima under the mentioned conditions. The solution of this problem employs artificial potential fields as harmonic functions (Axler et.al. 1992) which have to be constructed according to the boundary conditions. Harmonic functions do indeed not contain local minima but are difficult to construct. This thesis examines the solution of finding an artificial potential field which is a harmonic function under the certain boundary conditions due to configuration obstacles and goal configuration(s). The solution employs the well-known Boundary Element Method, leading to a harmonic function without local minima in the configuration space of the robot. Finally, the solution which is applicable even for high dimensional robots, has been implemented and some results are included in this thesis.

1.4 Outline and Scope of the Thesis

This thesis is organized as follows. In chapter 2 related research is cited. More attention has been paid concerning the potential field method. Especially some methods have been addressed which have a direct relation with the present thesis.

Next, in chapter 3 we start with the kinematics of a robot including the direct and inverse kinematics and we end up with a dynamic model of a robot. We proceed with a simple control strategy, based on the latter model, which lays the fundamentals for the introduction of a control strategy involving artificial potential fields.
Following the requirements stated by the control strategy concerning the artificial potential field, in chapter 5 we examine the artificial potential fields. After some definitions and requirements, harmonic functions are introduced. Solving the problem of finding a harmonic function under the stated constraints by using the Boundary Element Method concludes this chapter.
The method has been implemented and tested. In chapter 6 different scenarios have been discussed to evaluate the main properties of the potential field method using the BEM.
In the last chapter 7 the summary and conclusions of the thesis are presented. Besides some ideas about eventually future development of the method have been addressed concluding the thesis.

Chapter 2

Robot Motion Planning: A Survey

Before we discuss the methods and algorithms considered in the next chapters, we describe the related research cited. The main objective is to give the necessary background to get insight in the issues that follow in this thesis. We focus our attention to the artificial potential fields in robot motion planning, giving accordingly a brief survey of the existing work of other researchers.

Every method concerning robot motion planning has its own advantages and application domains but also its disadvantages and constraints. Therefore it would be rather difficult either to compare methods or to motivate the choice of a method upon others.
In contrast to many methods, robot motion planning through artificial potential fields considers simultaneously the problem of obstacle avoidance and that of trajectory planning. In addition the dynamics of the manipulator are directly taking into account, which leads in our opinion to a more natural motion of the robot.
Although the method has been significantly developed since it was proposed, it is still far from the practical usage level. The major problem in the potential field motion planning approach is the occurrence of local minima in the potential field which cause the untimely termination of the motion of the robot. In addition most of the proposed solutions are restricted to only two-dimensional robots. The motivation of this thesis is to present a solution of the motion planning problem which uses artificial potential fields without the mentioned drawbacks.

Starting with a survey concerning robot motion planning in general, we proceed with a brief explication of three specific methods concerning robot motion planning using artificial potential fields.

2.1 Robot Motion Planning and Artificial Potential Fields

Robot Motion Planning (MP) has been an important area in robotic research. According to the application objectives, different methods have been developed with their own applicability, complexity, assumptions and performance. Two distinct classes of robots, mobile or articulated, led to two different research areas. However, many methodologies find their application in both mobile and articulated robots. Robot motion planning considers in general the problem of programming a robot in order to accomplish a given task e.g. assembling or welding. In almost all such tasks it is inherently required to be able to move the robot from one position to another. Mostly, while executing the given task, undesired collisions with obstacles have to be prevented. A general description of different methodologies concerning robot motion planning can be found in (Ratering 1992; Latombe 1993; and Hwang and Ahuja 1992).
Latombe (Latombe 1993) distinguishes three different motion planning approaches: the *cell decomposition* method, the *roadmap* methods, and the *potential fields* methods.
In the cell decomposition approach, the free configuration space of the robot is subdivided into a finite number of simple connected *subcells*, such that planning motion between two configurations within the same subcell is straightforward. When a motion has to be planned between two different configurations belonging to different subcells a *connectivity graph* is used. Each node of the connectivity graph represents a subcell which is connected with another node (subcell) when these two subcells share a common boundary allowing direct crossing of the robot. By creating the connectivity graph the problem of robot motion planning is reduced to a graph searching problem: Find the begin and end subcell in which respectively the begin and end configuration of the motion problem lie. Determine next a path in the connectivity graph which connects the nodes corresponding to the begin and end subcells or report that no such a path exists. The "optimal" path can be determined according to some criterions like shortest distance or time. The found sequence of subcells together with some crossing rules from one subcell into another, are used to transform the sequence into a path for the robot from the begin to the end configuration. When a method guarantees to find a path if one exists it is called *exact* (mostly computationally expensive), on the contrary to methods called *approximate*

(mostly heuristic, fast and easy to implement) which sometimes fail to find a path even if one exists. In the case of the cell decomposition method we find two different approaches according to the division of the free space of the configuration space. *Exact cell decomposition* methods divide the free space of the configuration space into simple subcells such that the union of the subcells equals exactly the free space. This method is preeminently applicable in low dimensional situations or/and simple shaped obstacles. Example of exact cell decomposition methods can be found in (Halperin et.al. 1992; Ke and Rourke 1987; Schwartz and Sharir 1983a; Schwartz and Sharir 1984; Sharir and E. Ariel-Sheffi 1984). *Approximate cell decomposition* methods Brooks and Lozano-Perez 1983; Faverjon 1986; Kambhampati and Davis 1986; Zhu and Latombe 1991) divide the free space of the configuration space into subcells with uniform shapes e.g. balls or rectangloids. The union of the subcells forms in that case a subset of the free space. Occasional failure to return a path is evident from considering the difference between the free space and the union of the subcells.

In the *roadmap* method, the free space of the configuration space is retracted to, or mapped onto, a network of one-dimensional curves. This approach is also called the retraction, skeleton, or highway approach. Firstly motion planning requires the determination of two points on the roadmap accessible from the begin and end configuration of the motion problem. Motion planning is then reduced into a graph searching problem with these two configuration on the roadmap. Roadmap methods including *Voronoi diagram*, *visibility graph*, *silhouette* and the *subgoal network* can be found in (Canny 1987; and Canny 1988; Leven and Sharir 1987; Takahashi and Schilling 1989; Sifrony and Sharir 1987).

Potential field methods (Khatib 1987; Khosla and Volpe 1988; Koditschek 1987) construct a scalar function called potential that has a minimum when the robot is at the destination configuration, and a high value on obstacles. The motion is accomplished by following the gradient of the potential field which points along the steepest descent of the potential field towards the minimum of the potential field. Unfortunately, the motion might get stuck in a local minimum of the potential field, when such local minima are present. A lot of research has be done finding potential fields containing no local minima e.g. (Rimon and Koditschek 1989; Rimon and Koditschek 1990; Rimon and Koditschek 1992; Khosla and Volpe 1988; Connolly and Grupen 1992; Connolly, Burns and Weiss 1990; and Connolly, Burns and Weiss 1989). Escaping from local minima has also been considered, resulting in a number of techniques (Barraquand and Latombe 1990).

Next we discuss some examples of robot planning methodologies which employ potential fields. Although research concerning potential fields is going on up

to present days (Nam, Lee and Ko 1995; Ratering and Gini 1995; Masoud, Masoud and Bayoumi 1994; Ralli and Hirzinger 1994), we just address some methodologies which form to our opinion milestones in the development of this technique.

2.2 Robot Motion Planning through Potential Fields

The idea of using potential fields for robot planning and obstacle avoidance has been pioneered by Khatib (Khatib 1985). However, the idea of more flexibility at the control level regarding obstacle avoidance was already expressed in his previous work with Le Maitre (Khatib and Le Maitre 1978). Khatib introduced a potential field (a scalar function) which consists of two parts. The first part, the repulsive potential, is defined around the obstacles and keeps the manipulator away from the obstacles. The other part, the attractive potential, defined at the goal position of the manipulator pulls the manipulator to this position. The potential field is defined in the work space of the robot. The manipulator (actually the end-effector) will be controlled by the gradient of the potential field which induces a force directed towards the goal and keeping away from the obstacles. In our opinion there is a serious criticism regarding this method. The construction of the potential field was such that minima other than at the goal position could occur. So the robot may roll to some position other than the goal and stop.
Nevertheless, the introduction of potential fields in robotics has given new scientific inspiration to a number of researchers who had to contend with the next problems:

- The potential field has to exhibit no other minima than the minimum at the goal position defined by the specific task of the robot.
- The potential field around the obstacles has to faithfully enclose the shape of the obstacles even for complex unstructured obstacle surfaces.
- Preferably the potential field is constructed in the configuration space of the robot where the robot is represented by a single (controllable) point, although the obstacles exist in the physical space of the robot.

Khatib (Khatib 1987) has avoided the problem of the arbitrary shape of the obstacles, using only the shortest distance between specific points on the manipulator and the obstacles. However still the potential field introduced exhibits local minima other than at the goal position of the robot.

The need for an obstacle avoidance potential field that closely models the obstacles, yet does not generate local minima in the work space of the manipulator was obvious. Volpe and Khosla (Volpe and Khosla 1987) developed a new elliptical potential field in the work space that improved upon previous artificial potential fields by providing avoidance of obstacles without generating local minima. Also, since the contours of rectangular objects are followed, a modified version of the function may be used for object approach. In conjunction with these schemes, an algorithm has been presented that determines the interaction of the manipulator links with the artificial potential field. Later Volpe and Khosla (Khosla and Volpe 1988; Volpe and Khosla 1990) developed a novel superquadric potential field in work space that provides obstacle avoidance and object approach capabilities. Robust obstacle avoidance and goal acquisition is achieved by governing the end-effector motion with an avoidance potential field placed in a global attractive well. Local minima are not generated in the work space because of the asymptotically spherical nature of the superquadric potential field. Link collisions with the obstacles are also eliminated. For object approach, a second form of the superquadric potential field may be employed to generate deceleration forces. This scheme reduces contact velocities and forces to tolerable levels. Both the avoidance and approach potential fields have been implemented in simulations of two and three link manipulators. The results indicated an improvement over other local potential schemes.

The superquadric formulation is a generalization of the elliptical potential function method, and therefore is viable for a much larger class of object shapes. The superquadric potential function presented, changes from the object-shape near the object, to a spherical-shape away from it (circular in two dimensions), and satisfies four requirements:
- The potential field should have spherical symmetry for large distances to avoid the creation of local minima when this potential field is added to others.
- The potential field contours near the surface of obstacles should follow the surface contour so that large portions of the work space are not effectively eliminated.
- The potential field related to an obstacle should have a limited range of influence.
- The potential field and its gradient must be continuous.

Superquadric potential fields have been constructed to satisfy the above mentioned criteria, however with limited applicability concerning the shape of the obstacles. Volpe and Khosla (Khosla and R. Volpe 1987) have shown that superquadric potential fields can be constructed for simple shapes like square or triangular figures.
In addition the problem of local minima remains, because when no local min-

ima occur in the work space of a robot, this does not mean that also no local minima occur in the configuration space of the robot.
That is actually the reason to turn to methodologies finding potential fields in the configuration space of the robot. The contributions of Koditschek in (Koditchek 1989; and Koditchek 1987; Rimon and Koditschek 1989; Rimon and Koditschek 1990; and Rimon and Koditschek 1992) are worth to be mentioned because they introduced an analytic potential field in the configuration space of the robot without local minima. However the topology of the application range is limited to obstacles which have to be ball- or star-shaped otherwise no solution can be found.
Another serious attempt to construct a potential field in the configuration space of a robot without local minima has been given, introducing the so-called harmonic functions. Kim and Khosla in (Kim and Khosla 1991; and Kim and Khosla 1992) use harmonic functions to build a potential field, and additionally they develop a control strategy for navigating the robot in this potential field. Harmonic functions do not have any local minima within a given domain. They only attain their extreme values at the boundary of the domain.
At the same time Connolly and Grupen (Connolly and Grupen 1992), Connolly, Burns and Weiss (Connolly et.al. 1990; and Connolly et.al. 1989) describe a method to find a harmonic function in the free configuration space. The free configuration space of the robot consists of all configurations where no collision occurs. The boundary of the free configuration is formed by the configuration obstacles (all the configurations where a collision occurs) and the goal configuration.
The contributions of Connolly (Connolly 1994) and of Kim and Khosla (Kim and Khosla 1992) are in our opinion the most successful methods concerning robot motion planning with potential fields. The work presented in this thesis is closely related to the work of Connolly (Connolly 1994) and certainly related to the work of Kim and Khosla (Kim and Khosla 1992). Therefore we will give a brief description of these two methodologies. However, in order to introduce the reader in the notion of the potential fields we will first give a brief description of the method of Khatib (Khatib 1987).

2.2.1 FIRAS: birth of potential fields in robotics

Khatib's philosophy of the artificial potential field can be described as (Khatib 1985; and Khatib 1986):

> The manipulator moves in a field of forces. The position to be reached is an attractive pole for the end-effector, and the obstacles are repulsive surfaces for the manipulator parts.

Hence the introduced artificial potential field $U_{art}(\boldsymbol{x})$ consists of two terms, the attractive potential field $U_{attr}(\boldsymbol{x})$, and the repulsive potential field $U_{rep}(\boldsymbol{x})$. The total artificial potential field $U_{art}(\boldsymbol{x})$ is then the sum of these two potential fields:

$$U_{art}(\boldsymbol{x}) = U_{attr}(\boldsymbol{x}) + U_{rep}(\boldsymbol{x}) \tag{2.1}$$

The method has been applied in the work space of a robot which means that $\boldsymbol{x}$ denotes a point in that space. The negative of the gradient of the total potential field $U_{art}(\boldsymbol{x})$ consists of two terms, the force $F_{attr} = -\nabla U_{attr}(\boldsymbol{x})$ driving the end-effector to reach the destination position $\boldsymbol{x}_d$, and the force $F_{rep} = -\nabla U_{rep}(\boldsymbol{x})$. The force F_{rep} keeps the manipulator away from the obstacles, hence the name *Force Inducing an Artificial Repulsion from the Surface* of the obstacle (FIRAS, from the French).
The attractive potential field is given by:

$$U_{attr}(\boldsymbol{x}) = \frac{1}{2}k(\boldsymbol{x} - \boldsymbol{x}_d)^2 \tag{2.2}$$

with k a scalar constant. $U_{rep}(\boldsymbol{x})$ is a non-negative continuous and differentiable function whose value tends to infinity as the end-effector approaches the obstacle's surface. The influence of this potential field has been limited to a given region surrounding the obstacles. The proposed repulsive potential field has the following form:

$$U_{rep}(\boldsymbol{x}) = \begin{cases} \frac{1}{2}\eta(\frac{1}{\rho} - \frac{1}{\rho_o})^2, & \text{if } \rho \leq \rho_o \\ 0, & \text{if } \rho > \rho_o \end{cases} \tag{2.3}$$

where ρ_o represents the limit distance of the potential field influence and ρ the shortest distance to the obstacle. Any point on the manipulator can be subjected to the artificial potential field. The control of a *point subjected to the potential* (PSP) with respect to an obstacle O is achieved by using the gradient of the corresponding FIRAS function, given by:

$$F_{(O,PSP)}(\boldsymbol{x}) = \begin{cases} \eta(\frac{1}{\rho} - \frac{1}{\rho_o})\frac{1}{\rho^2}\frac{\partial \rho}{\partial \boldsymbol{x}}, & \text{if } \rho \leq \rho_o \\ 0, & \text{if } \rho > \rho_o \end{cases} \tag{2.4}$$

where $\frac{\partial \rho}{\partial x}$ denotes the partial derivative vector of the distance from the PSP to the obstacle:

$$\frac{\partial \rho}{\partial \boldsymbol{x}} = \left(\frac{\partial \rho}{\partial x}, \frac{\partial \rho}{\partial y}, \frac{\partial \rho}{\partial z}\right)^T \tag{2.5}$$

When more than one different obstacle is taken into account related to a specific PSP, then the total repulsive force is given by:

$$F_{PSP} = \sum_i F_{(O_i,PSP)} \tag{2.6}$$

The joint forces corresponding to $F_{PSP}(\boldsymbol{x})$ are obtained using the Jacobian matrix associated with this PSP. On a comparable manner the joint limits of the manipulator can be modelled such that during motion the manipulator stays inside these joint limits.
The main drawback of this method is the possibility of local minima of the potential field except at the destination point $\boldsymbol{x}_d$. In the next two sections we examine respectively two different methods which cope with this problem.

2.2.2 Analytic harmonic functions

Kim and Khosla (Kim and Khosla 1992) examined motion planning in the configuration space of a robot. A configuration of a robot is represented by the n-dimensional vector $\boldsymbol{q}$ where n denotes the number of joints or degrees of freedom of the robot. In configuration space, the robot is represented by a single point $\boldsymbol{q}$. Kim and Khosla (Kim and Khosla 1992) employed harmonic functions as potential fields to guide a robot in the configuration space. Harmonic functions are functions which satisfy the following equation

$$\nabla^2_{\boldsymbol{q}}\varphi(\boldsymbol{q}) = 0 \tag{2.7}$$

also called the Laplace equation.
The reason to use harmonic functions is that they possess a number of interesting properties, the two most important of which are:

- The Laplace equation is a linear equation. This means that a superposition of harmonic functions is again a harmonic function.
- Harmonic functions do not exhibit local minima within a certain domain where they are defined.

The Laplace equation (2.7) can be written in general polar coordinates (Kim and Khosla 1992) as

$$\nabla^2\varphi = \frac{\partial^2\varphi}{\partial r^2} + \frac{n-1}{r}\frac{\partial\varphi}{\partial r} + \text{angular terms} = 0 \tag{2.8}$$

Because we assume the artificial potential function φ to be a function of r only, the angular terms are zero. After rearranging and integrating with respect

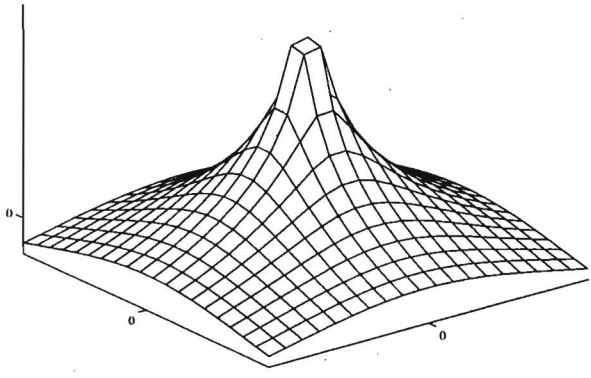

Figure 2.1: Harmonic artificial potential field of a point obstacle in two dimensions.

to r (2.8) becomes a general formula for constructing a harmonic function of arbitrary dimension:

$$\frac{\partial \varphi}{\partial r} = \frac{c}{r^{n-1}} \tag{2.9}$$

For a two-dimensional configuration space ($n = 2$) the solution of (2.9) is given by:

$$\varphi = c \ln(r) + c_1 \tag{2.10}$$

and for higher dimensions ($n > 2$) by:

$$\varphi = \frac{c/(2-n)}{r^{n-2}} + c_1 \tag{2.11}$$

where

$$r = \sqrt{(q_1 - q_{o1})^2 + (q_2 - q_{o2})^2 + \cdots + (q_n - q_{on})^2}$$

with $\boldsymbol{q}_o$ being an arbitrary point.
Depending on the sign of the constant scalar c, (2.10) and(2.11) can be used to represent a source or a sink. A source can be used to represent a point obstacle (figure2.1) at $\boldsymbol{q}_o$ and a sink can be used to represent the goal position at $\boldsymbol{q}_o = \boldsymbol{q}_d$.

Obstacles in configuration space with an arbitrary shape can be represented by a number of panels (Kim and Khosla 1992). A panel $\mathcal{S}^{n-1}$ is a shape with dimension $n-1$ and is defined by a parameter representation:

$$\begin{aligned} \mathcal{S}^{n-1} &= \{\boldsymbol{r} = \boldsymbol{r}_0 + \lambda_1 \boldsymbol{r}_1 + \lambda_2 \boldsymbol{r}_2 + \cdots \lambda_{n-1} \boldsymbol{r}_{n-1} \mid \\ &\quad \lambda_1 \in [-\bar{\lambda}_1, \bar{\lambda}_1]; \ldots ; \lambda_{n-1} \in [-\bar{\lambda}_{n-1}, \bar{\lambda}_{n-1}]\} \end{aligned} \tag{2.12}$$

where $\boldsymbol{r}_0$ is vector in $\mathcal{R}^n$ and represents the origin of the panel. The parameters λ_i, which are scalars, define the panel in the independent directions $\boldsymbol{r}_i$. For example, a panel in two dimensions is a line segment with parameter representation

$$\mathcal{S}^1 = \{\boldsymbol{r} | \boldsymbol{r} = \boldsymbol{r}_0 + \lambda_1 \boldsymbol{r}_1\} \tag{2.13}$$

The potential field of a panel can be constructed as a superposition of potentials of point obstacles. The potential field for these point obstacles is defined in (2.10) or (2.11). The potential field of a panel can be calculated by:

$$\begin{aligned} -\varphi_{\text{panel}}(\boldsymbol{r}) &= \int_{-\bar{\lambda}_1}^{\bar{\lambda}_1} \int_{-\bar{\lambda}_2}^{\bar{\lambda}_2} \cdots \int_{-\bar{\lambda}_{n-1}}^{\bar{\lambda}_{n-1}} \varphi \left(| \boldsymbol{r} - \boldsymbol{r}_0 - \lambda_1 \boldsymbol{r}_1 \right. \\ &\quad \left. - \lambda_2 \boldsymbol{r}_2 - \cdots - \lambda_{n-1} \boldsymbol{r}_{n-1} | \right) \, \mathrm{d}\lambda_1 \, \mathrm{d}\lambda_2 \ldots \mathrm{d}\lambda_{n-1} \end{aligned} \tag{2.14}$$

In two dimensions the potential field of a panel $\mathcal{S}^1$ (2.13) with length $2L$ is

$$-\varphi_{\text{panel}}(\boldsymbol{r}) = \int_{\lambda_1=-L}^{\lambda_1=L} \varphi \left(\boldsymbol{r} - \boldsymbol{r}_0 - \lambda_1 \boldsymbol{r}_1 \right) \, \mathrm{d}\lambda_1 \tag{2.15}$$

and is shown in figure 2.2.
At large distances from the goal point the influence of the attractive potential field is very small. To assist the attractive potential a field of uniform flow is added:

$$\varphi_{\text{uniform}}(\boldsymbol{q}) = -k \cdot (\boldsymbol{q} \, , \, \boldsymbol{k}_d) \tag{2.16}$$

where $\boldsymbol{k}_d = \frac{\boldsymbol{q}-\boldsymbol{q}_d}{|\boldsymbol{q}-\boldsymbol{q}_d|}$ and k is an arbitrary constant scalar representing the flow strength. The uniform flow field is also a harmonic function.
The total artificial potential field is a summation of the attractive potential field of the goal position, the uniform flow and the repulsive field of the m panels:

$$\varphi(\boldsymbol{q}) = \varphi_{\text{goal}}(\boldsymbol{q}) + \varphi_{\text{uniform}}(\boldsymbol{q}) + \sum_{j=1}^{m} \varphi_{\text{panel, j}}(\boldsymbol{q}). \tag{2.17}$$

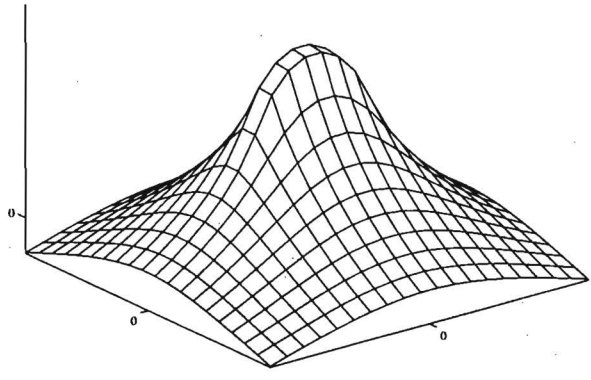

Figure 2.2: Harmonic artificial potential field of a panel obstacle in two dimensions.

When the figures 2.1 and 2.2 are compared it can be seen that the potential on a panel is not infinite, as on a point, but has become finite. This could result in a path through a panel. To prevent this, the normal velocity component $\frac{\partial \varphi(\boldsymbol{q})}{\partial n}$ of the potential field must be directed away from panel i at all times:

$$\frac{\partial \varphi(\boldsymbol{q})}{\partial n} \geq V_i \qquad \forall \boldsymbol{q} \in \mathcal{S}_i^{n-1} \tag{2.18}$$

where V_i is some positive constant. When (2.17) is substituted into (2.18) a set of m equations in m unknowns is obtained. By solving these equations the potential field strength of the panels is determined, which guarantees that a generated path will lead around the panels.

2.2.3 Numerical harmonic functions

Another approach to the calculation of an artificial harmonic potential field is the use of numerical algorithms as proposed by Sato (Sato 1993) and Connolly (Connolly 1994). The method is also applied in the configuration space of a robot.
The basis for this method is the homogeneous Laplace equation

$$\nabla_{\boldsymbol{q}}^2 \phi(\boldsymbol{q}) = 0 \tag{2.19}$$

This equation can be written as a difference equation by replacing each derivative of (2.19) by

$$\frac{\partial \phi}{\partial q_k} = \frac{\phi_{i+1} - \phi_i}{\Delta q_k} \tag{2.20}$$

where Δq_k is the grid size and ϕ_i is the value of ϕ atthe grid point $q_k = i\Delta q_k$. Apparently, the configuration space is represented by a regularly spaced n-dimensional grid.
In two dimensions equation (2.19) becomes

$$\begin{aligned} \nabla^2\phi = \frac{\partial^2\phi}{\partial q_1^2} + \frac{\partial^2\phi}{\partial q_2^2} &= \frac{\phi_{i+1,j} - 2\phi_{i,j} + \phi_{i-1,j}}{2(\Delta q_1)^2} \\ &+ \frac{\phi_{i,j+1} - 2\phi_{i,j} + \phi_{i,j-1}}{2(\Delta q_2)^2} = 0 \end{aligned} \tag{2.21}$$

When the grid sizes Δq_1 and Δq_2 are chosen equal, (2.21) can be rewritten as

$$\phi_{i,j} = \frac{1}{4}(\phi_{i+1,j} + \phi_{i-1,j} + \phi_{i,j+1} + \phi_{i,j-1}). \tag{2.22}$$

Equation (2.22) states that the value of ϕ at the grid point $(i\Delta q_1, j\Delta q_2)$ equals the average of the neighbouring points. In three or more dimensions this principle remains the same.
The calculation of the potential field starts with a division of the configuration space in a regular grid. The goal point is fixed at a potential $\phi = 0$ while the obstacle points are fixed at a value $\phi = 1$. For each grid point the potential is calculated using (2.22). The goal and obstacle points are skipped because their potential is known. This procedure is repeated until the change of potential between two successive iterations is small enough.
This method can also be used in a dynamic environment. The new obstacle points are set on a fixed value 1. The iterative process is repeated. The potential field before the change of the obstacles, is used as initial value for the new iterative process.

Chapter 3

Robot Modelling and Control

In this chapter the kinematic and dynamic models of a robot are introduced which form the basic mathematical models for the robot control analysis and design. The kinematic model defines the relation between the position and orientation of the TCP and the values of each joint of the robot. Hence, the kinematics of the robot can be analysed in terms of the direct kinematics and its counterpart the inverse kinematics. For the kinematics of the robot a standard representation is given based on the Denavit-Hartenberg(D-H) (Denavit and Hartenberg 1955) approach of establishing coordinate systems to each link of an articulated chain.

The dynamic model describes the dynamics of the robot expressed in terms of torque inputs, and joint positions, velocities and accelerations. The Langrange-Euler formulation of the dynamic model adopted here incorporates the influence of the robot characteristics: geometry and mass of the links, dynamics of the actuators. These characteristics are included in the dynamic model of the robot through the Coriolis, centrifugal, gravitation and friction forces and the manipulator inertia.

We examine a robot control method which has some interesting advantages related to the requirement of minimal prior knowledge of the robot characteristics and the direct usage of artificial potential fields. In the first place, we analyse the control strategy when an n-axis proportional-plus-derivative (PD-type) controller is employed. The aim of the PD-type controller is to regulate the robot towards a prescribed constant *goal state.* This is known as the *regulator* problem, or set-point problem.

Finally, this PD-type controller will be extended to a more general controller

including artificial potential fields which are going to be examined in the next chapter.

3.1 Robot Model

Generally, a robot can be modeled as a chain of rigid bodies (*links*) which are interconnected to one another by variable *joints* (figure 3.1). One end of the chain of links is fixed to a base, while the other end is free to move. The

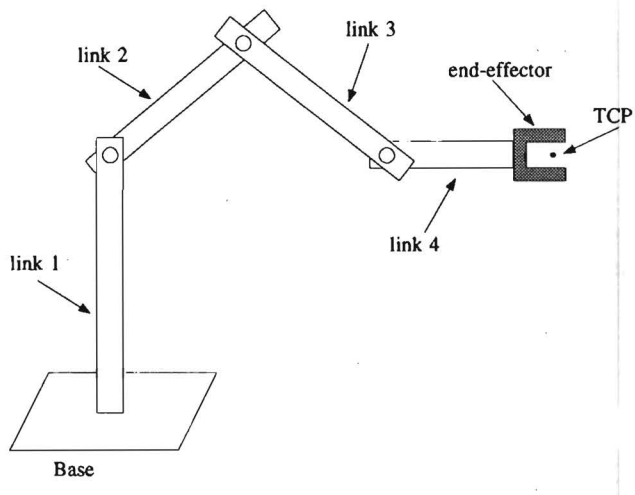

Figure 3.1: A chain of interconnected rigid bodies

mobile end has a flange, or face plate, with a *tool*, or *end-effector*, attached to it. A predefined point at the end-effector the so-called *tool centre point* (TCP) will be used as the reference point of the motion of the robot. In addition a local coordinate system is assigned to the TCP which can be used to define the orientation of the end-effector in the space. The objective is to control both the position and the orientation of the TCP. In order to accomplish the robot motion, we must first formulate the relation between the joint variables and the position and orientation of the TCP. This is called the *direct kinematics problem.*The inverse kinematics problem considers the determination of the joint variables given a position and orientation of the TCP. In figure 3.2 the direct and inverse kinematics are diagrammatically depicted.

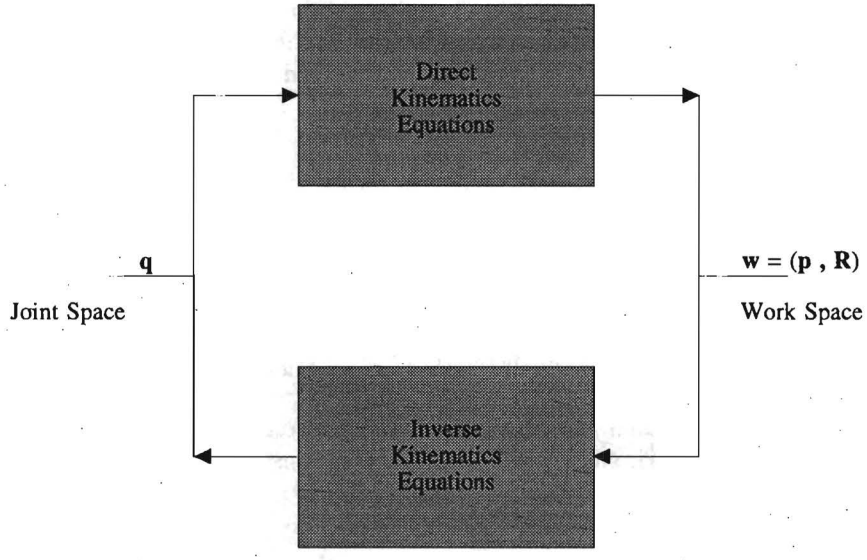

Figure 3.2: Direct and inverse kinematics of a robot

The inverse kinematics equations are important because the motion tasks are naturally formulated in the work space of the robot and in addition the obstacles in the environment of the robot are sensored also in the work space of the robot, though the motion planning takes place in the joint space of the robot. The transformation of the position and orientation of the TCP and all the configurations where the robot collides to an obstacle uses the inverse kinematics of the robot as will be discussed in the next chapter.
Before starting with the direct and inverse kinematics of the robot, we need to define the two different spaces where the robot can be described, the *joint space* $\mathcal{J}$ and the so-called *work space* $\mathcal{W}$ of the robot.

3.1.1 Direct Kinematics of the Robot

Recalling that only articulated robots with revolute axes are considered, we identify the joint variables as the angles of the joints of the robot. The joint space of the robot $\mathcal{J}$, is a subset of $\mathcal{R}^n$ [1], where n is the number of joints

[1] More precise by the joint space of a robot is an n-dimensional torus. By doing so, it is possible to model the property of a joint variable to get the value 0 instead of 2π by a

of the robot. We denote an element of $\mathcal{J}$ by $\boldsymbol{q}$ which is an n-dimensional vector representing the n angles of the joints of the robot. Let $\underline{q}_i$ and $\bar{q}_i$ be, respectively, the minimal and maximal bounds of the joint coordinate q_i. The manipulator configuration $\boldsymbol{q}$ in joint space is confined to the convex polyhedron in $\mathcal{R}^n$ of the following general form:

$$\mathcal{Q} = \{\, \boldsymbol{q} \in \mathcal{J} : \underline{q}_i < q_i < \bar{q}_i \,\} \tag{3.1}$$

The open set $\mathcal{Q}$ of all feasible configurations is denoted as the *operational configuration space* of the robot.

The work space of a robot is defined as: $\mathcal{W} \triangleq \mathcal{R}^3 \times SO(3)$. Where

$$SO(3) \triangleq \{R \in \mathcal{R}^{3\times 3} | R^T R = I \; and \; \det(R) > 0\} \tag{3.2}$$

is the set of rotations in $\mathcal{R}^3$ with positive orientation (see also Arnold 1978). Accordingly, the work space consists of all positions and orientations of the TCP.

We assume that coordinate frames are assigned to each link in accordance with the convention developed by Denavit and Hartenberg (Denavit and Hartenberg 1955) for spatial mechanisms. Because the establishment of the coordinate systems is not unique, different algorithms are proposed by different authors (Paul 1982; and McKerrow 1991). In the present treatment we use the algorithm found in (Paul 1982). According to this algorithm the coordinate systems of the 6-axis PUMA robot 3.3(a) has been assigned as shown in figure 3.3(c). According to this assignment we can define a homogeneous transformation matrix ${}^{i-1}T_i(q_i)$ which relates the i-th and $(i-1)$-th link-coordinate frames as follows:

$${}^{i-1}T_i(q_i) = \begin{bmatrix} \cos(q_i) & -\cos(\alpha_i)\sin(q_i) & \sin(\alpha_i)\sin(q_i) & a_i\cos(q_i) \\ \sin(q_i) & \cos(\alpha_i)\cos(q_i) & -\sin(\alpha_i)\cos(q_i) & a_i\sin(q_i) \\ 0 & \sin(\alpha_i) & \cos(\alpha_i) & d_i \\ 0 & 0 & 0 & 1 \end{bmatrix}$$

where

- q_i is the joint angle from the x_{i-1} axis to the x_i axis about the z_{i-1} axis (using the right-hand rule).
- d_i is the distance from the origin of the $(i-1)$-th coordinate frame to the intersection of the z_{i-1} axis with the x_i axis along the z_{i-1} axis.

complete rotation of the link.

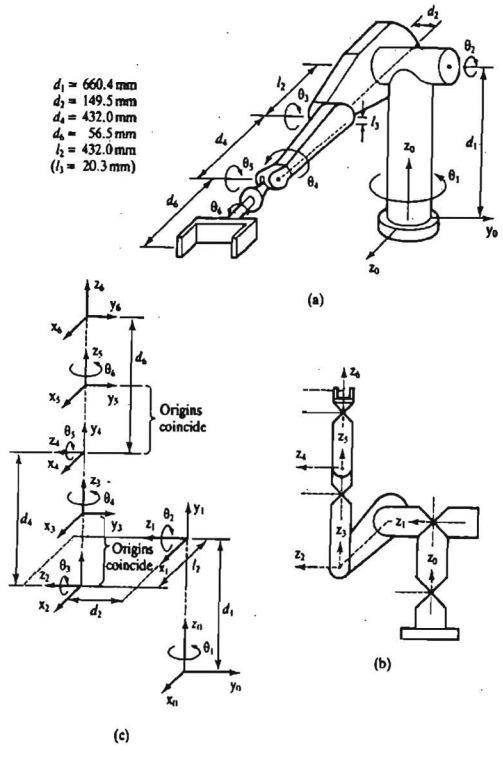

Figure 3.3: Example of coordinate systems.

- a_i is the offset distance from the intersection of the z_{i-1} axis with the x_i axis to the origin of the i-th frame along the x_i axis (or shortest distance between the z_{i-1} and z_i axes).
- α_i is the offset angle from the z_{i-1} axis to the z_i axis about the x_i axis (using the right-hand rule).

For a robot with all joints of the revolute type, only q_i is variable and the remaining parameters are known and constant.
The homogeneous matrix ${}^0T_i$ specifies the position and orientation of the end point of link i with respect to the base coordinate system. The matrix ${}^0T_i$ is the chain product of successive coordinate matrices, expressed as

$$ {}^0T_i = {}^0T_1\,{}^1T_2 \cdots {}^{i-1}T_i = \prod_{j=1}^{i} {}^{j-1}T_j \tag{3.3} $$

Comparably, successive transformations between adjacent coordinate frames, connecting the TCP and the base of the robot, lead to the so-called *arm matrix* given by:

$$ {}^0T_n(\boldsymbol{q}) = \prod_{j=1}^{n} {}^{j-1}T_j(q_j) \tag{3.4} $$

or

$$ {}^0T_n(\boldsymbol{q}) = \begin{bmatrix} R(\boldsymbol{q}) & \boldsymbol{p}(\boldsymbol{q}) \\ \mathbf{0} & 1 \end{bmatrix} \tag{3.5} $$

The arm matrix ${}^0T_n$ represents the position $\boldsymbol{p} \in \mathcal{R}^3$ and orientation $R = [\boldsymbol{r}_1, \boldsymbol{r}_2, \boldsymbol{r}_3] \in SO(3)$ of the TCP with respect to the base frame as a function of the joint variables $\boldsymbol{q}$. The TCP position and orientation is defined by the element $\boldsymbol{w}(\boldsymbol{q}) = (\boldsymbol{p}, R)$ which is an element of the work space.
For a given robot configuration $\boldsymbol{q}$ is then possible to find the TCP position $\boldsymbol{p}(\boldsymbol{q})$ and orientation $R(\boldsymbol{q})$ using the arm matrix. That is actually the solution of the *direct kinematics* problem.
Obviously, for general joint boundaries, the set of all TCP positions and orientations $\mathcal{T} = \{\boldsymbol{w}(\boldsymbol{q}) : \boldsymbol{q} \in \mathcal{Q}\}$ form the operational space of the robot, which is a subset of $\mathcal{W}$.

3.1.2 Inverse Kinematics of the Robot

The *inverse kinematics* problem is in fact the opposite of the direct kinematics problem. It can be formulated as follows: for a given position $\boldsymbol{p}$ and orientation R of the TCP, find the corresponding joint coordinates $\boldsymbol{q}$. Here we assume that the solutions of the inverse kinematics problem can be found by methods described in the literature e.g. (McKerrow 1991; Schilling 1990). Further exploitation of the inverse kinematics of a specific manipulator will be fully worked out when the transformation of the obstacles from the work space to the joint space will be analysed, in chapter 4. Notice that it is possible to find more than one solution for the inverse kinematics problems even for a nonredundant robot. Despite other definitions of redundancy i.e. (McKerrow 1991), in the present treatment a robot is called redundant when the dimension of the joint space is higher than the dimension of the work space (Schilling 1990). However, it is possible that the inverse kinematics problem has more than one solution. For example, consider the robot depicted in figure (3.4). In that case two distinct solutions are possible for the same position and orientation of the TCP.
Traditionally, one of these solutions is going to be chosen by the motion planning problem. We allow both solutions as valid goal configurations which can

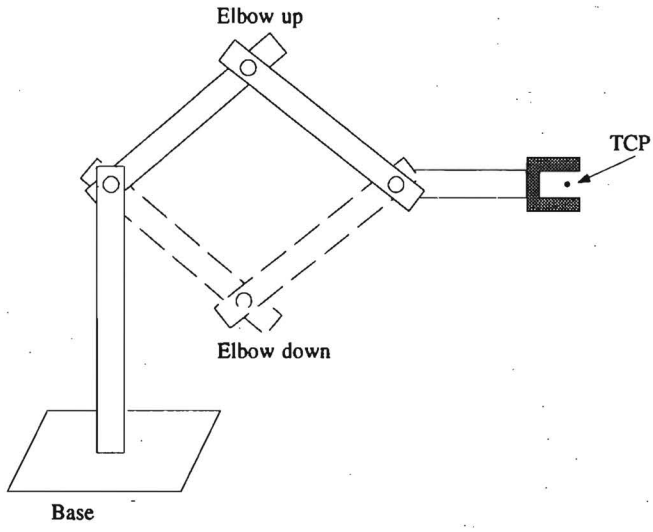

Figure 3.4: Multiple solutions with a nonredundant robot

arbitrarily be reached by the robot. Of course, the possibility remains to explicitly choose one of them and exile the other one as explained in the next subsection.

3.1.3 The Goal State of the Motion Planning Problem

Robot motion planning has been in the present treatment restricted to the point-to-point type. That means that the robot has to reach a given goal position and orientation $\boldsymbol{w}_d \in \mathcal{T}$ or a given goal configuration $\boldsymbol{q}_d \in \mathcal{Q}$. We define the set of goal states as:

Set of Goal Configurations *The set of goal configurations $\mathcal{G}$ is defined as:*

- *for a given goal configuration $\boldsymbol{q}_d \in \mathcal{Q}$*

$$\mathcal{G} = \{\boldsymbol{q}_d\} \tag{3.6}$$

or

- *for a given goal TCP position and orientation $\boldsymbol{w}_d = (\boldsymbol{p}_d, R_d) \in \mathcal{T}$*

$$\mathcal{G} = \{\boldsymbol{q} : \boldsymbol{p}(\boldsymbol{q}) = \boldsymbol{p}_d \text{ and } R(\boldsymbol{q}) = R_d\} \tag{3.7}$$

Through the definition of the set of goal configurations $\mathcal{G}$, we can define the objective of the motion planning problem as instructing the robot to reach a goal configuration $\boldsymbol{q}_d$ belonging to $\mathcal{G}$. Hence, the motion planning problem is formulated in the joint space of the robot.

3.1.4 Dynamic Model of the Robot

The equations of motion of an n-axis robotic arm can be expressed in the following general form:

$$D(\boldsymbol{q})\ddot{\boldsymbol{q}} + C(\boldsymbol{q},\dot{\boldsymbol{q}})\dot{\boldsymbol{q}} + \boldsymbol{h}(\boldsymbol{q}) + \boldsymbol{b}(\dot{\boldsymbol{q}}) = \boldsymbol{\tau} \tag{3.8}$$

where $\boldsymbol{q}$ represents the joint angles of the robot, $\dot{\boldsymbol{q}}$ represents the joint angle velocities of the robot, $\boldsymbol{\tau}$ the input torque vector, $D(\boldsymbol{q})$ is an $n \times n$ matrix representing the *inertia* of the robot, $C(\boldsymbol{q},\dot{\boldsymbol{q}})$ represents the Coriolis and centrifugal effects, $\boldsymbol{h}(\boldsymbol{q})$ represents the gravitation torques, and $\boldsymbol{b}(\dot{\boldsymbol{q}})$ represents the friction torques.
The matrix $C(\boldsymbol{q},\dot{\boldsymbol{q}})$ is linear in $\dot{\boldsymbol{q}}$, and $D(\boldsymbol{q})$, $C(\boldsymbol{q},\dot{\boldsymbol{q}})$ and $\boldsymbol{h}(\boldsymbol{q})$ all vary in $\boldsymbol{q}$ by polynomials of transcendental functions.
Following the notation in (Schilling 1990) pp. 236, we recall the next proposition.

Proposition 3.1.1 (State-Space Representation) *The equation of motion of a robotic arm in (3.8) can be represented by the following first-order state-space model:*

$$\begin{aligned} \dot{\boldsymbol{q}} &= \boldsymbol{v} \\ \dot{\boldsymbol{v}} &= D^{-1}(\boldsymbol{q})[\boldsymbol{\tau} - \boldsymbol{h}(\boldsymbol{q}) - C(\boldsymbol{q},\boldsymbol{v})\boldsymbol{v} - \boldsymbol{b}(\boldsymbol{v})] \end{aligned} \tag{3.9}$$

where $\boldsymbol{v} \triangleq \dot{\boldsymbol{q}}$.
Proof. (see also (Schilling 1990), pp. 236, proposition 7-2-1). By definition, $\dot{\boldsymbol{q}} = \boldsymbol{v}$. Using (3.9) and the definition of $\boldsymbol{v}$, we then have:

$$\begin{aligned} \dot{\boldsymbol{v}} &= \ddot{\boldsymbol{q}} \\ &= D^{-1}(\boldsymbol{q})[\boldsymbol{\tau} - \boldsymbol{h}(\boldsymbol{q}) - C(\boldsymbol{q},\dot{\boldsymbol{q}})\dot{\boldsymbol{q}} - \boldsymbol{b}(\dot{\boldsymbol{q}})] \\ &= D^{-1}(\boldsymbol{q})[\boldsymbol{\tau} - \boldsymbol{h}(\boldsymbol{q}) - C(\boldsymbol{q},\boldsymbol{v})\boldsymbol{v} - \boldsymbol{b}(\boldsymbol{v})] \end{aligned}$$

□
For the derivation of the control strategy in the next section we only need an explicit expression of the friction term $\boldsymbol{b}(\dot{\boldsymbol{q}})$, expressed in the three distinct components: the *viscous friction*, the *dynamic friction* and the *static friction*.

Friction Torques. For joint k we assume the following frictional torque model (Schilling 1990):

$$b_k(\dot{q}_k) = b_k^v \dot{q}_k + sgn(\dot{q}) \left[b_k^d \left(1 - \exp \frac{-|\dot{q}_k|}{\epsilon} \right) + b_k^s \exp \frac{-|\dot{q}_k|}{\epsilon} \right] \tag{3.10}$$

for $1 \leq k \leq n$. The first term in (3.10) represents the *viscous friction* where b_k^v is the coefficient of viscous friction for joint k. The second term in (3.10) represents *dynamic friction* where b_k^d is the coefficient of dynamic friction for joint k. Finally, the last term in (3.10) represents *static friction* or Coulomb friction, where b_k^s is the coefficient of static friction for joint $k$and ϵ is a small positive parameter. The model of frictional torques acting on the k-th joint is depicted in figure 3.5.

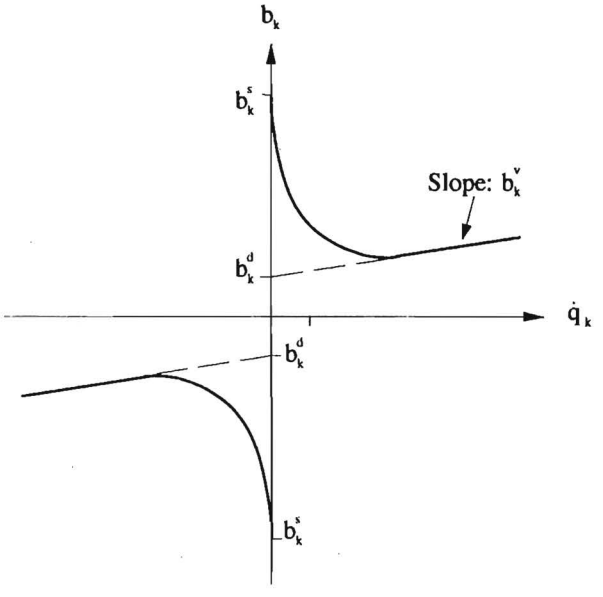

Figure 3.5: Friction model for joint k

3.2 Robot Control

A *robot control* problem aims to issuing the robot either to follow a prescribed trajectory or to reach a prescribed goal configuration. Numerous techniques

have been proposed for its solution such as: the *computed-torque* method, single-axis *PID control* and the PD-plus-Gravity Control (Schilling 1990). The latter control strategy has the advantage that no explicit knowledge of the manipulator dynamic characteristics is required. In addition the extension to the usage of artificial potential fields is evident as will be shown. However, for this kind of control scheme, the exact cancellation of the gravitational torques is needed and the goal configuration has to remain constant.
The proof of stability of the controller towards the goal configuration will be included based on the pioneer work of Koditschek, (Koditchek 1984; Koditchek 1986; Koditchek 1991) and also described in (Schilling 1990). We recall the fundamentals of this control strategy as it forms the basis for further exploitation when a more general feedback law is introduced which is related with artificial potential fields.
Artificial potential fields will be introduced in a general way since they are extensively analysed in chapter 5.

3.2.1 Fundamentals of Nonlinear Systems

As the state equations of a robot (3.9) are highly nonlinear, we introduce some fundamental analysis applicable to nonlinear system in general. We restrict our attention to a nonlinear system S of the following explicit form:

$$\dot{\boldsymbol{x}} = \boldsymbol{f}(\boldsymbol{x}, \boldsymbol{u}) \tag{3.11}$$

The independent time variable, denoted as t, is left implicit. The vector $\boldsymbol{x}(t) \in \mathcal{R}^m$ is the state of S at time t and the vector $\boldsymbol{u}(t) \in \mathcal{R}^p$ is the input to S at time t. The system S is a *nonautonomous* system because it has an time-varying input $\boldsymbol{u}(t)$. In the case of constant inputs, the system S becomes an *autonomous* system. Autonomous systems are easier to analyse because they often posses one or more constant solutions called *equilibrium points.*

Equilibrium Points. *Let $\boldsymbol{u}(t) = \boldsymbol{r}$ for $t \geq 0$ for some $\boldsymbol{r} \in \mathcal{R}^p$. Then $\hat{\boldsymbol{x}} \in \mathcal{R}^m$ is an equilibrium point of the system S associated with the input $\boldsymbol{u}(t) = \boldsymbol{r}$ if and only if:*

$$\boldsymbol{f}(\hat{\boldsymbol{x}}, \boldsymbol{r}) = 0 \tag{3.12}$$

From (3.11) it is evident that at each equilibrium point of a system S, $\dot{\boldsymbol{x}} = 0$. That means that if $\boldsymbol{x}(0) = \hat{\boldsymbol{x}}$, then $\boldsymbol{x}(t) = \hat{\boldsymbol{x}}$ for $t \geq 0$. That is, equilibrium points are constant solutions of S. When the solution start near an equilibrium

point $\hat{\boldsymbol{x}}$ in the sense that $||\boldsymbol{x}(0) - \hat{\boldsymbol{x}}||$ is small, we define the important notion of *asymptotic stability* as:

Asymptotic Stability. *An equilibrium point $\hat{\boldsymbol{x}}$ of a system S described by (3.11) is asymptotic stable if and only if for each $\epsilon > 0$ there exists a $\delta > 0$ such that if $||\boldsymbol{x}(0) - \hat{\boldsymbol{x}}|| < \delta$, then $||\boldsymbol{x}(t) - \hat{\boldsymbol{x}}|| < \epsilon$ for $t \geq 0$ and:*

$$\boldsymbol{x}(t) \rightarrow \hat{\boldsymbol{x}} \qquad as \qquad t \rightarrow \infty \tag{3.13}$$

Each asymptotically stable equilibrium point has an open region surrounding it called a *domain of attraction.* The domain of attraction is a set $\Omega_\rho \subset \mathcal{R}^m$ with the following property:

$$\boldsymbol{x}(0) \in \Omega_\rho \Rightarrow \boldsymbol{x}(t) \rightarrow \hat{\boldsymbol{x}} \qquad \text{as} \qquad t \rightarrow \infty \tag{3.14}$$

There is a relative simple sufficient condition, called *Lyapunov's second method,* that can be used to both establish the asymptotic stability of an equilibrium point and to estimate its domain of attraction. First, we define a Lyapunov function as follows.

Lyapunov Function *Let Ω_ρ be an open region in $\mathcal{R}^m$ containing the origin. A function $V_L : \Omega_\rho \rightarrow \mathcal{R}$ is a* Lyapunov function *on Ω_ρ if and only if:*

1. *$V_L(\boldsymbol{x})$ has a continuous time derivative.*
2. *$V_L(\mathbf{0}) = 0$*
3. *$V_L(\boldsymbol{x}) > 0$ for $\boldsymbol{x} \neq \mathbf{0}$*

To verify the asymptotic stability of $\hat{\boldsymbol{x}}$, we evaluate $V_L(\boldsymbol{x}(t))$ along solutions of the system S. For simplicity, we assume that the equilibrium point is located at the origin. If this is not the case, we can always perform a change of variables to translate it to the origin. If we can demonstrate that $V_L(\boldsymbol{x}(t))$ decreases along solutions of S, then it must be the case that $V_L(\boldsymbol{x}(t)) \rightarrow 0$ as $t \rightarrow \infty$. But since $V_L(\boldsymbol{x})$ is a Lyapunov function, this implies that $\boldsymbol{x}(t) \rightarrow 0$ as $t \rightarrow \infty$. The Lyapunov's second method can now be formulated as follows.

Proposition 3.2.1 Lyapunov's Second Method. *Let $\hat{\boldsymbol{x}} = \mathbf{0}$ be an equilibrium point of a system S described by (3.11) associated with a constant input $\boldsymbol{u}(t) = \boldsymbol{r}$. Next, let $V_L : \Omega_\rho \rightarrow \mathcal{R}$ be a Lyapunov function on Ω_ρ where $\Omega_\rho = \{x : V_L(x) < \rho\}$ for some $\rho > 0$. Then $\hat{\boldsymbol{x}}$ is asymptotically stable with domain of attraction Ω_ρ if, along solutions of S:*

1. $\dot{V}_L(\boldsymbol{x}(t)) \leq 0$

2. $\dot{V}_L(\boldsymbol{x}(t)) \equiv 0 \Rightarrow \boldsymbol{x}(t) \equiv 0$

The Lyapunov's second method, also called the direct method, appears very attractive for the analysis of nonlinear systems since the conditions of the above stated proposition can be checked without solving the nonlinear system. Indeed from (3.11), the time derivative of $V_L(\boldsymbol{x}(t))$, evaluated along solutions of S, is:

$$\dot{V}_L(\boldsymbol{x}) = \nabla_{\boldsymbol{x}} V_L(\boldsymbol{x})\, \dot{\boldsymbol{x}} = \nabla_{\boldsymbol{x}} V_L(\boldsymbol{x})\, \boldsymbol{f}(\boldsymbol{x}, \boldsymbol{r}) \tag{3.15}$$

That means that only the gradient $\nabla_{\boldsymbol{x}} V_L(\boldsymbol{x})$ has to be calculated where no solutions of $\boldsymbol{f}(\boldsymbol{x}, \boldsymbol{r})$ are involved. This is important since in most cases an explicit expression for the solution of (3.11) does not exist.

3.2.2 PD-Plus-Gravity Control

We consider a robot described by the dynamical system of (3.9). Suppose that for the performance of a specific task, the robot has to be controlled to reach the prescribed goal state $(\boldsymbol{q}_d, \boldsymbol{0}) \in \mathcal{Q} \times T\mathcal{Q}$. The control strategy introduced is given by the explicit expression of torque input:

$$\boldsymbol{\tau} = \boldsymbol{h}(\boldsymbol{q}) - K_1(\boldsymbol{q} - \boldsymbol{q}_d) - K_2 \boldsymbol{v} \tag{3.16}$$

This algorithm requires neither an explicit knowledge of the inertia matrix $D(\boldsymbol{q})$ nor the matrix $C(\boldsymbol{q}, \dot{\boldsymbol{q}})$ which depend upon particular features of the task like grasping a load. However, we notice that the gravitation forces $\boldsymbol{h}(\boldsymbol{q})$ which do depend upon the particular features of the task, need to be calculated explicitly. Furthermore, we will notice that this control strategy works if and only if the reference signal $\boldsymbol{q}_d$ remains constant. Since our problem formulation is restricted to reaching a constant goal state, it seems that the PD-type controller satisfies the given requirements. The gravitation forces, on the other hand, are relatively easy to calculate but still depend on the specific task to be accomplished. Some work has been done (Koditchek 1984) to incorporate this term in the control law in an adaptive way but still not satisfactory.
In the next theorem, we recall the proof of the asymptotic stability of the PD-type controller under the state feedback algorithm (3.16).

Theorem 3.2.1 *(Takegaki and Arimoto 1981; Koditschek 1984) Let the operational joint space $\mathcal{Q}$ be a simply connected subset of $\mathcal{R}^n$. The system (3.9), under the state feedback algorithm (3.16),*

$$\begin{aligned} \dot{\boldsymbol{q}} &= \boldsymbol{v} \\ \dot{\boldsymbol{v}} &= -D^{-1}(\boldsymbol{q})[(K_2 + C(\boldsymbol{q}, \boldsymbol{v}))\boldsymbol{v} + K_1(\boldsymbol{q} - \boldsymbol{q}_d) - \boldsymbol{b}(\boldsymbol{v})] \end{aligned} \tag{3.17}$$

is globally asymptotically stable with respect to the state $(\boldsymbol{q}_d, \mathbf{0})$ *for any positive definite symmetric matrices* K_1 *and* K_2.

Proof: First we perform a change of variables to move the equilibrium point to the origin. Let $\boldsymbol{z} \triangleq \boldsymbol{q} - \boldsymbol{q}_d$. Then, the closed-loop equations in (3.17) can be recast in terms of $\boldsymbol{z}$ and $\boldsymbol{v}$ as:

$$\begin{aligned} \dot{\boldsymbol{z}} &= \boldsymbol{v} \\ \dot{\boldsymbol{v}} &= -D^{-1}(\boldsymbol{z}+\boldsymbol{q}_d)[(K_2 + C(\boldsymbol{z}+\boldsymbol{q}_d, \boldsymbol{v}))\boldsymbol{v} + K_1\boldsymbol{z} + \boldsymbol{b}(\boldsymbol{v})] \end{aligned} \tag{3.18}$$

Since $C(\boldsymbol{z}+\boldsymbol{q}_d, 0) = 0$ and $\boldsymbol{b}(0) = 0$), it follows that the state $(0,0)$ is an equilibrium point of the transformed system. To show that this equilibrium point is asymptotically stable, we use Lyapunov's second method. Consider the positive definite Lyapunov candidate

$$V(\boldsymbol{z}, \boldsymbol{v}) \triangleq \frac{1}{2}(\boldsymbol{z}^T K_1 \boldsymbol{z} + \boldsymbol{v}^T D(\boldsymbol{z}+\boldsymbol{q}_d)\boldsymbol{v}) \tag{3.19}$$

The time derivative of V is given by:

$$\dot{V}(\boldsymbol{z}, \boldsymbol{v}) = \boldsymbol{z}^T K_1 \boldsymbol{v} + \frac{1}{2}\boldsymbol{v}^T \dot{D}(\boldsymbol{z}+\boldsymbol{q}_d)\boldsymbol{v} + \boldsymbol{v}^T D(\boldsymbol{z}+\boldsymbol{q}_d)\dot{\boldsymbol{v}} \tag{3.20}$$

Substituting (3.17) in (3.20) yields:

$$\begin{aligned} \dot{V}(\boldsymbol{z}, \boldsymbol{v}) &= \boldsymbol{z}^T K_1 \boldsymbol{v} + \frac{1}{2}\boldsymbol{v}^T \dot{D}(\boldsymbol{z}+\boldsymbol{q}_d)\boldsymbol{v} - \\ &\quad \boldsymbol{v}^T[K_1\boldsymbol{z} + K_2\boldsymbol{v} + C(\boldsymbol{z}+\boldsymbol{q}_d, \boldsymbol{v})\boldsymbol{v} + \boldsymbol{b}(\boldsymbol{v})] \\ &= \boldsymbol{v}^T\left[\frac{1}{2}\dot{D}(\boldsymbol{z}+\boldsymbol{q}_d) - C(\boldsymbol{z}+\boldsymbol{q}_d, \boldsymbol{v})\right]\boldsymbol{v} - \boldsymbol{v}^T[K_2\boldsymbol{v} + \boldsymbol{b}(\boldsymbol{v})] \end{aligned} \tag{3.21}$$

It is proven (Koditchek 1984) that $C(\boldsymbol{q}, \boldsymbol{v})$, the Coriolis and centrifugal term in (3.17), may be written as the half sum of the time derivative of the positive definite symmetric inertia matrix $D(\boldsymbol{q})$, and a skew-symmetric matrix, $F(\boldsymbol{q}, \boldsymbol{v})$. That $F(\boldsymbol{q}, \boldsymbol{v})$ is a skew-symmetric matrix implies that $F^T(\boldsymbol{q}, \boldsymbol{v}) = -F(\boldsymbol{q}, \boldsymbol{v})$. Hence:

$$C(\boldsymbol{z}+\boldsymbol{q}_d, \boldsymbol{v}) = \frac{1}{2}(\dot{D}(\boldsymbol{z}+\boldsymbol{q}_d) - F(\boldsymbol{z}+\boldsymbol{q}_d, \boldsymbol{v})) \tag{3.22}$$

Substituting (3.22) in (3.21) yields the following expression for $\dot{V}(\boldsymbol{z}, \boldsymbol{v})$, taking

into account that $v^T F v$ vanishes:

$$\begin{aligned}
\dot{V}(z,v) &= \frac{1}{2}v^T F(z+q_d,v)v - v^T[K_2 v + b(v)] \\
&= -v^T[K_2 v + b(v)] \\
&= -v^T K_2 v - \sum_{k=1}^{n} v_k b_k(v_k) \\
&= -v^T K_2 v - \sum_{k=1}^{n} v_k \left[b_k^v v_k + \right. \\
&\quad \left. sgn(v_k)[b_k^d(1 - \exp(\frac{-|v_k|}{\epsilon})) + b_k^s \exp(\frac{-|v_k|}{\epsilon})]\right] \\
&= -v^T K_2 v - \sum_{k=1}^{n} \left[b_k^v (v_k)^2 + \right. \\
&\quad \left. |v_k|[b_k^d(1 - \exp(\frac{-|v_k|}{\epsilon})) + b_k^s \exp(\frac{-|v_k|}{\epsilon})]\right] \qquad (3.23)
\end{aligned}$$

Recalling that K_2 is positive definite, and that the friction coefficients are all nonnegative implies that $\dot{V}(z(t)+q_d, v(t)) \leq 0$ along solutions of (3.18). Accordingly, the first condition of proposition 3.2.1 is satisfied.
Since K_2 is positive definite:

$$\begin{aligned}
\dot{V}(z(t)+q_d, v(t)) \equiv 0 &\Rightarrow v(t) \equiv 0 \\
&\Rightarrow \dot{v}(t) \equiv 0 \\
&\Rightarrow D^{-1}(z(t)+q_d)K_1 z(t) \equiv 0 \\
&\Rightarrow z(t) \equiv 0 \qquad (3.24)
\end{aligned}$$

Thus, the second condition of proposition (3.2.1) is satisfied, and from proposition (3.2.1), the equilibrium point $(z,v) = (0,0)$ is asymptotically stable. □
The domain of attraction is the set Ω_ρ where:

$$\begin{aligned}
\Omega_\rho &= \{(z,v) : V(z,v) < \rho\} \\
&= \left\{(z,v) : \frac{z^T K_1 z + v^T D(z+q_d)v}{2} < \rho\right\} \qquad (3.25)
\end{aligned}$$

$V(z,v)$ is a Lyapunov function on Ω_ρ and conditions 1 and 2 of proposition (3.2.1) are satisfied on Ω_ρ for every $\rho > 0$. Furthermore, since K_1 and $D(z+q_d)$ are positive-definite matrices, $V(z,v) \to \infty$ as $\|z\| + \|v\| \to \infty$. Thus the domain of attraction is the entire state space $\Omega_\rho = \mathcal{R}^n$. That is, the equilibrium point $(q,v) = (q_d, 0)$ is asymptotically stable in the large. It is

noticeable that in this control strategy not any more a reference trajectory but a goal state $(\boldsymbol{q}_d, \mathbf{0})$ plays a role. Nevertheless it seems clear that the solution of the robotic system or the trajectory followed, is left to the "mechanical computer" formed by the robot arm itself.
There are two serious criticisms to be made of any robot controller based upon this result.

- The control law requires the exact cancellation of any gravitational disturbance. While $\boldsymbol{h}(\boldsymbol{q})$ has a much simpler structure than the moment of inertia matrix, $D(\boldsymbol{q})$, or the Coriolis matrix $C(\boldsymbol{q}, \boldsymbol{v})$, exact knowledge of the load parameters would still be required, in general, to permit the computation of the gravitational torques.
- This result yields very little understanding of the trajectory that the arm will follow as it moves towards $(\boldsymbol{q}_d, \mathbf{0})$. This is in fact the reason of the choice of the name of this method as "Natural Motion" in (Koditchek 1991; Koditchek 1986; Koditchek 1985; Koditchek 1984).

3.2.3 Robot Control using Artificial Potential Fields

In the previous analysis of the robot control we have shown that it is possible to control the robot to a goal state $(\boldsymbol{q}_d, \mathbf{0})$. The basic concept of this control strategy is that the inputs of the robot are torque commands created by a simple PD-controller. In fact we want to send the robot to a specific position without colliding with obstacles in the environment of the robot. By defining an *Artificial Potential Field* (APF) $\mathrm{U}(\boldsymbol{q}) : \mathcal{Q} \rightarrow \mathcal{R}$, depending on these obstacles, it is possible to calculate a set of torques which keep the robot away from the obstacles and enforce the robot to attain a goal configuration $\boldsymbol{q}_d \in \mathcal{Q}$.
We consider again a robot to be described by the dynamical system of (3.9). The control strategy introduced here is an extended version of the one already described in subsection (3.2.2). Using an APF $\mathrm{U}(\boldsymbol{q})$ we define the following control strategy for the system described by (3.9), given by the torque:

$$\boldsymbol{\tau}(\boldsymbol{q}) = \boldsymbol{h}(\boldsymbol{q}) - \nabla_{\boldsymbol{q}}\mathrm{U}(\boldsymbol{q}) - K_2\boldsymbol{v} \tag{3.26}$$

We can prove that a state $(\boldsymbol{q}_d, \mathbf{0})$ of the system (3.9) is asymptotically stable for the new control strategy (3.26) as theorem 3.2.2 states.

Theorem 3.2.2 *Let the operational joint space $\mathcal{Q}$ be a simply connected subset of $\mathcal{R}^n$. The system of (3.9), under the state feedback algorithm (3.26),*

$$\begin{aligned} \dot{\boldsymbol{q}} &= \boldsymbol{v} \\ \dot{\boldsymbol{v}} &= -D^{-1}(\boldsymbol{q})[(K_2 + C(\boldsymbol{q}, \boldsymbol{v}))\boldsymbol{v} + \nabla_{\boldsymbol{q}}\mathrm{U}(\boldsymbol{q}) + \boldsymbol{b}(\boldsymbol{v})] \end{aligned} \tag{3.27}$$

is asymptotically stable with respect to the state $(\boldsymbol{q}_d, \mathbf{0})$ *for any* $\boldsymbol{q}_d \in \mathcal{Q}$ *for any positive definite symmetric matrix* K_2 *and for any function* $\mathtt{U}(\boldsymbol{q}) : \mathcal{Q} \rightarrow \mathcal{R}$ *which satisfies the following conditions:*

1. $\mathtt{U}(\boldsymbol{q})$ *has a continuous time derivative.*
2. $\mathtt{U}(\boldsymbol{q}) > 0$ *for all* $\boldsymbol{q} \neq \boldsymbol{q}_d$.
3. $\mathtt{U}(\boldsymbol{q}_d) = 0$.
4. $\nabla_{\boldsymbol{q}}\mathtt{U}(\boldsymbol{q}_d) = \mathbf{0}$.
5. $\nabla_{\boldsymbol{q}}\mathtt{U}(\boldsymbol{q}) \neq \mathbf{0}$ *for all* $\boldsymbol{q} \neq \boldsymbol{q}_d$.

Proof: For the proof of this theorem, we follow the same steps as for the theorem (3.2.1). First we perform a change of variables to move the equilibrium point to the origin. Let $\boldsymbol{z} \triangleq \boldsymbol{q} - \boldsymbol{q}_d$. Then, the closed-loop equations in (3.27) can be recast in terms of $\boldsymbol{z}$ and $\boldsymbol{v}$ as:

$$\begin{aligned} \dot{\boldsymbol{z}} &= \boldsymbol{v} \\ \dot{\boldsymbol{v}} &= -D^{-1}(\boldsymbol{z}+\boldsymbol{q}_d)[(K_2 + C(\boldsymbol{z}+\boldsymbol{q}_d, \boldsymbol{v}))\boldsymbol{v} + \\ &\qquad \nabla_{\boldsymbol{q}}\mathtt{U}(\boldsymbol{z}+\boldsymbol{q}_d) + \boldsymbol{b}(\boldsymbol{v})] \end{aligned} \tag{3.28}$$

Since $C(\boldsymbol{z}+\boldsymbol{q}_d, 0) = 0$, $\nabla_{\boldsymbol{q}}\mathtt{U}(\boldsymbol{z}+\boldsymbol{q}_d) = \mathbf{0}$ and $\boldsymbol{b}(\mathbf{0}) = \mathbf{0}$, it follows that $(z, 0) = (0, 0)$ is an equilibrium point of the transformed system (3.28). To show that this equilibrium point is asymptotically stable, we use Lyapunov's second method. Consider the positive [2] definite Lyapunov function:

$$V(\boldsymbol{z}, \boldsymbol{v}) \triangleq \mathtt{U}(\boldsymbol{z}+\boldsymbol{q}_d) + \frac{1}{2}\boldsymbol{v}^T D(\boldsymbol{z}+\boldsymbol{q}_d)\boldsymbol{v} \tag{3.29}$$

The time derivative of V is given by:

$$\begin{aligned} \dot{V}(\boldsymbol{z}, \boldsymbol{v}) &= \boldsymbol{v}^T\nabla_{\boldsymbol{q}}\mathtt{U}(\boldsymbol{z}+\boldsymbol{q}_d) + \frac{1}{2}\boldsymbol{v}^T\dot{D}(\boldsymbol{z}+\boldsymbol{q}_d)\boldsymbol{v} + \boldsymbol{v}^T D(\boldsymbol{z}+\boldsymbol{q}_d)\dot{\boldsymbol{v}} \\ &= \boldsymbol{v}^T\nabla_{\boldsymbol{q}}\mathtt{U}(\boldsymbol{z}+\boldsymbol{q}_d) + \frac{1}{2}\boldsymbol{v}^T\dot{D}(\boldsymbol{z}+\boldsymbol{q}_d)\boldsymbol{v} - \boldsymbol{v}^T[\nabla_{\boldsymbol{q}}\mathtt{U}(\boldsymbol{z}+\boldsymbol{q}_d) + \\ &\quad K_2\boldsymbol{v} + C(\boldsymbol{z}+\boldsymbol{q}_d, \boldsymbol{v})\boldsymbol{v} + \boldsymbol{b}(\boldsymbol{v})] \\ &= \boldsymbol{v}^T\left[\frac{1}{2}\dot{D}(\boldsymbol{z}+\boldsymbol{q}_d) - C(\boldsymbol{z}+\boldsymbol{q}_d, \boldsymbol{v})\right]\boldsymbol{v} - \boldsymbol{v}^T[K_2\boldsymbol{v} + \boldsymbol{b}(\boldsymbol{v})] \end{aligned}$$

The right-hand side of this expression is actually identical to the right-hand side of (3.21), which means that in the same way we can prove that $\dot{V}(\boldsymbol{z}(t) +$

[2] Note that this function is positive definite because the second condition put on $\mathtt{U}(\boldsymbol{q})$.

$q_d, v(t)) \leq 0$ along solutions of (3.27). Hence, the first condition of proposition 3.2.1 is satisfied.
Since K_2 is positive-definite:

$$\begin{aligned} \dot{V}(z(t)+q_d, v(t)) \equiv 0 &\Rightarrow v(t) \equiv 0 \\ &\Rightarrow \dot{v}(t) \equiv 0 \\ &\Rightarrow D^{-1}(z(t)+q_d)\nabla_q \mathrm{U}(q) \equiv 0 \\ &\Rightarrow z(t) \equiv 0 \end{aligned} \tag{3.30}$$

since $D(z(t)+q_d)$ is positive definite. Using the second and third conditions put on $\mathrm{U}(q)$ we can deduce that $\nabla_q \mathrm{U}(q) = 0$ implies that $z(t) = 0$. Thus, also the second condition of proposition 3.2.1 is satisfied which means that the equilibrium point $(z, v) = (0, 0)$ is asymptotically stable. □

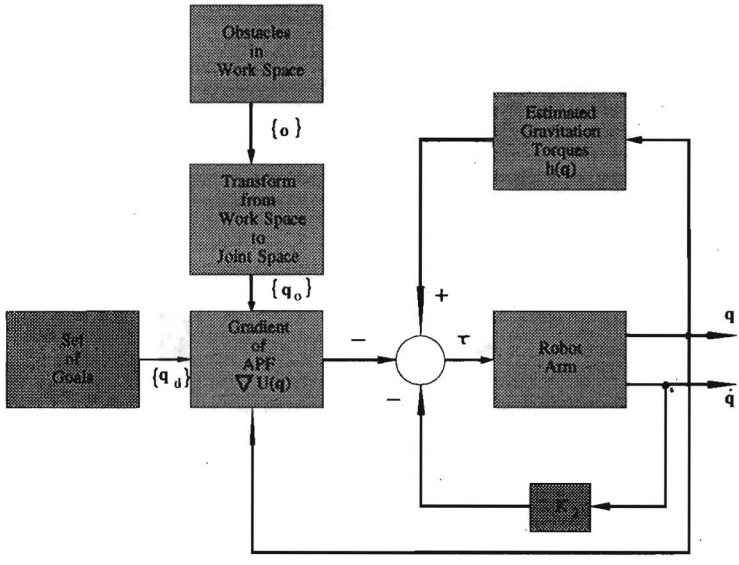

Figure 3.6: Block diagram of the controlled robot arm

In figure 3.2.3 the above mentioned control system is shown schematically.

Chapter 4

The Environment of the Robot

Before an artificial potential field can be constructed in the configuration space of the robot, information about the configurations where a collision occurs must be obtained. The physical (euclidean) space where the robot operates contains objects. Since these objects have to be avoided during execution of the motion of the robot, they will also be denoted as obstacles.

Motion planning is performed in this thesis in the configuration space of a robot. Therefore the configurations of the robot at which a part of the robot collides with a physical obstacle have to be calculated. These configurations will be called the configuration obstacles. Obviously, the calculation of the configuration obstacles depends on the geometry of the obstacles and on the geometry of the manipulator itself. Even for low-dimensional robots when the precise geometry of the robot and obstacles is taken into account, the calculation of the configuration obstacles can be extremely complicated. Therefore certain simplifications will be introduced concerning the modelling of the obstacles in the physical and configuration space of the robot and the geometry of the manipulator itself.

Even with the introduced simplifications it will be rather difficult to find a unified method to calculate the configuration obstacles, due to the variety of mechanical constructions of a manipulator. However, it is possible to find explicit expressions describing the configuration obstacles comparable to the solution of the inverse kinematics of the robot, though specific to the robot under consideration.

In this chapter we calculate the configuration obstacles for a specific robot

(the ASEA IRB-6) as an illustrative example of the method. Firstly, some simplifications concerning the spaces where a robot can be represented are given. Next a brief description of the kinematics of the robot is given which leads to the solution of the configuration obstacles.

4.1 Simplifications of the Physical and Configuration Space of a Robot

Obstacles in the environment of a robot can be seen as rigid bodies with arbitrary geometry, defined in the three (or two) dimensional euclidean space where the robot operates. In order to make a distinction with the work space of the robot, which also contains the orientation of the end-effector of the robot, we introduce the physical space of a robot. The euclidean space $\mathcal{P} \subset \mathcal{R}^k$ where a robot operates will be called the *physical space* of the robot. For robots operating on a plane $k = 2$ and accordingly for robots operating in a three dimensional space $k = 3$. The physical space of a robot is confined to the convex polyhedron in $\mathcal{R}^k$ of the following general form:

$$\mathcal{P} = \{ \boldsymbol{p} \in \mathcal{R}^k : \underline{p}_i \leq p_i \leq \bar{p}_i \} \tag{4.1}$$

where $\underline{p}_i$ and $\bar{p}_i$ denote the minimum and maximum values of the points which can be reached by at least one point of the manipulator.
When it should be possible to represent any arbitrary geometry of the obstacles, both the physical space $\mathcal{P}$ and the configuration space $\mathcal{Q}$ are represented by a regularly spaced grid. The physical space $\mathcal{P}$ is divided in $L \times \ldots \times L$ cells, as depicted in figure 4.1. The constant grid size of the i-th coordinate d_i can be calculated by

$$d_i = \frac{\bar{p}_i - \underline{p}_i}{L} \tag{4.2}$$

for $i = 1, \ldots, k$. An arbitrary point $\boldsymbol{p}$ is hardly ever exactly on a grid point. Instead of the actal coordinates of $\boldsymbol{p}$ the nearest grid point $\boldsymbol{k} \in \mathcal{P}^k$ is used, given by:

$$\boldsymbol{k} = \left((k_1 + \frac{1}{2}) d_1, \ldots, (k_k + \frac{1}{2}) d_k \right) \tag{4.3}$$

where $k_i \in \mathcal{Z}$, for $i = 1, \ldots, k$.
The configuration space $\mathcal{Q}$ is also divided into a grid of $M \times \ldots \times M$ cells, as depicted in figure 4.2. The constant grid size of the i-th coordinate D_i can be

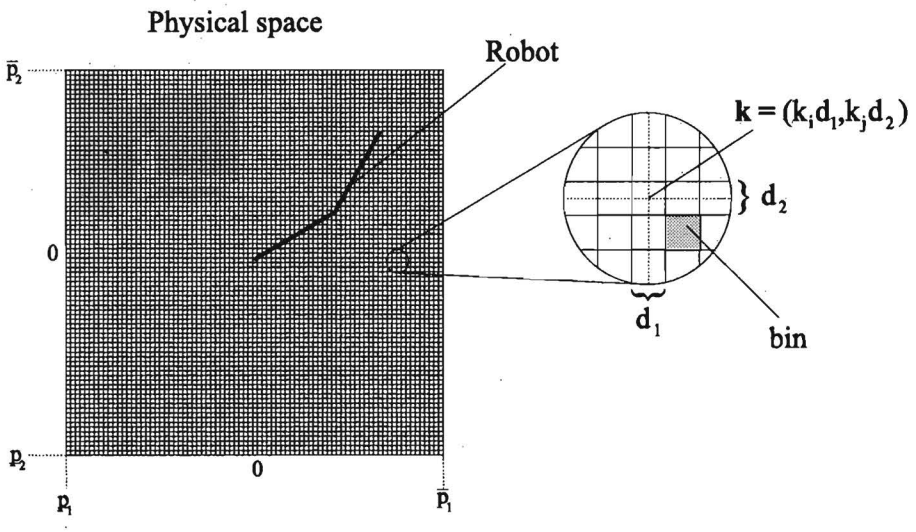

Figure 4.1: Grid representation of the physical space of a two-dimensional robot

calculated by

$$D_i = \frac{\bar{q}_i - \underline{q}_i}{M} \tag{4.4}$$

for $i = 1, \ldots, n$. Again instead of the actual point $\boldsymbol{q}$, the nearest grid point $\boldsymbol{m} \in \mathcal{Q}$ is used, given by:

$$\boldsymbol{m} = \left((m_1 + \frac{1}{2})D_1, \ldots, (m_n + \frac{1}{2})D_n \right) \tag{4.5}$$

where $m_i \in \mathcal{Z}$, for $i = 1, \ldots, n$.
Generally, a grid can be seen as an array of bins. The centre of a bin coincides with the grid point $\boldsymbol{k}$ or $\boldsymbol{m}$ as defined in respectively (4.3) and (4.5). The size of a bin is determined by the spacing of the grid respectively $d_1 \times \ldots \times d_k$ and $D_1 \times \ldots \times D_n$. The corresponding bin of a grid point $\boldsymbol{k}$ is defined as the hyper-volume around the grid point given by:

$$\mathcal{O}^{\mathcal{P}}_{\boldsymbol{k}} = \left\{ x \in \mathcal{P} : ||k_i + x_i|| \leq \frac{1}{2} d_i \, \forall i = 1 \ldots k \right\} \tag{4.6}$$

The next definition of an occupied grid point is going to be used in the definition of the problem of finding the configuration obstacles.

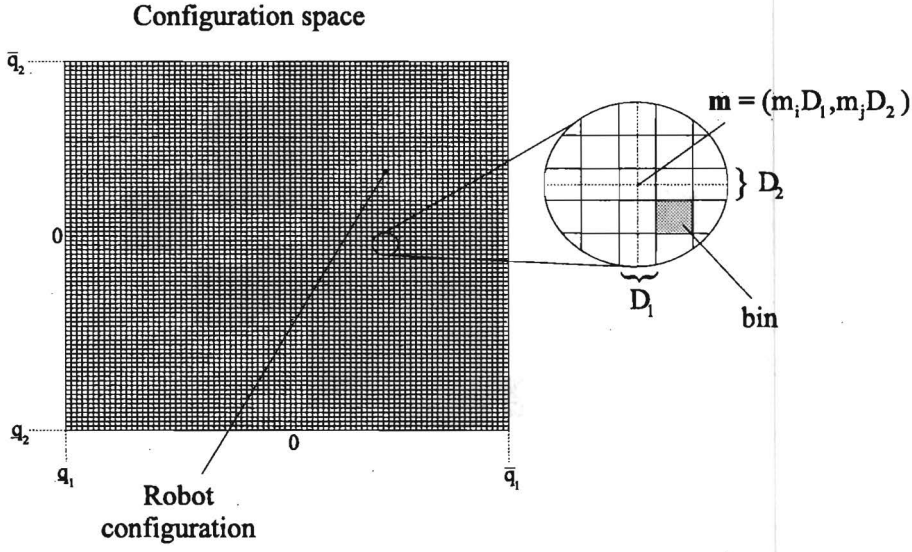

Figure 4.2: Grid representation of the configuration space of a two-dimensional robot

Occupied Grid Point *A grid point* $\boldsymbol{k}$ *of the physical space of a robot is said to be occupied, when at least one point inside the whole corresponding bin* $\mathcal{O}^{\mathcal{P}}_{\boldsymbol{k}}$ *is occupied by a point of an obstacle. The set* $\mathcal{K}$ *of all occupied grid points is called the set of the occupied grid points.*

Notice in the above definition that the set $\mathcal{K}$ is a denumberable set. Assuming that there are N_p occupied grid points [1] $\boldsymbol{k}_{n_p}$ with $n_p = 1 \ldots N_p$ in the physical space of a robot we define the set

$$\mathcal{O}^{\mathcal{P}} = \bigcup_{n_p=1}^{N_p} \mathcal{O}^{\mathcal{P}}_{\boldsymbol{k}_{n_p}} \tag{4.7}$$

of all bins corresponded to the occupied grid points $\boldsymbol{k}_{n_p} \in \mathcal{K}$. Notice that the set $\mathcal{O}^{\mathcal{P}} \subset \mathcal{P}$ is bounded and closed.
Mostly the robot arm is also simplified to a wire model as shown for example in figure 3.3. Each link of the robot is represented by a line segment connecting two sequential joints. We say that a collision occurs at a specific configuration of a robot when a point of the wire model of the robot touches at least one

[1] The scalar N_p is also the number of elements of the set $\mathcal{K}$.

occupied grid point of the physical space of the robot. As we will see, mostly there is more than one configurations where a collision occurs between the robot and a specific occupied grid point of the physical space of the robot.
The corresponding bin of a grid point $\boldsymbol{m}$ is defined as the hyper-volume around the grid point given by:

$$\mathcal{O}_{\boldsymbol{m}}^{\mathcal{Q}} = \left\{ \boldsymbol{q} \in \mathcal{Q} : ||m_i + q_i|| \leq \frac{1}{2} D_i \forall i = 1 \ldots n \right\} \tag{4.8}$$

Comparable to the term occupied grid point in the physical space of the robot, we introduce the term of the prohibited grid point in the configuration space.

Prohibited Grid Point *A grid point $\boldsymbol{m}$ of the configuration space of a robot is said to be prohibited, when on at least one configuration inside the whole corresponding bin $\mathcal{O}_{\boldsymbol{m}}^{\mathcal{Q}}$, a collision occurs between any point of the wire model of the robot and a occupied grid point of the physical space of the robot. The set $\mathcal{M}$ of all prohibited grid points is called the set of the prohibited grid points.*

Using the above given definitions we are able now to address the problem of finding the configuration obstacles, as follows. Given the set of all occupied grid points $\mathcal{K}$ in the physical space of a robot, find the set $\mathcal{M}$ of the prohibited grid points. Thereby the robot is completely described by means of its kinematics (actually the geometry of the robot wire model corresponding to a given configuration).
When the set $\mathcal{M}$ of the prohibited grid points is found we need to construct the set of the corresponding bins to the prohibited grid points. The set

$$\mathcal{O}^{\mathcal{Q}} = \bigcup_{n_q=1}^{N_q} \mathcal{O}_{\boldsymbol{m}_{n_q}}^{\mathcal{Q}} \, \forall \boldsymbol{m}_{n_q} \in \mathcal{M} \tag{4.9}$$

of all corresponding bins to the N_q prohibited grid points $\boldsymbol{m}_{n_q}$ of the configuration space of a robot is denoted by the term *configuration obstacles* and is a subset of the configuration space of the robot, hence $\mathcal{O}^{\mathcal{Q}} \subseteq \mathcal{Q}$.
An example of the problem of finding the configuration obstacles is given for a two-dimensional robot.

Example 4.1.1 *Given a planar RR robot with two links, as shown in figure 4.3(a). The length of the i-th link is denoted by l_i and the physical space of the robot $\mathcal{P} \subset \mathcal{R}^2$ is confined to the circle with radius equal to $l_1 + l_2$. Suppose that there is one occupied grid point $\boldsymbol{p} = (x_p, y_p)$ in the physical space of a robot. We want to find the configuration obstacles for this situation, which*

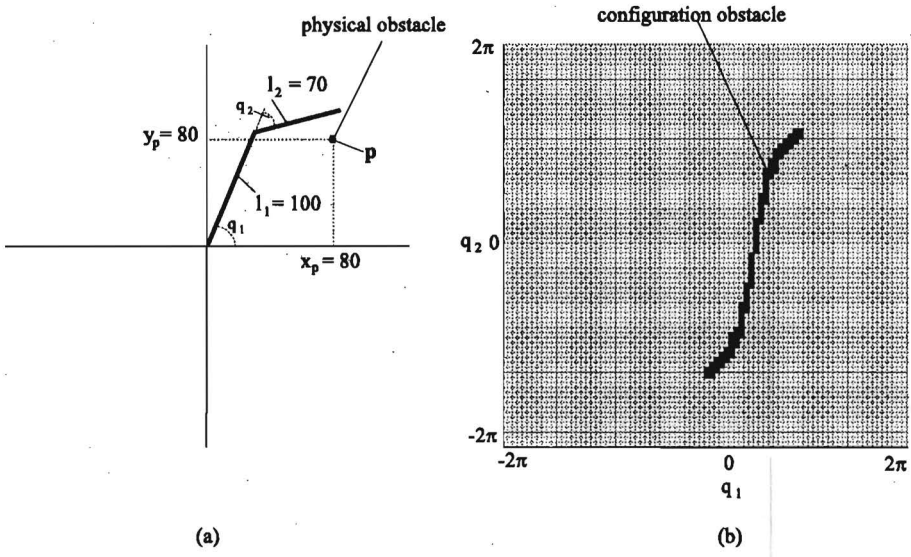

Figure 4.3: A point obstacle in the physical space of a robot on the plane and the corresponded configuration obstacles

means that we want to find all the set of prohibited configurations. A prohibited configuration is depicted for instance in figure 4.4.

Solution:
Using the cosines rule we obtain the following equations:

$$l_1^2 + r^2 + 2l_1 r\cos(q_1 - \theta_p) = s^2 \tag{4.10}$$

$$l_1^2 + s^2 - 2l_1 s\cos(q_2) = r^2 \tag{4.11}$$

where $r = |\boldsymbol{p}|$ *and* $\theta_p = \arctan(\frac{y_p}{x_p})$. *Equations 4.10 and 4.11 can be used to obtain the solution of the corresponding configuration obstacle.*

$$q_1 = \pm\arccos\left(\frac{s^2 - l_1^2 - r^2}{2l_1 r}\right) + \theta_p \tag{4.12}$$

$$q_2 = \mp\arccos\left(\frac{r^2 - l_1^2 - s^2}{2l_1 s}\right) \tag{4.13}$$

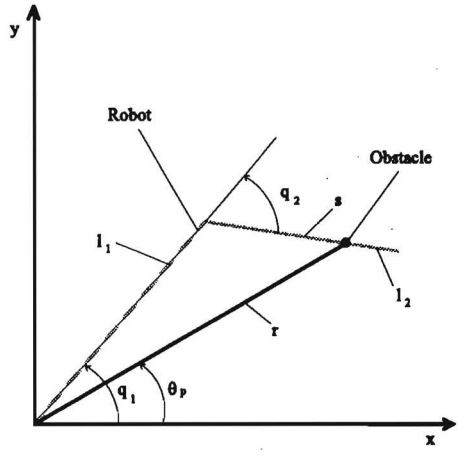

Figure 4.4: A prohibited configuration of a robot on the plane

Letting the parameter s take values from the interval $[|r - l_1|, \min(r + l_1, l_2)]$ *the prohibited grid points in the configuration space can be calculated, as depicted in figure 4.3(b).*

4.2 Robot Configuration Obstacles

In this section the solution of the problem of finding the configuration obstacles is examined. First we consider the general situation for an arbitrary robot. Next we consider a robot with five degrees of freedom, which is also used during the implementation of the method as explained in chapter 6.

4.2.1 Configuration Obstacles in n dimensions

As in the previous example we consider one occupied grid point $\boldsymbol{p} = (x_p, y_p, z_p)$ in the physical space of a robot. In addition we assume that the direct kinematics of the n-dimensional robot are given, as explained in section 3.1. We have determined a homogeneous transformation matrix ${}^{i-1}T_i(q_i)$ which relates the i-th and $(i-1)$-th link coordinate frames as follows:

$$ {}^{0}T_i(q_i) = \begin{bmatrix} \cos(q_i) & -\cos(\alpha_i)\sin(q_i) & \sin(\alpha_i)\sin(q_i) & a_i\cos(q_i) \\ \sin(q_i) & \cos(\alpha_i)\cos(q_i) & -\sin(\alpha_i)\cos(q_i) & a_i\sin(q_i) \\ 0 & \sin(\alpha_i) & \cos(\alpha_i) & d_i \\ 0 & 0 & 0 & 1 \end{bmatrix} $$

Comparable to the arm matrix defined in section 3.1 the i-th link coordinate frame in reference to the base coordinate frame can be expressed by the matrix ${}^0T_i(\boldsymbol{q})$, given by:

$$ {}^0T_i(\boldsymbol{q}) = \prod_{j=1}^{i} {}^{j-1}T_j(q_j) \tag{4.14} $$

We consider a point ${}^i\boldsymbol{p}_r$ at the i-th link of the robot, in reference to the i-th coordinate system. That point can be expressed in reference to the 0-th coordinate system by using the following equation:

$$ \begin{pmatrix} \boldsymbol{p}_r(\boldsymbol{q}) \\ 1 \end{pmatrix} = {}^0T_i(\boldsymbol{q}) \begin{pmatrix} {}^i\boldsymbol{p}_r \\ 1 \end{pmatrix} \tag{4.15} $$

According to the above definitions we reformulate the problem of finding the configuration obstacle for a given occupied point $\boldsymbol{p}$ in the physical space of a robot by:
Find the configurations $\boldsymbol{q}$ which satisfy the equations

$$ \boldsymbol{p}_r(\boldsymbol{q}) = \boldsymbol{p} \tag{4.16} $$

for all points $\boldsymbol{p}_r(\boldsymbol{q})$ on the wire model of the robot.
It appears that an explicit solution $\boldsymbol{q}_i(\boldsymbol{s})$ exists which depends on some parameters $\boldsymbol{s}$, corresponding to the i-th link of the robot. In the next section we consider the solution of this problem for a specific 5-dimensional robot.

4.2.2 ASEA-Irb6 and Configuration Obstacles

We consider a robot with five degrees of freedom depicted in figure 4.5(a). The corresponding wire model of this robot is given in figure 4.5(b). Considering just one occupied grid point of the physical space of the robot $\boldsymbol{p} = (x_p, y_p, z_p)$, we derive the corresponding configuration obstacles ${}^i\mathcal{O}^{\mathcal{Q}}$ related to the i-th link. Consequently, the total configuration obstacles is the union of the configuration obstacles related to each link, hence:

$$ \mathcal{O}^{\mathcal{Q}} = \bigcup_{i=1}^{5} {}^i\mathcal{O}^{\mathcal{Q}} \tag{4.17} $$

In the following equations the length of the i-th link of the robot is denoted by l_i. In addition the following variables are going to be often used as shown in figure 4.6. The angle

$$ \theta_p = \arctan\left(\frac{\sqrt{x_p^2 + y_p^2}}{z_p - l_1} \right) \tag{4.18} $$

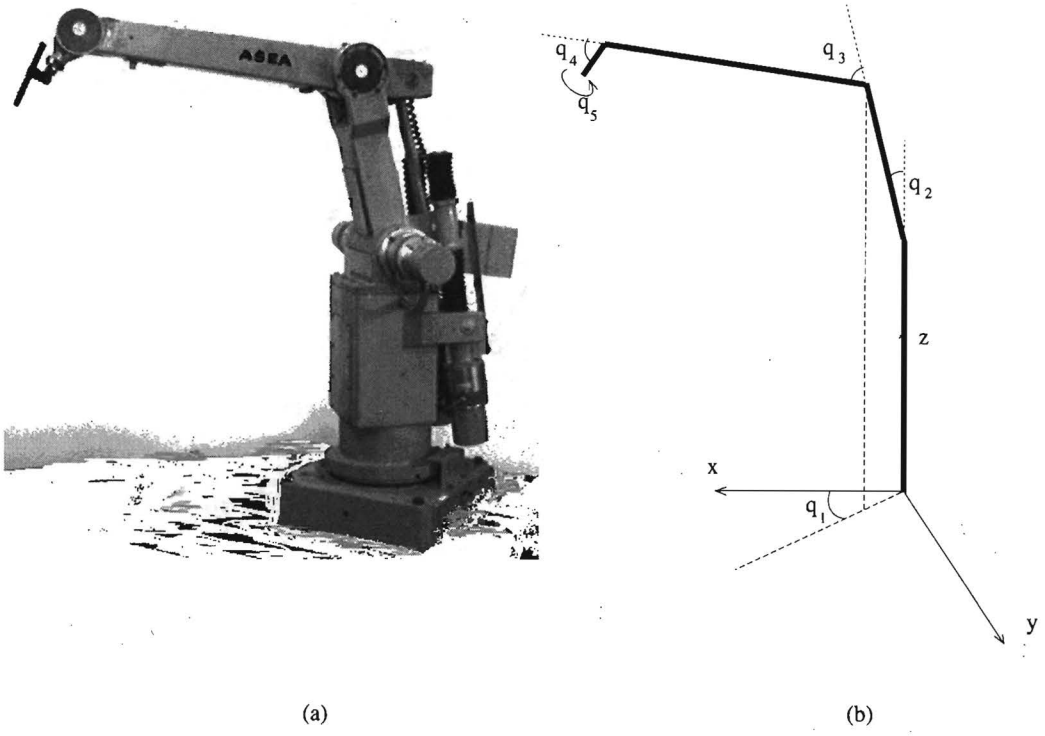

Figure 4.5: Wire model of a 5-DOF manipulator

the angle

$$\phi_p = \arctan\left(\frac{y_p}{x_p}\right) \tag{4.19}$$

and finally the length

$$r = \sqrt{p_x^2 + p_y^2 + (p_z - l_1)^2} \tag{4.20}$$

- **Link 1:** If $p_x = 0$ and $p_y = 0$ and $p_z \leq l_1$ then each configuration of the robot is prohibited, hence

$$^1\mathcal{O}^{\mathcal{Q}} = \bar{\mathcal{Q}} \tag{4.21}$$

otherwise the configuration obstacles related to the first link $^1\mathcal{O}^{\mathcal{Q}}$ is empty.

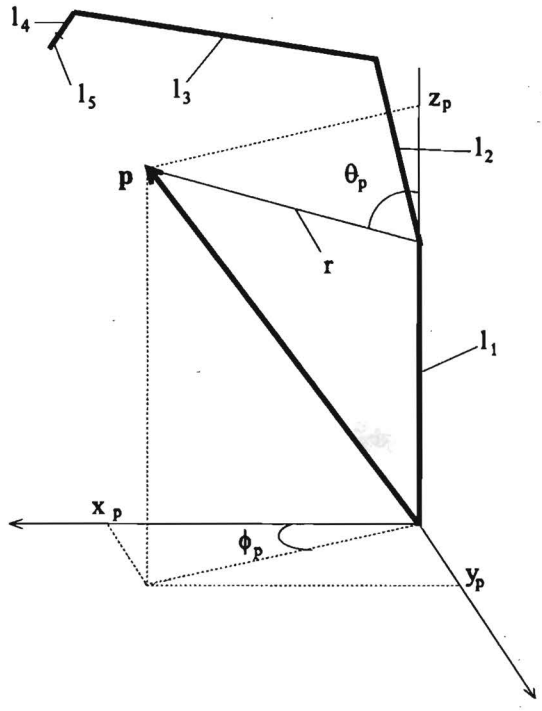

Figure 4.6: An point obstacle in the physical space of a robot

- **Link 2:** If $r \leq l_2$ then the point $\boldsymbol{p}$ can be reached by the second link of the robot and the corresponding configuration obstacles related to the second link are given by:

$$^2\mathcal{O}^{\mathcal{Q}} = \{ \boldsymbol{q} \in \mathcal{Q} : q_1 = \phi_p \text{ and } q_2 = \theta_p \} \tag{4.22}$$

otherwise the point $\boldsymbol{p}$ can not be reached by the second link, hence the configuration obstacles related to the second link $^2\mathcal{O}^{\mathcal{Q}}$ is empty.

- **Link 3:** The configuration obstacles related to the third link (Meyer 1988) is given by:

$$^3\mathcal{O}^{\mathcal{Q}} = {}^{+3}\mathcal{O}^{\mathcal{Q}} \bigcup {}^{-3}\mathcal{O}^{\mathcal{Q}} \tag{4.23}$$

where

$$^{+3}\mathcal{O}^{3}\mathcal{Q} = \left\{ \boldsymbol{q} \in \mathcal{Q} : q_1 = \phi_p, q_2 = \arccos\left(\frac{s^2 - l_2^2 - r^2}{2l_2 r}\right) + \theta_p \text{ and } q_3 = -\arccos\left(\frac{r^2 - l_1^2 - s^2}{2l_1 s}\right), \forall s \in [|r - l_2|, \min(r + l_2, l_3)] \right\} \quad (4.24)$$

and

$$^{-3}\mathcal{O}^{\mathcal{Q}} = \left\{ \boldsymbol{q} \in \mathcal{Q} : q_1 = \phi_p, q_2 = -\arccos\left(\frac{s^2 - l_2^2 - r^2}{2l_2 r}\right) + \theta_p \text{ and } q_3 = \arccos\left(\frac{r^2 - l_1^2 - s^2}{2l_1 s}\right), \forall s \in [|r - l_2|, \min(r + l_2, l_3)] \right\} \quad (4.25)$$

- **Link 4 and 5:** The configuration obstacles related to the fourth link is given by:

$$^{4}\mathcal{O}^{\mathcal{Q}} = {}^{++4}\mathcal{O}^{\mathcal{Q}} \bigcup {}^{+-4}\mathcal{O}^{\mathcal{Q}} \bigcup {}^{-+4}\mathcal{O}^{\mathcal{Q}} \bigcup {}^{--4}\mathcal{O}^{\mathcal{Q}} \quad (4.26)$$

where

$$\begin{aligned} {}^{++4}\mathcal{O}^{\mathcal{Q}} = \{ \boldsymbol{q} \in \mathcal{Q} : q_1 &= \phi_p, \\ q_2 &= \arccos\left(\frac{s_1^2 - l_2^2 - l_3^2}{2l_2 l_3}\right), \\ q_3 &= \arccos\left(\frac{l_3^2 - l_2^2 - s_1^2}{2l_2 s_1}\right) + \arccos\left(\frac{s_2^2 - s_1^2 - r^2}{2s_1 r}\right) + \theta_p, \\ q_4 &= \arccos\left(\frac{l_2^2 - l_3^2 - s_1^2}{2l_3 s_1}\right) + \arccos\left(\frac{r^2 - s_1^2 - s_2^2}{2s_1 s_2}\right) \\ \forall s_1 \in [|l_2 - l_3|, l_2 + l_3] \text{ and } \forall s_2 &\in [|r - s_1|, \min(r + s_1, l_4)] \}, \end{aligned} \quad (4.27)$$

$$\begin{aligned} {}^{+-4}\mathcal{O}^{\mathcal{Q}} = \{ \boldsymbol{q} \in \mathcal{Q} : q_1 &= \phi_p, \\ q_2 &= \arccos\left(\frac{s_1^2 - l_2^2 - l_3^2}{2l_2 l_3}\right), \\ q_3 &= \arccos\left(\frac{l_3^2 - l_2^2 - s_1^2}{2l_2 s_1}\right) + \arccos\left(\frac{s_2^2 - s_1^2 - r^2}{2s_1 r}\right) + \theta_p, \\ q_4 &= -\arccos\left(\frac{l_2^2 - l_3^2 - s_1^2}{2l_3 s_1}\right) - \arccos\left(\frac{r^2 - s_1^2 - s_2^2}{2s_1 s_2}\right) \\ \forall s_1 \in [|l_2 - l_3|, l_2 + l_3] \text{ and } \forall s_2 &\in [|r - s_1|, \min(r + s_1, l_4)] \}, \end{aligned} \quad (4.28)$$

$$
\begin{aligned}
{}^{-+4}\mathcal{O}^{\mathcal{Q}} = \{ q \in \mathcal{Q} : q_1 &= \phi_p, \\
q_2 &= \arccos\left(\frac{s_1^2 - l_2^2 - l_3^2}{2l_2l_3}\right), \\
q_3 = -\arccos\left(\frac{l_3^2 - l_2^2 - s_1^2}{2l_2s_1}\right) &- \arccos\left(\frac{s_2^2 - s_1^2 - r^2}{2s_1r}\right) + \theta_p, \\
q_4 = \arccos\left(\frac{l_2^2 - l_3^2 - s_1^2}{2l_3s_1}\right) &+ \arccos\left(\frac{r^2 - s_1^2 - s_2^2}{2s_1s_2}\right) \\
\forall\, s_1 \in [|l_2 - l_3|, l_2 + l_3] \text{ and } \forall\, s_2 &\in [|r - s_1|, \min(r + s_1, l_4)] \}, \quad (4.29)
\end{aligned}
$$

and

$$
\begin{aligned}
{}^{--4}\mathcal{O}^{\mathcal{Q}} = \{ q \in \mathcal{Q} : q_1 &= \phi_p, \\
q_2 &= \arccos\left(\frac{s_1^2 - l_2^2 - l_3^2}{2l_2l_3}\right), \\
q_3 = -\arccos\left(\frac{l_3^2 - l_2^2 - s_1^2}{2l_2s_1}\right) &- \arccos\left(\frac{s_2^2 - s_1^2 - r^2}{2s_1r}\right) + \theta_p, \\
q_4 = -\arccos\left(\frac{l_2^2 - l_3^2 - s_1^2}{2l_3s_1}\right) &- \arccos\left(\frac{r^2 - s_1^2 - s_2^2}{2s_1s_2}\right) \\
\forall\, s_1 \in [|l_2 - l_3|, l_2 + l_3] \text{ and } \forall\, s_2 &\in [|r - s_1|, \min(r + s_1, l_4)] \} \quad (4.30)
\end{aligned}
$$

When also the 5-th link is taken into consideration, the situation does not substantially change. In that case, the above equations can be used with $l_4 + l_5$ instead l_4, due to the fact that the fourth and fifth link can be seen as one link with length $l_4 + l_5$.

Chapter 5

Artificial Potential Fields

Before we give an exact description of a potential field, we first elucidate the notion of potential fields and the way they can be used for robot motion planning, through an illustrative metaphor.
Suppose we face the situation as depicted in figure 5.1(a). On a plane where obstacles are present (vertical sticks in the figure), we want to drive a marble to a destination point (dot point) without colliding with the obstacles. By

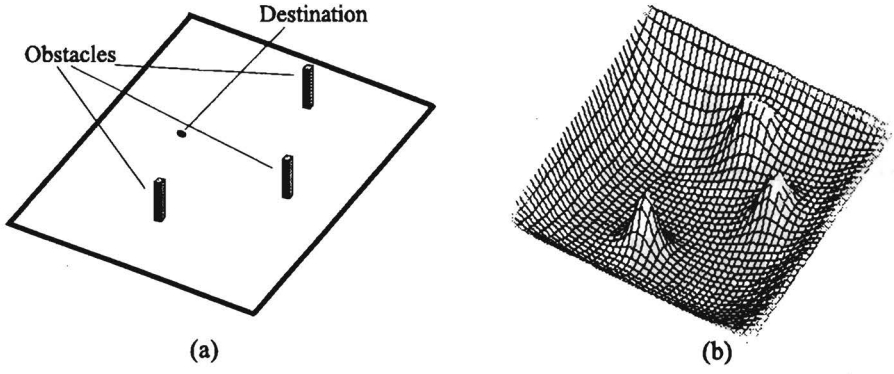

Figure 5.1: An example of an Artificial Potential Field

stretching a rubber sheet along the whole plane, the obstacle-sticks enforce the sheet to form little heightenings whereas a nail keeps the sheet fixed at the plane at the destination point. By doing this, we create the situation drawn in figure 5.1(b). In addition extra obstacles have been introduced at the edges of

the plane to ensure that the marble is going to remain inside the plane. In this example it is obvious that from any beginning point we can let the marble roll down to the destination point, avoiding collisions to any obstacle.
Nevertheless, this example is very specific and it will give a solution in any given situation unless certain condition are satisfied related to the plane, the obstacles, the destination point and the rubber sheet.
When the plane of the example represents the joint space of a robot, it is easy to see the correspondence of the marble to the robot. The height of the rubber sheet represents the potential field used to guide the robot (marble) to a goal configuration (the destination point) independently of its initial configuration.

An *Artificial Potential Field* (APF) is a scalar function defined at each point of the joint space of the robot. Two major issues are important. Namely, we have to avoid collisions with the obstacles and a goal configuration has to be reached from any initial configuration when it is possible. That means that the APF has to attain its maximum values at the obstacles and no other wells must occur except at the goal configuration(s).
The idea behind the usage of artificial potential fields in robot motion planning is based on the fact that the negative gradient of a potential field points to the direction of maximum decrease (steepest descent) of the potential field. That means that when the negative gradient of the potential field is followed, a minimum of the potential field will be reached. However certain conditions have to be satisfied to ensure for example that the minimum reached is indeed a goal configuration (and not another minimum, mostly called a local minimum); and no collisions with obstacles occur. In figure 5.2(a) a comparable situation as the previous example is drawn where local minima are present. Apparently, starting at certain points the destination point it will not be reached, but rather the local minimum as depicted in figure 5.2(b). Still, many questions arise such as: does such a potential field exists and how can we construct such a field? For existence and construction of the APF, harmonic functions can be used which have been extensively analysed in the framework of the so-called potential theory. Harmonic functions have already being proposed in robot motion planning (Connolly 1992; Kim and Khosla 1992; Connolly 1990). Many physical phenomena can be modelled by harmonic functions like temperature flow, pressure and electrical fields. For instance temperature flow does not exhibit local minima as it will be illustrated by the following fact. Considering a building (with insulated walls) where even using only one heating element, it is possible to ever warm every room up, independently of the structure of the building.
However, finding an harmonic function satisfying the applied constraints appears a rather hard problem. In this thesis, a solution is formulated, utilizing the *Boundary Element Method.*

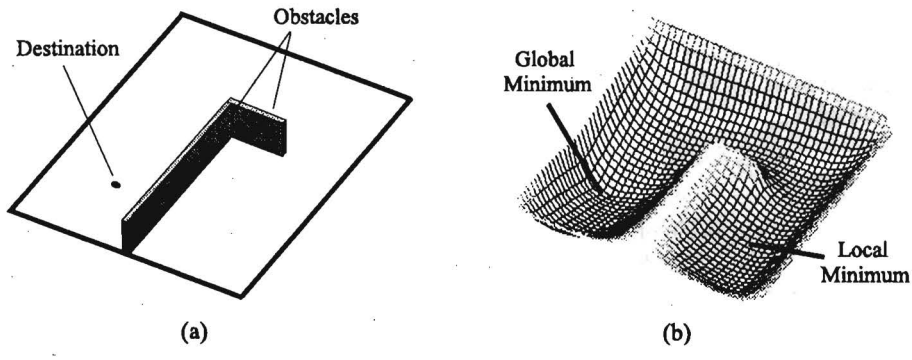

Figure 5.2: An example of a field with local minima

The Boundary Element Method (BEM) is a technique ideally suited to the solution of many two- and three-dimensional problems in potential theory. The theory concerning the BEM will be extensively discussed, related with the specific problem of finding a potential field for robot motion planning. We conclude the chapter with an elaborate example of finding a potential field in a two-dimensional space, to make the method more accessible.

5.1 APF definitions and requirements

Generally, a scalar field is a function $\mathtt{V}$ which associates a scalar, a real number, with each point in a subspace Ω. Because the scalar fields used in the current treatment can be seen as representation of potential energy added to the robot, we employ here the term *potential field* to denote a scalar field. However, the potential fields constructed are merely fictitious potential fields modelled in a computer, that is why the term *artificial potential fields* has been introduced. An artificial potential field is defined as:

Artificial Potential Field. *A scalar function* $\mathtt{V}(\boldsymbol{x}) : \Omega \rightarrow \mathcal{R}$ *is an Artificial Potential Field defined at each point* $\boldsymbol{x} \in \Omega$, *where* Ω *is a subset of* $\mathcal{R}^m$.

The gradient $\nabla_{\boldsymbol{x}}\mathtt{V}$ defined as:

$$\nabla_{\boldsymbol{x}}\mathtt{V}(\boldsymbol{x}) = \left(\frac{\partial \mathtt{V}}{\partial x_1}, \frac{\partial \mathtt{V}}{\partial x_2}, \cdots, \frac{\partial \mathtt{V}}{\partial x_m} \right)^T \tag{5.1}$$

determines a vector field in Ω. By definition, a potential field $\mathtt{V}(\boldsymbol{x})$ has a *global minimum* in Ω at a point $\boldsymbol{x}_0$ if $\mathtt{V}(\boldsymbol{x}) \geq \mathtt{V}(\boldsymbol{x}_0)$ for all $\boldsymbol{x}$ in Ω. Similarly, $\mathtt{V}(\boldsymbol{x})$

has a *global maximum* at $\boldsymbol{x}_0$ if $\mathtt{V}(\boldsymbol{x}) \leq \mathtt{V}(\boldsymbol{x}_0)$ for all $\boldsymbol{x}$ in Ω. Minima and maxima together are called extrema. Furthermore, $\mathtt{V}(\boldsymbol{x})$ is said to have a *local minimum* at $\boldsymbol{x}_0$ if $\mathtt{V}(\boldsymbol{x}) \geq \mathtt{V}(\boldsymbol{x}_0)$ for all $\boldsymbol{x}$ in a neighbourhood of $\boldsymbol{x}_0$, say, for all $\boldsymbol{x}$ satisfying

$$|\boldsymbol{x} - \boldsymbol{x}_0| < \epsilon \tag{5.2}$$

where $\epsilon > 0$ is sufficiently small. A *local maximum* is defined similarly.
If $\mathtt{V}(\boldsymbol{x})$ is differentiable and has an extremum at a point $\boldsymbol{x}_0$ in the interior of Ω, then the gradient $\nabla\mathtt{V}(\boldsymbol{x})$ vanishes at that point. The points where the gradient of the potential field $\mathtt{V}(\boldsymbol{x})$ vanishes are called stationary points. A way to examine the nature of a stationary point of a potential field is based on the Hessian matrix of the potential field, defined as:

$$H(\boldsymbol{x}) = \begin{bmatrix} \frac{\partial^2 \mathtt{V}}{\partial x_1 \partial x_1} & \frac{\partial^2 \mathtt{V}}{\partial x_2 \partial x_1} & \cdots & \frac{\partial^2 \mathtt{V}}{\partial x_m \partial x_1} \\ \frac{\partial^2 \mathtt{V}}{\partial x_1 \partial x_2} & \frac{\partial^2 \mathtt{V}}{\partial x_2 \partial x_2} & \cdots & \frac{\partial^2 \mathtt{V}}{\partial x_m \partial x_2} \\ \vdots & \vdots & \ddots & \vdots \\ \frac{\partial^2 \mathtt{V}}{\partial x_1 \partial x_m} & \frac{\partial^2 \mathtt{V}}{\partial x_2 \partial x_m} & \cdots & \frac{\partial^2 \mathtt{V}}{\partial x_m \partial x_m} \end{bmatrix} \tag{5.3}$$

When the eigenvalues of the Hessian $H(\boldsymbol{x})$ of a potential field $\mathtt{V}(\boldsymbol{x})$ at a stationary point $\boldsymbol{x}_0$ are:

- all negative then $\mathtt{V}$ has a maximum at $\boldsymbol{x}_0$;
- all positive then $\mathtt{V}$ has a minimum at $\boldsymbol{x}_0$;
- both positive and negative then $\mathtt{V}$ has a saddle point at $\boldsymbol{x}_0$.

When a potential field is not constant, it can only exhibit extrema or saddles at stationary points. Saddles denote stationary points which are not extrema. In figure 5.1 different stationary points are depicted in a two-dimensional region. In addition the corresponding level curves are drawn.
Level curves are the special case of the *level set* of a potential field. The level set $\mathcal{L}(c)$ of a potential field $\mathtt{V}(\boldsymbol{x})$ is defined as:

$$\mathcal{L}(c) = \{\boldsymbol{x} | \boldsymbol{x} \in \Omega \text{ and } \mathtt{V}(\boldsymbol{x}) = c\} \tag{5.4}$$

When $\Omega \subset \mathcal{R}^2$, the level set $\mathcal{L}(c)$ is called a *level curve*; and when $\Omega \subset \mathcal{R}^3$, it is called a *level surface*. Sometimes some other terms are used denoting level sets depending on the kind of the scalar field under consideration. For example for a temperature field the term *isotherms* is used and for potential fields the term *isopotentials*. Visualizing the level set $\mathcal{L}(c)$ of a potential field for different values of the varialbe c can give a good impression of the potential field itself

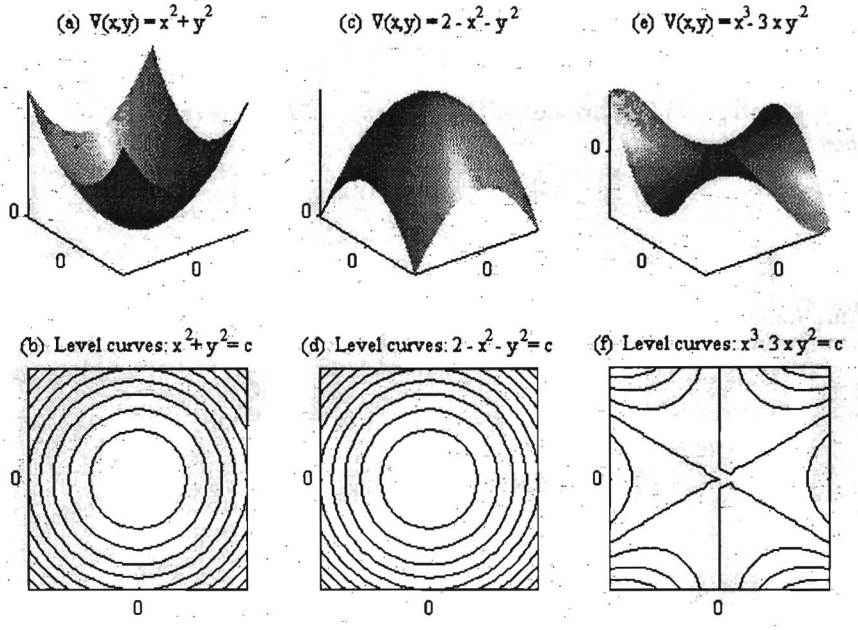

Figure 5.3: Stationary points

and its gradient. That can be concluded considering an arbitrary level set $\mathcal{L}(\hat{c})$ for a given $c = \hat{c}$. Given a point $\boldsymbol{a} \in \mathcal{L}(\hat{c})$, the gradient $\nabla V(\boldsymbol{a})$ at that point $\boldsymbol{a}$ is normal to the level set $\mathcal{L}(\hat{c})$ (Apostol 1967).

The negative gradient of the potential field points to the direction of maximum decrease (steepest descent) of the potential field. That means that when we follow the negative gradient of a potential field that does not exhibit local minima, we are "mostly" able to reach its global minimum. Even there are no local minima, following the negative gradient of the potential field, a saddle point can be reached where the gradient vanishes. Fortunately, it is possible to proceed following the negative gradient of the potential field starting at a point in the neighbourhood of the saddle point.

On the basis of the control strategy discussed in chapter 3, equation (3.26) the gradient of such a potential field can be used in the control feedback aiming two goals. Firstly, to reach any goal configuration $\boldsymbol{q} \in \mathcal{G}$ and secondly to avoid collisions with the obstacles in the environment of the robot. Consequently, the designed potential field depends on the set of goal configurations $\mathcal{G}$ and the geometry of the objects in the environment of the robot $\mathcal{O}$.

The APF is defined in the operational joint space $\mathcal{Q}$ excluding configurations

occupied by the goal configurations $\mathcal{G}$ and the obstacles $\mathcal{O}$. Accordingly, we define the *free configuration space* of the robot as follows.

Free Configuration Space *The free configuration space of the robot is the open set $\mathcal{F}$ defined as:*

$$\mathcal{F} = \{\boldsymbol{q} \in \mathcal{Q} : \boldsymbol{q} \notin \mathcal{G} \wedge \boldsymbol{q} \notin \mathcal{O}\} \tag{5.5}$$

Consequently, holds that:

$$\mathcal{Q} = \mathcal{F} \cup \mathcal{G} \cup \mathcal{O} \tag{5.6}$$

and by defining the *obstacle boundary* $\Gamma_o = \partial\mathcal{Q} \cup \partial\mathcal{O}$ and the *goal boundary* $\Gamma_d = \partial\mathcal{G}$, it follows that:

$$\partial\mathcal{F} = \Gamma_o \cup \Gamma_d \tag{5.7}$$

where $\partial\Omega$ of a set Ω denotes the boundary of the set.
The problem faced here can be formulated as follows:
Find an APF $\mathtt{U}(\boldsymbol{q}) : \mathcal{F} \rightarrow \mathcal{R}$ which attains its maximum value c_o at the obstacle boundary Γ_o and vanishes at the goal configurations boundary Γ_d. In addition it does not have any local minima in the free configuration space $\mathcal{F}$.
Using the Hessian matrix to examine the stationary points of a potential field can be rather complicated. Therefore, we introduce the harmonic functions which inherently do not exhibit any local minima in the region defined. Requiring that the APF is a harmonic function defined in the free configuration space of the robot, guarantees that no local minima occur. The next step is to find a harmonic function which meets the conditions related to the boundaries Γ_o and Γ_d.

5.2 Harmonic Functions

Harmonic functions are scalar functions defined on open subsets of real Euclidean spaces. Let Ω be an open, non-empty subset of $\mathcal{R}^m$. A twice continuously differentiable, function $\mathtt{V}$ defined on Ω is *harmonic* on Ω if

$$\triangle \mathtt{V} = \frac{\partial^2 \mathtt{V}}{\partial x_1^2} + \frac{\partial^2 \mathtt{V}}{\partial x_2^2} + \cdots + \frac{\partial^2 \mathtt{V}}{\partial x_m^2} \equiv 0 \tag{5.8}$$

The operator $\triangle$ is called the*Laplacian* and equation (5.8) is called the *Laplace's equation*. Notice that the operator $\triangle$ is equivalent to the divergence of the gradient $(\nabla \cdot \nabla)$, sometimes denoted by the operator ∇^2.

We can show that a harmonic function defined in an open set Ω, does not contain local minima in Ω. Therefore, the next theorem is used.

Theorem 5.2.1 Maximum Principle *(Axler, Bourdon and Ramey 1992). Let Ω be a connected set, and let $\mathtt{V}$ be a harmonic and real-valued function on Ω. If $\mathtt{V}$ has either a minimum or a maximum in Ω, then $\mathtt{V}$ is constant.*

The proof is given in (Axler, Bourdon and Ramey 1992) p. 6. According to this theorem a harmonic function which is not constant has no local minima or maxima in Ω. Its minima or maxima occur actually at the boundary of Ω as the next corollary states.

Corollary 5.2.1 *Suppose Ω is bounded and $\mathtt{V}$ is a continuous real-valued function on $\partial\Omega$ that is harmonic on Ω. Then $\mathtt{V}$ attains its maximum and minimum value over $\bar{\Omega}$ on $\partial\Omega$.* [1]

The proof is given in (Axler, Bourdon and Ramey 1992) p. 7.
A simple example of a harmonic function in $\mathcal{R}^n \setminus \{0\}$ for $n = 2$ is

$$\mathtt{V}(\boldsymbol{x}) = \log\left(\frac{1}{|\boldsymbol{x}|}\right) \tag{5.9}$$

and for $n > 2$ is

$$\mathtt{V}(\boldsymbol{x}) = |\boldsymbol{x}|^{2-n} \tag{5.10}$$

5.3 The Boundary Element Method

As it stated before, potential theory examines the solutions of the Laplace equation (5.8) when certain boundary conditions have to be met. The solution of the Laplace equation is actually a special case of the so-called *boundary value problems*. Boundary value problems are problems involving a partial differential equation which is applicable over a region $\Omega \subset \mathcal{R}^m$ enclosed by the boundary Γ, as shown in figure 5.4. For example the following differential equation (known as the Poisson's equation) represents a boundary value problem:

$$\left(\frac{\partial^2}{\partial x_1^2} + \frac{\partial^2}{\partial x_2^2} + \cdots + \frac{\partial^2}{\partial x_m^2}\right)\phi(\boldsymbol{x}) = f(\boldsymbol{x}) \tag{5.11}$$

where $\phi(\boldsymbol{x})$ is the unknown function to be determined and $f(\boldsymbol{x})$ is a given function applicable over Ω. The unknown potential field $\phi(\boldsymbol{x}) : \Omega \rightarrow \mathcal{R}$ at

[1] Suppose an open set Ω, then $\partial\Omega$ denotes the boundary of Ω and $\bar{\Omega}$ denotes closure of Ω, thus $\bar{\Omega} = \Omega \cap \partial\Omega$.

each point $\boldsymbol{x} = (x_1, x_2, \cdots, x_m) \in \Omega$ has to attain certain values over the boundary $\Gamma = \partial\Omega$. To be able to obtain a unique solution for any differential equation we have to specify some 'boundary conditions', which the unknown function $\phi(\boldsymbol{x})$ have to satisfy over the boundary Γ.
Among others, two kinds of boundary conditions can be formulated (figure 5.4).

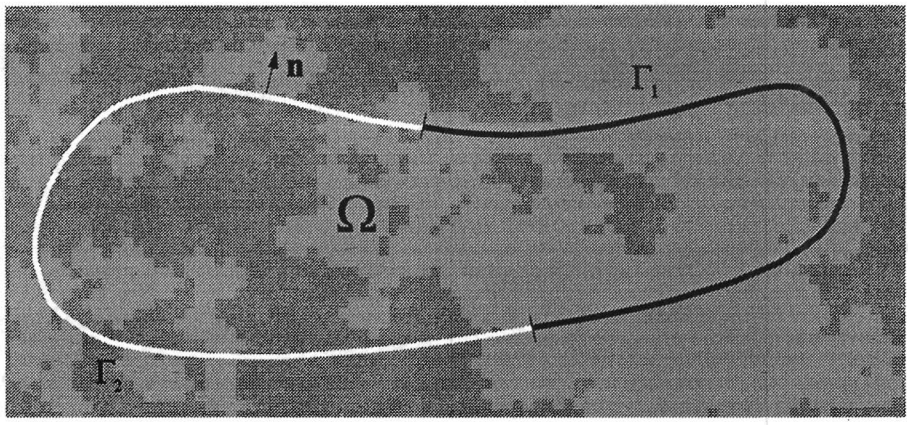

Figure 5.4: Boundary conditions related to potential problems

1. Conditions related to the value of $\phi(\boldsymbol{x})$ over a part of the boundary Γ, say Γ_1, as

$$\phi = \bar{\phi} \qquad \text{on} \quad \Gamma_1 \tag{5.12}$$

where $\bar{\phi}$ is a known quantity. This kind of conditions is also called the *Dirichlet type.*

2. Conditions related to the directional derivative of $\phi(\boldsymbol{x})$ over a part of the boundary Γ, say Γ_2, as

$$\frac{\partial\phi(\boldsymbol{x})}{\partial n} = \bar{\nu} \qquad \text{on} \quad \Gamma_2 \tag{5.13}$$

with $\partial\phi/\partial n$ the directional derivative of the function ϕ on Γ_2. The directional derivative $\partial\phi/\partial n$ of ϕ is defined by the equation:

$$\frac{\partial\phi}{\partial n} = \nabla\phi(\boldsymbol{x}) \cdot \boldsymbol{n} \tag{5.14}$$

where $\boldsymbol{n}$ denotes the outward unit normal on Γ_2. This kind of boundary conditions are denoted as the *Neumann type.*

A method to find a solution of boundary value problems is called the *Boundary Element Method* (BEM). The BEM has already been used for the solution of potential problems (Becker 1992; Brebbia 1980; and Brebbia 1977). The boundary element method is based on certain integral representation such as the Green's theorem, to reduce the dimensionality of the problem by one, i.e. transform the problem from the region Ω into the boundary Γ. The Green's theorem will be recalled in the following section before the BEM will be examined.
Next, the boundary elements method is investigated first when the region Ω is a subset of $\mathcal{R}^2$, and thereafter the general situation where Ω is a subset of $\mathcal{R}^m$ is considered.

5.3.1 Green's theorems

Green's theorem in the plane

Consider a bounded area $\Omega \subset \mathcal{R}^2$, enclosed by a piecewise smooth curve Γ. Suppose two potential fields $\phi(\boldsymbol{x})$ and $\psi(\boldsymbol{x})$ defined in Ω have continuous first and second derivatives with respect to the coordinates x_1 and x_2, where $\boldsymbol{x} = (x_1, x_2) \in \Omega$. The following theorem establishes a transformation of the variables ϕ and ψ between the area Ω and the curve Γ.

Theorem 5.3.1 Green's second identity *(two dimensions (Apostol 1967)). Let Ω be a compact subset of $\mathcal{R}^2$ with $\boldsymbol{n}$ the outward unit normal on $\partial\Omega$. Let $\phi(\boldsymbol{x})$ and $\psi(\boldsymbol{x})$ be two scalar fields on Ω. Denote the volume element of Ω by $d\omega_2$, and that of $\partial\Omega$ by $d\omega_1$. Then*

$$\int_{\Omega} (\phi \nabla^2 \psi - \psi \nabla^2 \phi) d\omega_2 = \int_{\partial\Omega} \left(\phi \frac{\partial \psi}{\partial n} - \psi \frac{\partial \phi}{\partial n} \right) d\omega_1 \tag{5.15}$$

Green's theorem in higher dimensions

Generally, the Green's theorem appears connecting variables defined in a plane or a volume. However, it is possible to extend it for higher dimensions as it will be shown. First, the formulation of the so-called *divergence theorem* is given. This theorem involves the divergence of a vector field $\boldsymbol{f}(\boldsymbol{x}) = (f_1(\boldsymbol{x}), f_2(\boldsymbol{x}), \ldots, f_m(\boldsymbol{x}))$ with $f_i(\boldsymbol{x})$ a scalar field in $\Omega \subset \mathcal{R}^m$ as

$$\nabla \cdot \boldsymbol{f}(\boldsymbol{x}) = \frac{\partial f_1}{\partial x_1} + \frac{\partial f_2}{\partial x_2} + \ldots + \frac{\partial f_m}{\partial x_m} \tag{5.16}$$

where $\boldsymbol{f}(\boldsymbol{x}) \in \mathcal{R}^m$ and $\boldsymbol{x} = (x_1, x_2, \cdots, x_m) \in \Omega$. The divergence theorem (Spivak 1979) is formulated as follows.

Theorem 5.3.2 *Let Ω be a compact subset of $\mathcal{R}^m$ with $\boldsymbol{n}$ the outward unit normal on $\partial\Omega$. Let $\boldsymbol{f}(\boldsymbol{x})$ be a vector field on Ω. Denote the volume element of Ω by $d\omega_m$, and that of $\partial\Omega$ by $d\omega_{m-1}$. Then*

$$\int_{\Omega} \nabla \cdot \boldsymbol{f}(\boldsymbol{x}) d\omega_m = \int_{\partial\Omega} (\boldsymbol{f}, \boldsymbol{n}) d\omega_{m-1} \tag{5.17}$$

Using the divergence theorem, we can prove the next theorem which is the extension of Green's second identity in higher dimensions than two.

Theorem 5.3.3 Green's second identity *(higher dimensions). Let Ω be a compact subset of $\mathcal{R}^m$ with $\boldsymbol{n}$ the outward unit normal on $\partial\Omega$. Let $\phi(\boldsymbol{x})$ and $\psi(\boldsymbol{x})$ be two scalar fields on Ω. Denote the volume element of Ω by $d\omega_m$, and that of $\partial\Omega$ by $d\omega_{m-1}$. Then*

$$\int_{\Omega} (\phi \nabla^2 \psi - \psi \nabla^2 \phi) d\omega_m = \int_{\partial\Omega} \left(\phi \frac{\partial \psi}{\partial n} - \psi \frac{\partial \phi}{\partial n} \right) d\omega_{m-1} \tag{5.18}$$

Proof: Suppose two potential fields $\phi(\boldsymbol{x})$ and $\psi(\boldsymbol{x})$ defined in Ω have continuous first derivatives with respect to the coordinates x_i with $i = 1 \ldots m$. We define a vector field $\boldsymbol{f}(\boldsymbol{x})$ by:

$$\boldsymbol{f}(\boldsymbol{x}) = \phi(\boldsymbol{x}) \nabla \psi(\boldsymbol{x}) \tag{5.19}$$

Substituting the vector field $\boldsymbol{f}(\boldsymbol{x})$ in (5.17) we obtain:

$$\int_{\Omega} \left((\nabla \psi(\boldsymbol{x}), \nabla \phi(\boldsymbol{x})) + \phi \nabla^2 \psi \right) d\omega_m = \int_{\partial\Omega} \phi \frac{\partial \psi}{\partial n} d\omega_{m-1} \tag{5.20}$$

We define the vector field $\boldsymbol{f}(\boldsymbol{x})$ by:

$$\boldsymbol{f}(\boldsymbol{x}) = \psi(\boldsymbol{x}) \nabla \phi(\boldsymbol{x}) \tag{5.21}$$

From (5.17) we obtain:

$$\int_{\Omega} \left((\nabla \phi(\boldsymbol{x}), \nabla \psi(\boldsymbol{x})) + \psi \nabla^2 \phi \right) d\omega_m = \int_{\partial\Omega} \psi \frac{\partial \phi}{\partial n} d\omega_{m-1} \tag{5.22}$$

Subtracting (5.20) and (5.22) we obtain (5.18).
□

5.3.2 Boundary Element Method in Potential Problems

Recall that the problem faced here can be formulated as follows:
Given a compact domain $\Omega \subset \mathcal{R}^m$, find a potential field $\phi(\boldsymbol{x})$, which is harmonic in Ω and satisfies the given Dirichlet conditions $\phi = \bar{\phi}$ on the boundary $\Gamma = \partial\Omega$ of the domain Ω.

Starting with Green's second identity, we state that $\phi(\boldsymbol{x})$ is the unknown potential field and $\psi(\boldsymbol{x})$ is the solution of the following equation:

$$\nabla^2\psi(\boldsymbol{x}) + \delta(\boldsymbol{x} - \boldsymbol{x}_i) = 0 \tag{5.23}$$

where δ is the Dirac delta function. This solution is also called the *fundamental solution*. In the two dimensional case ($m = 2$) the fundamental solution is given (Brebbia 1980) by:

$$\psi_i(\boldsymbol{x}) = \frac{1}{2\pi}\log\left(\frac{1}{|\boldsymbol{x} - \boldsymbol{x}_i|}\right) \tag{5.24}$$

For higher dimensions ($m > 2$) the fundamental solution is given by:

$$\psi_i(\boldsymbol{x}) = \frac{1}{4\pi|\boldsymbol{x} - \boldsymbol{x}_i|^{m-2}} \tag{5.25}$$

The fundamental solution has the following property when weighted by any function ϕ:

$$\int_\Omega \phi\,\nabla^2\psi_i\,d\omega_m = -\int_\Omega \phi\,\delta_i\,d\omega_m = -\phi(\boldsymbol{x}_i) = -\phi_i \tag{5.26}$$

where ϕ_i represents the value of the unknown function ϕ at the point of application of the potential, $\boldsymbol{x}_i$. In addition, in the sequel the notation ψ_{ij} will be used to denote the function $\psi_i(\boldsymbol{x}_j)$.
Using this property, (5.18) becomes:

$$\phi_i + \int_\Gamma \phi\,\frac{\partial\psi_i}{\partial n}\,d\omega_{m-1} = \int_\Gamma \frac{\partial\phi}{\partial n}\,\psi_i\,d\omega_{m-1} \tag{5.27}$$

Equation (5.27) relates the value of ϕ at the point $\boldsymbol{x}_i$ with the values of its partial derivative $\frac{\partial\phi}{\partial n}$ and ϕ over the boundary Γ.
The above equation is called the *Boundary Integral Equation* and forms the starting equation of the formulation of the BEM. We assume that only boundary conditions on the potential field (Dirichlet type conditions) have been stated and not on the directional derivative of the potential field (Neumann type conditions). In that case the source (or indirect) formulation of the boundary

elements method can be used (Brebbia 1980).

Assume now that ϕ' is the solution of Laplace's equation within the external region Ω'[2] of Ω. In addition we assume that ϕ' generates the same potentials as the potential field ϕ around Γ, hence $\phi' = \phi$ on Γ. In that case we get the following equation, instead of (5.27):

$$-\int_{\Gamma} \phi' \frac{\partial \psi_i}{\partial n} d\omega_{m-1} = \int_{\Gamma} \frac{\partial \phi'}{\partial n} \psi_i \, d\omega_{m-1} \tag{5.28}$$

Notice that because the point $\boldsymbol{x}_i$ is now external to Ω' the corresponding first term of (5.18) is now zero. Besides, the sign of $\partial\psi_i/\partial n$ has been changed in (5.28) due to the reversed sign of the normal vector on the boundary of Ω'.
By adding (5.27) and (5.28) we obtain the next basic form of the indirect formulation of BEM for an internal point in Ω:

$$\phi_i = \int_{\Gamma} (\frac{\partial \phi}{\partial n} + \frac{\partial \phi'}{\partial n}) \psi_i \, d\omega_{m-1} = \int_{\Gamma} \sigma \, \psi_i d\omega_{m-1} \tag{5.29}$$

where σ represents the initially unknown density distribution of ψ over Γ in order to generate ϕ_i via (5.29). Equation (5.29) can also be used even when the point $\boldsymbol{x}_i$ is on the boundary Γ which is the way to calculate the unknown densities σ from the next equation:

$$\bar{\phi}_i = \int_{\Gamma} \sigma \, \psi_i \, d\omega_{m-1} \tag{5.30}$$

Up to this stage, numerical approximations have not been applied in arriving at the integral (5.30). If the closed boundary of the domain Ω could be described by a simple equation and the function $\sigma(\boldsymbol{x})$ was explicitly given, then an explicit solution of (5.29) might be possible, though very tedious. However, to be able to cover any geometry we perform the integration of (5.30) by dividing the integral into small segments. In this treatment these segments are called *boundary elements* and they will be modelled as small hyperplanes (in two dimensions line segments, and in three dimensions patches).
Dividing the boundary of the domain under consideration in N elements Γ_j, and discretising (5.30) we obtain the next equation:

$$\bar{\phi}_i = \sum_{j=1}^{N} \int_{\Gamma_j} \sigma^j \, \psi_{ij} \, d\omega_{m-1} \tag{5.31}$$

[2]The external region is defined as $\Omega' = \mathcal{R}^m \setminus \bar{\Omega}$

where 'j' denotes the element index, and σ^j denotes the density distribution of ψ over the jth boundary element. The points $\boldsymbol{x}_i$ where the unknown values are considered are called *nodes* and can be arbitrarily chosen on the boundary elements. Suppose that M nodes are chosen on the ith boundary element, denoted by $\boldsymbol{x}_{ik}$ representing the kth node of the ith boundary element where $k = 1, \ldots, M$. Accordingly, ϕ_{ik} denotes the value of the unknown potential field at the $\boldsymbol{x}_{ik}$ node.

Example 5.3.1 *When the boundary elements in the two-dimensional case are small planes as shown in figure 5.5(a), we can define four nodes at the four corners of such an element. The variable σ^j corresponding to*

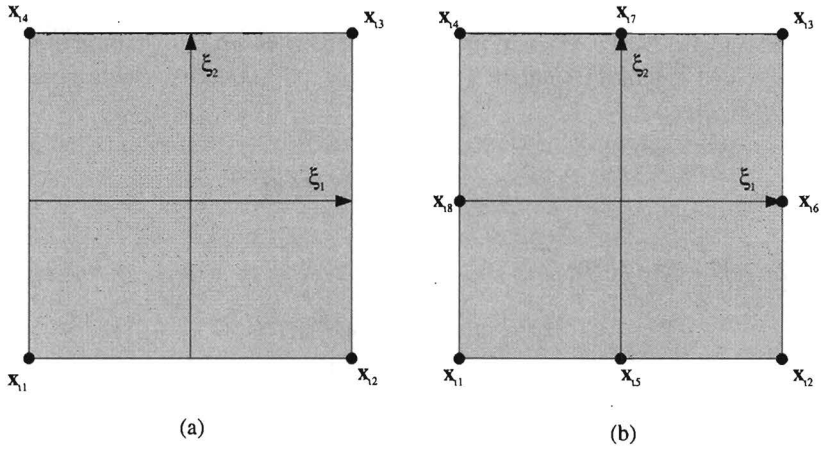

Figure 5.5: Two dimensional boundary elements with: (a) four nodes, (b) eight nodes

the jth boundary element can then be defined by:

$$\sigma^j = \sum_{k=1}^{4} \rho_k^j(\boldsymbol{\xi})\, \sigma_k^j \tag{5.32}$$

with

$$\begin{aligned}
\rho_1^j(\boldsymbol{\xi}) &= \frac{1}{4}(1-\xi_1)(1-\xi_2) \\
\rho_2^j(\boldsymbol{\xi}) &= \frac{1}{4}(1+\xi_1)(1-\xi_2) \\
\rho_3^j(\boldsymbol{\xi}) &= \frac{1}{4}(1+\xi_1)(1+\xi_2) \\
\rho_4^j(\boldsymbol{\xi}) &= \frac{1}{4}(1-\xi_1)(1+\xi_2)
\end{aligned}$$

A local coordinate system $\boldsymbol{\xi}$ has been defined at the middle point $\boldsymbol{x}_j$ of the jth boundary element, and the interpolation functions have been chosen in such a way that:

$$\begin{aligned}
\rho_l^j(\boldsymbol{x}_j - \boldsymbol{x}_{ik}) &= 1 \qquad \text{when } l = k \\
\rho_l^j(\boldsymbol{x}_j - \boldsymbol{x}_{ik}) &= 0 \qquad \text{when } l \neq k
\end{aligned}$$

Example 5.3.2 *We can improve the approximation by taking more nodes on each boundary element (figure 5.5(b)). In that case the approximation of σ^j given by*

$$\sigma^j = \sum_{k=1}^{8} \rho_k^j(\boldsymbol{\xi})\, \sigma_k^j \tag{5.33}$$

can be used, where

$$\begin{aligned}
\rho_1^j &= \frac{1}{4}(1-\xi_1)(1-\xi_2)(-\xi_1-\xi_2-1) \\
\rho_2^j &= \frac{1}{4}(1+\xi_1)(1-\xi_2)(\xi_1-\xi_2-1) \\
\rho_3^j &= \frac{1}{4}(1+\xi_1)(1+\xi_2)(\xi_1+\xi_2-1) \\
\rho_4^j &= \frac{1}{4}(1-\xi_1)(1+\xi_2)(-\xi_1+\xi_2-1) \\
\rho_5^j &= \frac{1}{2}(1-\xi_1^2)(1-\xi_2) \\
\rho_6^j &= \frac{1}{2}(1-\xi_1^2)(1-\xi_2) \\
\rho_7^j &= \frac{1}{2}(1-\xi_1^2)(1+\xi_2) \\
\rho_8^j &= \frac{1}{2}(1-\xi_1^2)(1+\xi_2)
\end{aligned}$$

Generally when M nodes are defined on each boundary element, the variable σ^j is given by

$$\sigma^j = \sum_{k=1}^{M} \rho_k^j(\boldsymbol{\xi}) \sigma_k^j \tag{5.34}$$

where σ_k^j for $k = 1, \ldots, M$, are assumed constant. Substitution of (5.34) in (5.31) gives:

$$\bar{\phi}_{il} = \sum_{j=1}^{N} \int_{\Gamma_j} \sum_{k=1}^{M} \rho_k^j \, \sigma_k^j \, \psi_{il,j} \, d\omega_{m-1} \tag{5.35}$$

where $\bar{\phi}_{il}$ denotes the given value of the potential field at the point $\boldsymbol{x}_{il}$ which is the l-th node of the i-th boundary element, and $\psi_{il,j}$ represents the value of the fundamental solution related with the points $\boldsymbol{x}_{il}$ and $\boldsymbol{x}_j$. Equation (5.35) can be formulated for every $l = 1, \ldots, M$ which leads to the following matrix form:

$$\begin{bmatrix} \bar{\phi}_{11} \\ \vdots \\ \bar{\phi}_{1M} \\ \vdots \\ \bar{\phi}_{N1} \\ \vdots \\ \bar{\phi}_{NM} \end{bmatrix} = \begin{bmatrix} G^{11} & G^{21} & \ldots & G^{N1} \\ G^{12} & G^{22} & \ldots & G^{N2} \\ \vdots & \vdots & \ddots & \vdots \\ G^{1N} & G^{2N} & \ldots & G^{NN} \end{bmatrix} \begin{bmatrix} \sigma_1^1 \\ \vdots \\ \sigma_M^1 \\ \vdots \\ \sigma_1^N \\ \vdots \\ \sigma_M^N \end{bmatrix} \tag{5.36}$$

where G^{ij} is a $M \times M$ matrix with elements given by:

$$G_{lk}^{ij} = \int_{\Gamma_j} \rho_k^j \, \psi_{il,j} \, d\omega_{m-1} \tag{5.37}$$

Finally, we end up with the matrix formulation of the BEM as

$$G\boldsymbol{\sigma} = \bar{\boldsymbol{\phi}} \tag{5.38}$$

with G a $N \cdot M \times N \cdot M$ matrix, $\boldsymbol{\sigma}$ a $N \cdot M$ vector containing the unknown intensities at each node of each boundary element, and $\bar{\boldsymbol{\phi}}$ a $N \cdot M$ vector containing the given potential field values at each node of each boundary element. Equation (5.38) can be solved for the unknown $\boldsymbol{\sigma}$ using known techniques like LU-decomposition. When the vector $\boldsymbol{\sigma}$ has been calculated, (5.31) can be used

to calculate the potential at any interior point ϕ_i or even the gradient of ϕ using the following equation:

$$\nabla_{\boldsymbol{x}}\phi(\boldsymbol{x}) = \sum_{j=1}^{N} \int_{\Gamma_j} \sum_{k=1}^{M} \rho_k^j \sigma_k^j \nabla_{\boldsymbol{x}} \psi_i d\omega_{m-1} \tag{5.39}$$

Next some examples of the BEM will be analysed in the two-dimensional case as depicted in figure 5.6. The boundary elements in that case are line segments. Two different approximations of the variable σ_j will be given depending on the number of nodes taken on each element.

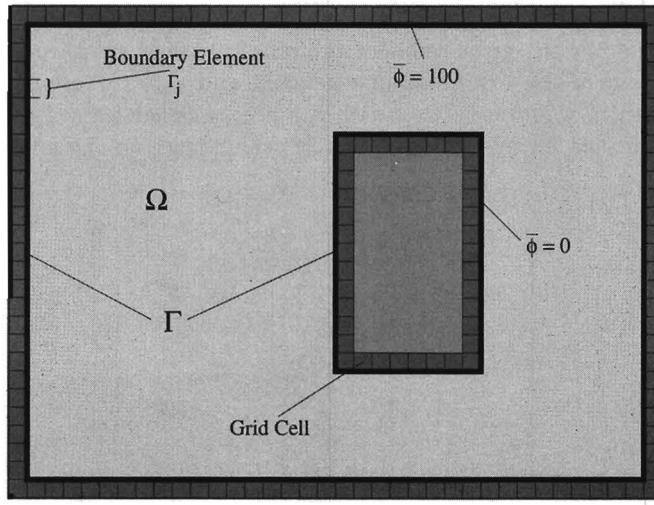

Figure 5.6: An example of a boundary element problem

Example 5.3.3 *In figure 5.6, a two-dimensional domain $\Omega \subset \mathcal{R}$ is depicted with certain boundary Γ. We would like to find a potential field $\phi(\boldsymbol{x})$ defined in Ω under the conditions given in the figure, which satisfies the Laplace equation (5.8).*

Applying the boundary elements method for the given situation we divide the boundary Γ in N line boundary elements Γ_j. By defining the nodes in the middle point $\boldsymbol{x}_j$ of each boundary element, the variables σ^j are assumed constant over the corresponded jth boundary element. Accordingly,

(5.35) gives:

$$\bar{\phi}_i = \sum_{j=1}^{N} \sigma_j \int_{\Gamma_j} \psi_{ij}\, d\omega_1 \tag{5.40}$$

and in matrix form:

$$G\sigma = \bar{\phi} \tag{5.41}$$

with $G_{ij} = \int_{\Gamma_j} \psi_{ij}\, d\omega_1$. *In the given example we distinguish two kinds of boundary elements:*

- *Horizontal elements, described by the vector* $\boldsymbol{x}_j + \boldsymbol{\xi}$, *where* $\boldsymbol{\xi} = (\xi, 0)$ *with* ξ *taking values in the interval* $[-\bar{\xi}, \bar{\xi}]$ *with* $2\bar{\xi}$ *the length of a boundary element.*
- *Vertical elements, described by the vector* $\boldsymbol{x}_j + \boldsymbol{\xi}$, *where* $\boldsymbol{\xi} = (0, \xi)$ *with* ξ *taking values in the interval* $[-\bar{\xi}, \bar{\xi}]$ *with* $2\bar{\xi}$ *the length of a boundary element.*

The elements of the matrix G are given by:

$$G_{ij} = \frac{1}{2\pi} \int_{-\bar{\xi}}^{\bar{\xi}} \log\left(\frac{1}{|\boldsymbol{x}_i - \boldsymbol{x}_j - \boldsymbol{\xi}|}\right) d\xi \tag{5.42}$$

For the specific kind of stated boundary elements, it is even possible to calculate analytically the integral of G_{ij}, *as given in appendix A.*

Solving (5.41) for the unknown densities $\boldsymbol{\sigma}$ *and using (5.31) we have obtained an analytic expression for the potential field* ϕ *shown in figure 5.7.*

Example 5.3.4 *Taking more nodes at each boundary element in the previous example can lead to a better approximation of the variables* σ^j. *By defining two nodes for instance at the points* $-\frac{1}{2}\bar{\xi}$ *and* $\frac{1}{2}\bar{\xi}$ *on each boundary element, the variables* σ^j *can then be described by the following equation.*

$$\sigma^j = \sum_{k=1}^{2} \rho_k^j(\boldsymbol{\xi})\, \sigma_k^j \tag{5.43}$$

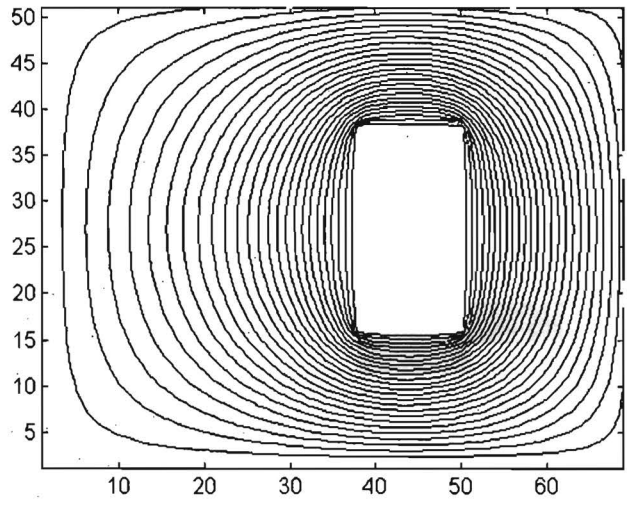

Figure 5.7: The found potential field (a) and its isopotential lines (b)

with

$$\rho_1^j(\xi) = \frac{1}{2}(\frac{\bar{\xi}}{2} - \xi)$$
$$\rho_2^j(\xi) = \frac{1}{2}(\frac{\bar{\xi}}{2} + \xi)$$

Accordingly (5.31) gives:

$$\bar{\phi}_{il} = \sum_{j=1}^{N} \int_{\Gamma_j} \sum_{k=1}^{2} \rho_k^j \, \sigma_k^j \, \psi_{il,j} \, d\omega_1 \tag{5.44}$$

and in matrix form:

$$\begin{bmatrix} \bar{\phi}_{11} \\ \bar{\phi}_{12} \\ \vdots \\ \bar{\phi}_{N1} \\ \bar{\phi}_{N2} \end{bmatrix} = \begin{bmatrix} G^{11} & G^{21} & \dots & G^{N1} \\ G^{12} & G^{22} & \dots & G^{N2} \\ \vdots & \vdots & \ddots & \vdots \\ G^{1N} & G^{2N} & \dots & G^{NN} \end{bmatrix} \begin{bmatrix} \sigma_1^1 \\ \sigma_2^1 \\ \vdots \\ \sigma_1^N \\ \sigma_2^N \end{bmatrix}. \tag{5.45}$$

Chapter 6

Experiments

In the previous chapters we have discussed how to incorporate artificial potential fields in the control scheme of each link of a robot, how to create an artificial potential field with the desired properties to use it in the control strategy, and how to transform the obstacles from the physical space of a robot into the configuration space of the robot.
The described method, BEM for finding an artificial potential field, has been implemented in the case of a planar RR robot. In this chapter we discuss some results concerning the performance of the method in various situations. The performance of the BEM related to robot motion planning concerns the presence of local minima in the interior and the boundary of the free configuration space of the robot. Basically, we have on one hand no theoretical (mathematical) background to measure the performance of the method and on the other hand no expectations or estimations concerning the results. Therefore we have designed a certain scenario of experiments to observe the influence of the change of some properties on the structure of the potential field.
Primarily, the requirements concerning a potential field are that it has no local minima and the APF has to satisfy the Dirichlet conditions on the boundary of the free configuration space of the robot. Of less importance in this phase of the experiments, we aim "fast" calculation of the APF in reference to real-time applications, and minimum computer memory effort.
The performance of the boundary element method depends on different parameters like the dimensions of the boundary elements; the minimum distance between boundary elements; and the "closeness" of a region of the domain of application.

- **Size of boundary elements.** In subsection 5.3.2 we have discussed how the BEM can be used in potential problems. The major approximation

has been done when the boundary of the domain has been divided in small segments the boundary elements. By doing so we have formulated the basic equation of the BEM (5.31). Obviously the smaller the boundary elements the better the approximation of the potential field.

- **Numerical approximations.** Another factor which plays an important role in the accuracy of the potential field is the calculation of the elements of the matrix G involved in the BEM. That issue has influence on the potential field only when numerical methods have been employed to solve the integrals in (5.31). Mostly it is difficult to find an exact solution of such integrals especially in higher dimensions. Therefore numerical methods like the *Gauss quadrature* method can be used. However such integration methods can give inaccurate results under certain circumstances like in our case when two boundary elements are lying too close to each other.

- **"Closeness".** Although it is rather difficult to give a mathematical definition of the term "closeness", intuitively we can state that the "closeness" of a region has something to do with the complexity of a path from a configuration inside that region to a destination configuration. Obviously, the more closed a region the more difficult to find a path to a destination point laying outside that region. Two extreme situations of closeness could be for instance a totally closed region where no path to a destination configuration exists and a region containing a destination configuration where a simple straight line from an initial configuration to the destination configuration could be a path. We investigate the influence of "closeness" on the potential field because we expect that its influence on the potential field is rather significant.

The experimental setup used consisted of two scenarios: first an obstacle situation is assumed as depicted in figure 6.1. Using this situation we investigate the influence of the mentioned parameters on the APF. Next, a three-dimensional configuration space of a robot is assumed where the solution of a simple motion planning problem is demonstrated.
Before we start analysing the results of the experiments, we give in the next section an algorithm of finding and using potential fields in robot motion planning. Some problems will be discussed and some solutions will be given.

6.1 Robot Motion Planning: the algorithm

When potential fields are employed in robot motion planning we have to solve the problem defined in section 5.1 as follows:

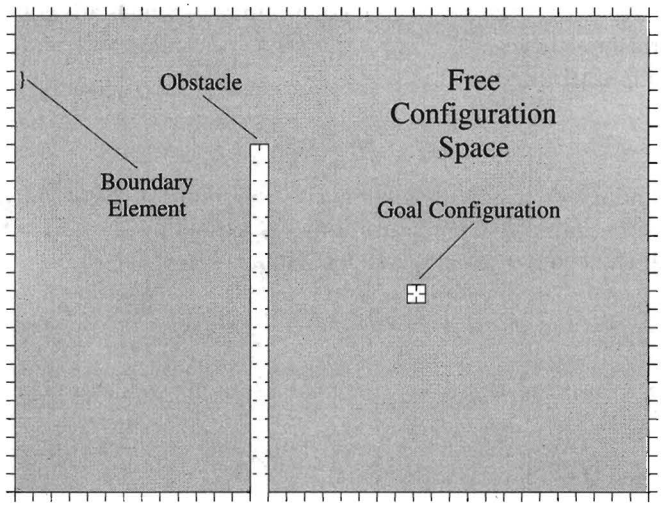

Figure 6.1: The experimental situation of a robot motion planning problem

Find an APF $\mathtt{U}(\boldsymbol{q}) : \mathcal{F} \rightarrow \mathcal{R}$ which attains its maximum value c_o at the obstacle boundary Γ_o and its minimum value c_d at the goal configurations boundary Γ_d. In addition this APF may not have any local minima in the free configuration space $\mathcal{F}$.
Solving this problem using the described method means that we have to undertake the following steps:

1. Find the configuration obstacles $\mathcal{O}^{\mathcal{Q}}$ (see section 4.2).
   Remark: The robot during its motion has to stay inside the configuration space. By considering the boundary $\partial\mathcal{Q}$ of the configuration space $\mathcal{Q}$ as an additional configuration obstacle we can enforce the robot to remain inside the configuration space. The boundary Γ_o now denotes the boundary of the total configuration obstacles $\mathcal{O} = \mathcal{O}^{\mathcal{Q}} \cup \partial\mathcal{Q}$.

2. Find the set of goal configurations $\mathcal{G}$ (see subsection 3.1.3).
   Remark: Apparently we are only interested in the goal configurations which can be reached by the robot or in other words the goal configurations inside the configuration space of the robot. Based on $\mathcal{G}$, we have to find the set of the reachable goal configurations defined by:

   $$\mathcal{G}_r = \mathcal{G} \cap \mathcal{Q} \tag{6.1}$$

   In addition, a goal configuration can be allowable when at that configuration the robot does not collide with any obstacles. Hence, based on

$\mathcal{G}_r$, we have to find the set of goal configurations which are not inside the configuration obstacles $\mathcal{O}^{\mathcal{Q}}$, i.e. the set of the allowable and reachable goal configurations given by:

$$\mathcal{G}_{ar} = \mathcal{G}_r \setminus (\mathcal{G}_r \cap \mathcal{O}^{\mathcal{Q}}) \tag{6.2}$$

The boundary Γ_d is now defined as the boundary of the set of the allowable and reachable goal configurations $\mathcal{G}_{ar}$ excluding the common boundary with the configuration obstacles. Hence,

$$\Gamma_d = \partial\mathcal{G}_{ar} \setminus (\partial\mathcal{O} \cap \partial\mathcal{G}_{ar}) \tag{6.3}$$

3. In order to use the Boundary Element Method, we define the following variables:

   (a) Define the boundary elements.
   Remark: Due to the discretization of the total configuration obstacles $\mathcal{O}$ and the set of the allowable and reachable goal configurations $\mathcal{G}_{ar}$, the boundaries Γ_o and Γ_d consist of sides of bins of the defined grid of the configuration space of the robot. That means that the boundary elements can be defined as the sides of the bins which belong to the boundaries Γ_o and Γ_d.

   (b) Define the number and position of the nodes on each boundary element.
   Remark: According to the position of the nodes on a boundary element we can define the interpolation functions $\rho_k^j(\boldsymbol{\xi})$ of the k-th node on the j-th boundary element, as described in subsection 5.3.2, by (5.34).

   (c) Determine the elements G_{lk}^{ij} of the dependency matrix G described in subsection 5.3.2, by (5.37).

   (d) Define the Dirichlet condition on the l-th node of the i-th boundary element of Γ_o, by a value c_o and on Γ_d, and on the l-th node of the i-th boundary element of Γ_d, by a value c_d with $c_d < c_o$.

4. Using these variables concerning the BEM we solve the system given by (5.38) for the unknown variables $\boldsymbol{\sigma}$.

5. Using (5.39) we calculate the gradient of the potential field at a point $\boldsymbol{q}$ of the free configuration space of the robot.

6. The gradient of the potential field is then included in the control law as described in subsection 3.2.3.

6.2 Practical Problems

In this section we address two problems of the usage of potential fields and we stress some ideas concerning their solution. First we examine whether the gradient of the potential field can be used in real applications where the robot actuators can only accept a bounded torque input. Second, we take a look of the real-time applicability of the potential fields for robot motion planning.

6.2.1 Admissibility of the gradient of the potential field

The first problem we would like to underline is the admissibility of the gradient of the potential field for control purposes described in subsection 3.2.3, by a real robot with real actuators. In order to get an idea of what a potential field will look like, the potential field has been calculated in the situation of figure 6.2. In that case only a single node at every boundary element has been used

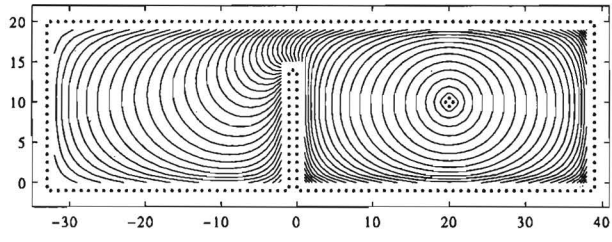

Figure 6.2: An example of an obstacle situation

(indicated by the dots in the figure) and the length of the boundary elements is 1. In figure 6.3 the corresponding potential field is shown and its isopotential lines are depicted in figure 6.2. Even if the main goal of avoiding local minima of the potential field is achieved, we ascertain the next problem. The potential field can in some areas be very flat and in some other areas very steep. Both the cases are problematic. Where the potential field is flat, the gradient of the potential is small and it is large at the areas where the potential field is steep. In fact the actuators of any robot have a certain range of admissible torques, which means that the input torques have to be limited, and accordingly the gradient of the potential field as well, hence

$$\left|\frac{\partial U}{\partial q_i}\right| \leq b_i \tag{6.4}$$

for $i = 1 \ldots n$, assuming that the bounds b_i are given. The solution of this problem is based on the fact that the potential field may not necessarily be a

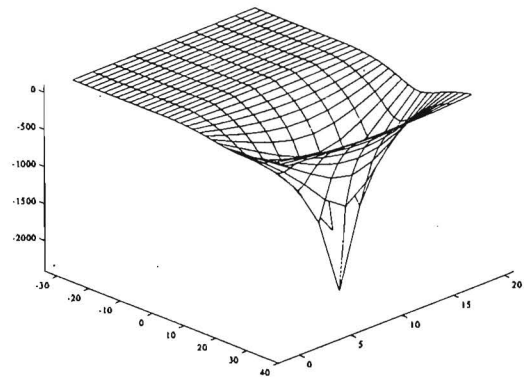

Figure 6.3: The potential field of the example

harmonic function but in any case must not exhibit local minima inside the free configuration space of the robot. We will prove that a potential field $f(\mathtt{U}(\boldsymbol{q}))$ does not exhibit any local minima under certain conditions as the next lemma states.

Lemma 6.2.1 *Suppose a harmonic function* $\mathtt{U}(\boldsymbol{q})$ *on a domain* Ω. *Any function* $f(\mathtt{U}(\boldsymbol{q}))$ *has the same stationary points as* $\mathtt{U}(\boldsymbol{q})$ *when*

$$\frac{df(\mathtt{U})}{d\mathtt{U}} \neq 0 \qquad \forall \boldsymbol{q} \in \Omega \tag{6.5}$$

Proof:
At a stationary point of the function $\mathtt{U}(\boldsymbol{q})$ it holds that:

$$\nabla_{\boldsymbol{q}}\mathtt{U}(\boldsymbol{q}) = 0 \tag{6.6}$$

The gradient of the function $f(\mathtt{U})$ is given by:

$$\nabla_{\boldsymbol{q}} f(\mathtt{U}) = \frac{df(\mathtt{U})}{d\mathtt{U}} \nabla_{\boldsymbol{q}}\mathtt{U}(\boldsymbol{q}) \tag{6.7}$$

That implies that the gradient of the function $f(\mathtt{U})$ under the given condition only vanishes at the stationary points of the potential field $\mathtt{U}$ or with other words has the same stationary points. □

In addition the gradient of any harmonic function $\mathtt{U}(\boldsymbol{q})$ is bounded, hence:

$$\left|\frac{\partial \mathtt{U}(\boldsymbol{q})}{\partial q_i}\right| \leq B_i \tag{6.8}$$

for $i = 1 \ldots n$, for some B_i.
The problem now is to define a proper function $f(\mathtt{U})$ and to determine the bounds B_i. The function $f(\mathtt{U})$ can be defined for instance by:

$$f(\mathtt{U}) = \ln(\mathtt{U}) \tag{6.9}$$

for which we have:

$$\frac{df(\mathtt{U})}{d\mathtt{U}} = \frac{1}{\mathtt{U}} \tag{6.10}$$

According to (6.7) the gradient of the new potential field $f(\boldsymbol{q})$ is given by:

$$\nabla_{\boldsymbol{q}} f(\boldsymbol{q}) = \frac{\nabla_{\boldsymbol{q}} \mathtt{U}(\boldsymbol{q})}{\mathtt{U}} \tag{6.11}$$

The minimum value of the potential field $\mathtt{U}(\boldsymbol{q})$ is defined by c_d at the goal configurations, which implies that:

$$\left|\frac{\partial f(\boldsymbol{q})}{\partial q_i}\right| = \left|\frac{\frac{\partial \mathtt{U}(\boldsymbol{q})}{\partial q_i}}{\mathtt{U}}\right| \leq \frac{B_i}{c_d} \tag{6.12}$$

That means that the value of c_d can be determined by the equation:

$$c_d \geq \frac{B_i}{b_i} \tag{6.13}$$

such that each coordinate $\frac{\partial f}{\partial q_i}$ of the gradient of the new potential field $f(\boldsymbol{q})$ is indeed bounded by b_i. In the case of the above example the potential field $f(\boldsymbol{q})$ is drawn in figure 6.4. Depending on the choice of the function $f(\mathtt{U})$ and the Dirichlet conditions applied it could be achieved that on the one hand the flat area is less flat and on the other hand the steep area around the goal configuration is less steep.

6.2.2 Real-time applicability

The second serious problem is the real-time applicability of the method. The main problem of using the BEM to calculate the potential field is the calculation of the vector $\boldsymbol{\sigma}$ in (5.38). To achieve this we need to calculate the inverse of the matrix G, which is the most time consuming operation. Generally it is

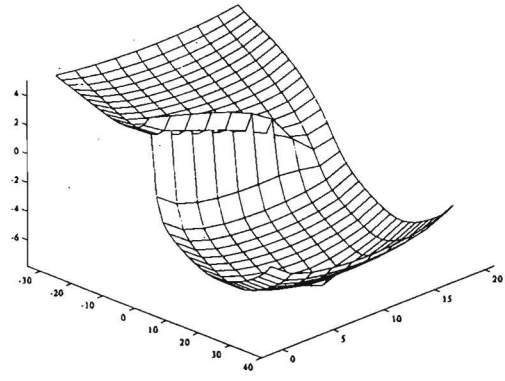

Figure 6.4: The transformed potential field of the example

difficult to use potential fields for real-time robot motion planning under the present computer performance and capacity. However, real-time applicability is actually required in two cases: when the environment of the robot changes in time and/or the obstacles in the environment of the robot are gradually sensored during motion of the robot. In both cases it means that some boundary elements of the free configuration space of the robot disappear and some other have to be added which leads to a new matrix G'. In these cases we introduce a method to calculate the inverse G'^{-1} of the new matrix G' based on the inverse G^{-1} of the old matrix G.

Adding new boundary elements Suppose that some boundary elements have to be added to the old ones, which means that a number of columns and rows have to be added to the matrix G. The number of the added columns or rows k_a is equal to the number of the new boundary elements times the number of nodes per boundary element [1].
Assuming that we have already calculated the inverse matrix G^{-1} of the matrix G we will show that the inverse of the new matrix G', can be derived from G^{-1} which is needed for the calculation of the new solution of the system:

$$G' \cdot \sigma' = b' \tag{6.14}$$

[1] In this text we have assumed without losing the generality of the method that every boundary element has the same number and type of nodes.

with b' the new Dirichlet conditions. The new matrix G' is given by:

$$G' = \begin{bmatrix} G & G_1 \\ G_2 & G_3 \end{bmatrix} \tag{6.15}$$

with G_1 a $(N \cdot M) \times k_a$ matrix, G_2 a $k_a \times (N \cdot M)$ matrix and G_3 a $k_a \times k_a$ matrix. The matrices G_1, G_2 and G_3 represent actually the added elements in the new matrix G' of the system (6.15) related to the added k_a nodes of the new boundary elements. Suppose that the LU decomposition of the matrix G' is given by:

$$L' = \begin{bmatrix} L & 0 \\ L_1 & L_2 \end{bmatrix} \tag{6.16}$$

with L_1 a $k_a \times (N \cdot M)$ matrix and L_2 a $k_a \times k_a$ matrix. And

$$U' = \begin{bmatrix} U & U_1 \\ 0 & U_2 \end{bmatrix} \tag{6.17}$$

with U_1 a $(N \cdot M) \times k_a$ matrix and U_2 a $k_a \times k_a$ matrix. Based on the fact that

$$G' = \begin{bmatrix} G & G_1 \\ G_2 & G_3 \end{bmatrix} = \begin{bmatrix} LU & LU_1 \\ L_1U & L_1U_1 + L_2U_2 \end{bmatrix} = L' \cdot U' \tag{6.18}$$

we can derive that:

$$L_1 = G_2 U^{-1} \tag{6.19}$$

$$U_1 = L^{-1} G_1 \tag{6.20}$$

$$L_2U_2 = G_3 - L_1U_1 \tag{6.21}$$

hence L_2, U_2 is the LU decomposition of the $k_a \times k_a$ matrix $G_3 - L_1U_1$. Substitution of (6.19) and (6.20) in (6.21) gives:

$$L_2U_2 = G_3 - G_2U^{-1}L^{-1}G_1 \tag{6.22}$$

Actually we do not need to calculate L_2 and U_2 but only the inverse matrix $K_2 = (L_2U_2)^{-1}$, with K_2 given by:

$$K_2 = (G_3 - G_2G^{-1}G_1)^{-1} \tag{6.23}$$

The inverses of the new L' and U' can be derived from (6.16) and (6.17) yielding:

$$L'^{-1} = \begin{bmatrix} L^{-1} & 0 \\ -L_2^{-1}L_1L^{-1} & L_2^{-1} \end{bmatrix} \tag{6.24}$$

and

$$U'^{-1} = \begin{bmatrix} U^{-1} & -U^{-1}U_1U_2^{-1} \\ 0 & U_2^{-1} \end{bmatrix} \tag{6.25}$$

For the solution of the new system we need the inverse of matrix G', given by $G'^{-1} = U'^{-1}L'^{-1}$ which can be calculated by:

$$G'^{-1} = \begin{bmatrix} G^{-1} + G^{-1}G_1K_2G_2G^{-1} & -G^{-1}G_1K_2 \\ -K_2G_2G^{-1} & K_2 \end{bmatrix} \tag{6.26}$$

Concluding we need the matrices G^{-1} and K_2 to calculate the inverse of the new matrix G'. The matrix G^{-1} was already calculated and the matrix K_2 has to be calculated using (6.23). The solution $\boldsymbol{\sigma}'$ of the new system can be calculated by:

$$\boldsymbol{\sigma}' = G'^{-1}\boldsymbol{b}' \tag{6.27}$$

Deleting boundary elements When new bins of the discretizised configuration space has been found as prohibited due to a new obstacle in the physical space of the robot, some boundary elements do not belong any more to the boundary of the free configuration space of the robot. These boundary elements are actually the common boundary elements of the new boundary elements and the existing boundary elements. That means that some boundary elements have to be deleted, which means that a number of columns and rows have to be deleted from the matrix G. The number of the deleted columns or rows k_d is equal to the number of the common boundary elements times the number of nodes per boundary element.
Assuming that we already have the $(N \cdot M) \times (N \cdot M)$ matrix G and its inverse matrix we will calculate the inverse of the new matrix G' after deleting the rows and columns corresponding to the deleted boundary elements. The inverse of the old matrix G is after certain pivoting, given by:

$$G^{-1} = \begin{bmatrix} D_1 & D_2 \\ D_3 & D_4 \end{bmatrix} \tag{6.28}$$

with D_1 a $((N \cdot M) - k_d) \times ((N \cdot M) - k_d)$ matrix, D_2 a $(N \cdot M) \times k_d$ matrix, D_3 a $k_d \times (N \cdot M)$ matrix and D_4 a $k_d \times k_d$ matrix. Suppose now that the LU decomposition of the matrix G' is given by:

$$L = \begin{bmatrix} L' & 0 \\ L_1 & L_2 \end{bmatrix} \tag{6.29}$$

with L_1 a $k_d \times (N \cdot M)$ matrix and L_2 a $k_d \times k_d$ matrix. And

$$U = \begin{bmatrix} U' & U_1 \\ 0 & U_2 \end{bmatrix} \tag{6.30}$$

with U_1 a $(N \cdot M) \times k_d$ matrix and U_2 a $k_d \times k_d$ matrix. The inverses of the old L and U can be derived from (6.29) and (6.30):

$$L^{-1} = \begin{bmatrix} L'^{-1} & 0 \\ -L_2^{-1}L_1L'^{-1} & L_2^{-1} \end{bmatrix} \tag{6.31}$$

and

$$U^{-1} = \begin{bmatrix} U'^{-1} & -U'^{-1}U_1U_2^{-1} \\ 0 & U_2^{-1} \end{bmatrix} \tag{6.32}$$

The inverse of matrix the matrix $G^{-1} = U^{-1}L^{-1}$ can be obtained from (6.31) and (6.32) giving:

$$G^{-1} = \begin{bmatrix} U'^{-1}L'^{-1} + U'^{-1}U_1U_2{}^{-1}L_2{}^{-1}L_1L'^{-1} & -U'^{-1}U_1U_2{}^{-1}L_2{}^{-1} \\ -U_2{}^{-1}L_2{}^{-1}L_1L'^{-1} & U_2{}^{-1}L_2{}^{-1} \end{bmatrix} \tag{6.33}$$

From (6.33) and (6.28) we get the following equations:

$$U'^{-1}L'^{-1} = D_1 - U'^{-1}U_1U_2{}^{-1}L_2{}^{-1}L_1L'^{-1} \tag{6.34}$$

$$-U'^{-1}U_1U_2{}^{-1} = D_2L_2 \tag{6.35}$$

and

$$-L_2{}^{-1}L_1L'^{-1} = U_2D_3 \tag{6.36}$$

By substitution of (6.35) and (6.36) in (6.34) we obtain

$$G'^{-1} = U'^{-1}L'^{-1} = D_1 - D_2L_2U_2D_3 \tag{6.37}$$

with

$$L_2U_2 = D_4{}^{-1} \tag{6.38}$$

This leads to the conclusion, we only need to calculate the inverse of the matrix D_4 and using (6.37) we can calculate the inverse of the new matrix G'. The solution $\boldsymbol{\sigma}'$ of the new system can be calculated by:

$$\boldsymbol{\sigma}' = G'^{-1}\boldsymbol{b}' \tag{6.39}$$

When new configuration obstacles are introduced, suppose that a number k_a boundary elements have to be added and a number k_d of boundary elements have to be deleted. When we want to apply the method we have to calculate the inverse matrix K_2 with dimension k_a and the inverse of the matrix D_4 with dimensions k_d. Typically k_a and k_d are much smaller than the dimension $(N \cdot M) + k_a - k_d$ of the new matrix G, which means that the calculation of the matrices K_2 and D_4 (plus some matrix multiplications) is much faster than the calculation of the inverse of the new matrix G.

7.1 Potential field calculations in two dimensions

The obstacle situation under consideration is shown in figure 6.1. Although it is a simple two-dimensional case it offers the possibility to investigate the influence of all the previous mentioned properties on the performance of the potential field. The most critical region is the "closed" region depicted in figure 7.1. In that region we are going to calculate and visualise the potential field under different conditions.

In the first place we take a look of the influence of the length ν_1 of the

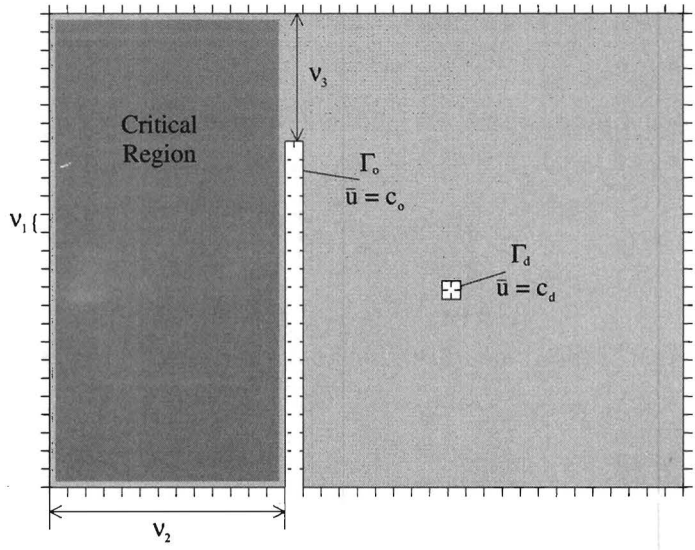

Figure 7.1: The critical region of the BEM

boundary elements on the potential field. Different values of ν_1 have been used to calculate the potential field depicted in figure 7.2 with $\nu_1 = 1$, figure 7.3 with $\nu_1 = 3$, figure 7.4 with $\nu_1 = 5$, and figure 7.5 with $\nu_1 = 7$.

The found potential field in every situation is actually a harmonic function which means that there are no local minima inside the free configuration space. However, sometimes (figures 7.4 and 7.5), saddle points occur inside the free configuration space which means that for robot motion planning purposes. the found potential field can not be used. In such cases there is a possibility that the robot will be driven through an obstacle. That implies that a potential field can be characterized as "good" meaning actually useful for robot motion planning

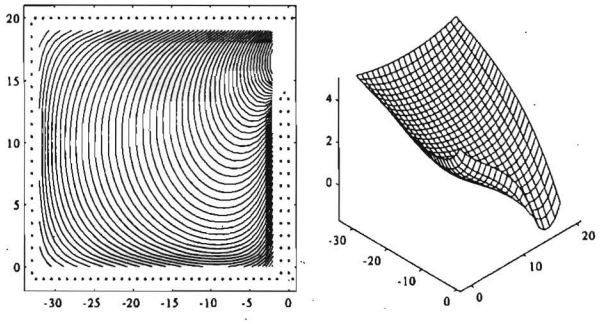

Figure 7.2: The obstacle situation and the found potential field for $\nu_1 = 1$

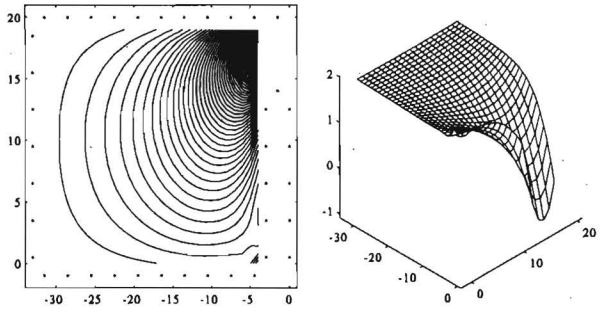

Figure 7.3: The obstacle situation and the found potential field for $\nu_1 = 3$

purposes which means an APF without local minima neither in the interior of the free configuration space nor at the boundary of the free configuration space of the robot.

As it was expected the smaller the boundary elements the better the potential field. As we will also see later on the length of the boundary elements ν_1 forms a powerful means for the improvement of the quality of the potential field. Nevertheless, the smaller the length of the boundary elements the higher the memory and time effort of the computer. The memory effort is quadratic related to the dimension of the matrix G, in terms of $(N \cdot M) \cdot (N \cdot M)$. In the present case the memory demand is of the order of respectively ($\nu_1 = 1$) 1.75 kB, ($\nu_1 = 3$) 1.53 kB, ($\nu_1 = 5$) 0.96 kB, and ($\nu_1 = 7$) 0.72 kB.

Next we investigate the influence of the "closeness" of a region on the quality of

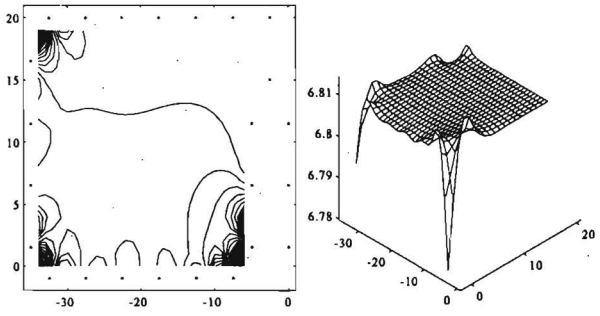

Figure 7.4: The obstacle situation and the found potential field for $\nu_1 = 5$

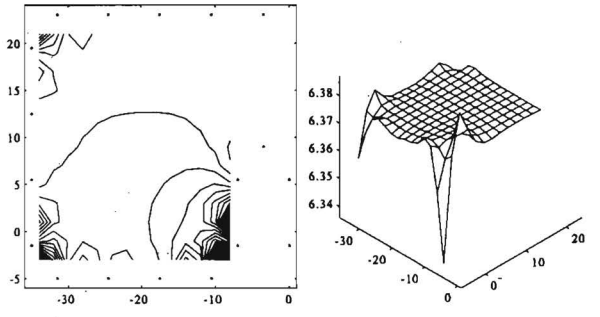

Figure 7.5: The obstacle situation and the found potential field for $\nu_1 = 7$

the potential field. Therefore we let the parameter ν_3 taking different values, and we calculate the potential field in the closed region of figure 7.1. The length of the boundary elements is $\nu_1 = 1$ and there is only a single node per boundary element. The width of the region is $\nu_2 = 32$. The results are depicted in figure 7.6 with $\nu_3 = 1$, and figure 7.7 with $\nu_3 = 2$. It appears that when the opening of the closed region is greater then two times the length of the boundary elements ν_1 that the potential field is good for robot motion purposes. However, that can not be a general conclusion as it appears from the next experiments. Even when $\nu_3 = 2$ when the region becomes narrower (varying the parameter ν_2) the potential field becomes worse. In figure 7.8 with $\nu_2 = 12$, figure 7.9 with $\nu_2 = 6$, and figure 7.10 with $\nu_2 = 2$, the parameter ν_3 is kept 2. The potential field becomes very flat and at last some saddles occur

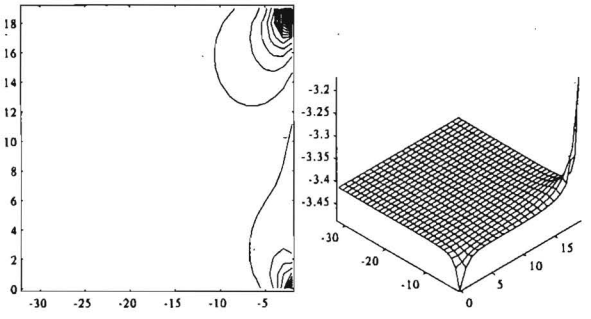

Figure 7.6: The obstacle situation and the found potential field for $\nu_3 = 1$

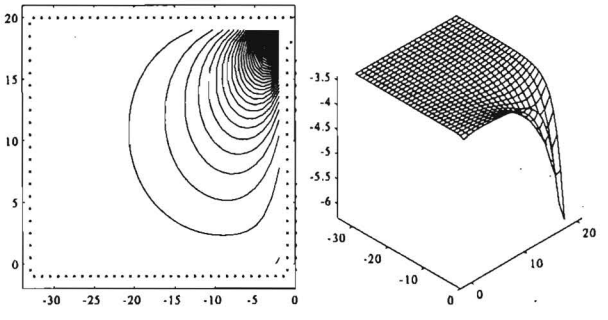

Figure 7.7: The obstacle situation and the found potential field for $\nu_3 = 2$

which make the potential field useless. When the situation becomes more complicated (or more closed) as the situation depicted in figure 7.11 the found potential can not be used for robot motion planning even when ν_3 is greater than twice the length of the boundary elements. In all the given situations we notice that a "good" potential field for robot motion purposes can only be obtained when the boundary elements are small enough.

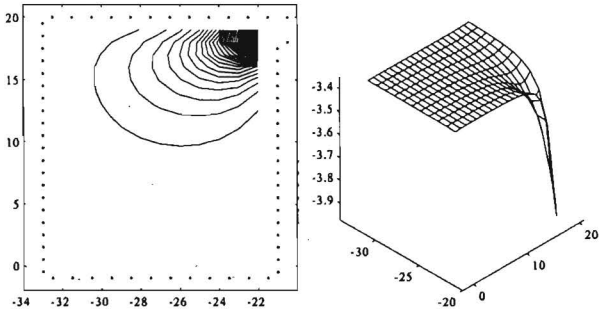

Figure 7.8: The obstacle situation and the found potential field for $\nu_2 = 12$

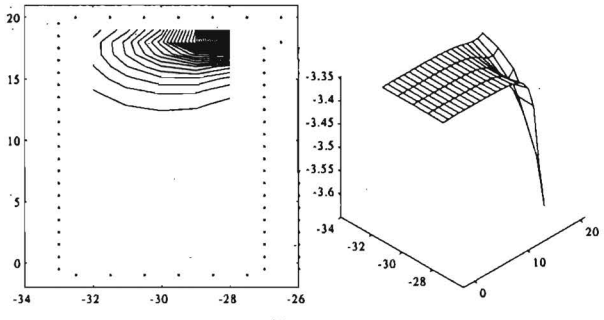

Figure 7.9: The obstacle situation and the found potential field for $\nu_2 = 6$

7.2 Potential field calculations in three dimensions

In this section a three-dimensional configuration space is considered. The major aim of this experiment is to demonstrate that it is possible to use the BEM in a three dimensional space. The obstacle situation used consists of a cube of dimensions 18 × 18 × 18 with a cubic obstacle at location (9, 9, 12) and a goal configuration at location (9, 9, 6). The boundary elements for the outer cube are patches with size 3 × 3. The obstacle cube and the goal configuration cube consist of six boundary elements with size 1 × 1.
It is obvious that in a three-dimensional space we miss the fourth dimension to visualise the found potential field. Therefore we have used two different ways

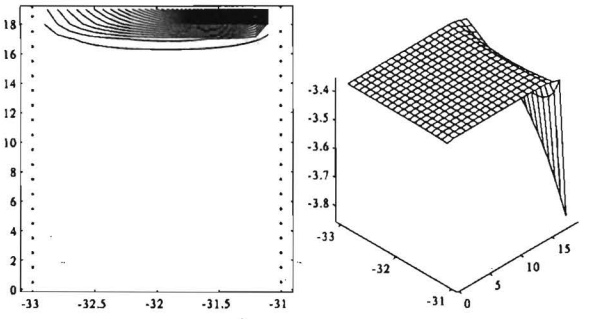

Figure 7.10: The obstacle situation and the found potential field for $\nu_2 = 2$

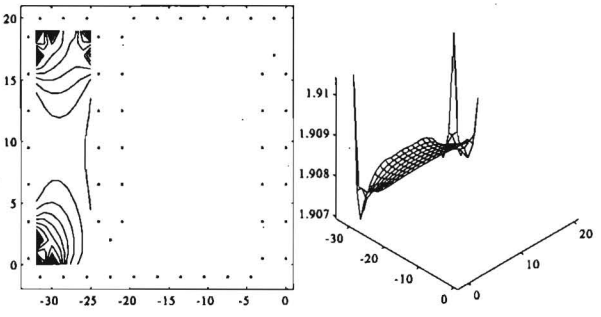

Figure 7.11: Situation with two obstacles and the found potential field

of showing the potential field. A path with the initial configuration (8, 8, 15) is calculated following the maximum negative gradient of the potential field. This path has been drawn in the space from three different viewpoints. In figures 7.12, 7.13, and 7.14 we see the path obtained with a view angle of 45°, 60° and 30°, respectively. The second way shows the potential field at different heights (different values of the q_3 coordinate) of the space. Notice that these "slices" of the potential field could contain local minima which does not necessarily mean that the potential field in general contains local minima. However, both ways of visualisation give a good impression of the potential field. In figures 7.15, 7.16, 7.17, 7.18, 7.19, 7.20, 7.21, 7.22, and 7.23 the potential field is depicted for $q_3 = 1$, $q_3 = 3$, $q_3 = 5$, $q_3 = 7$, $q_3 = 9$, $q_3 = 11$, $q_3 = 13$, $q_3 = 15$, and $q_3 = 17$, respectively.

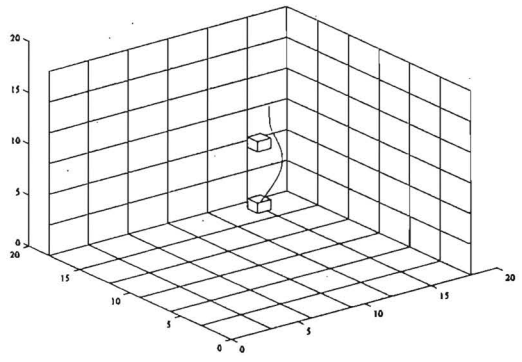

Figure 7.12: Path in a three-dimensional configuration space with a view angle of 45°.

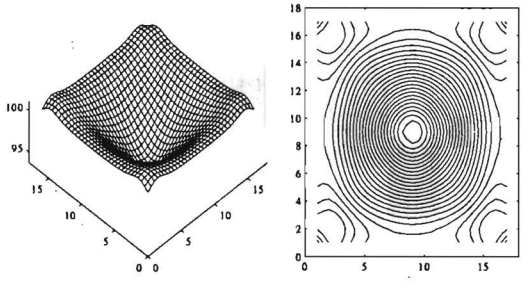

Figure 7.15: Potential field in a three-dimensional configuration space at $q_3 = 1$.

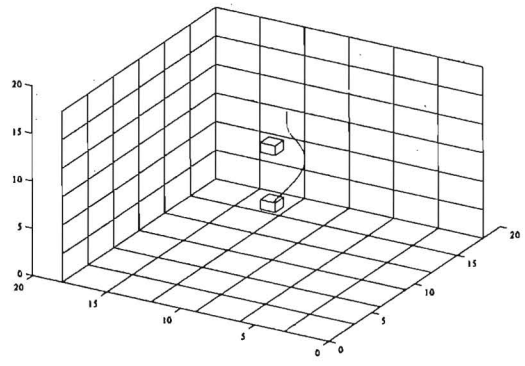

Figure 7.13: Path in a three-dimensional configuration space with a view angle of 60°.

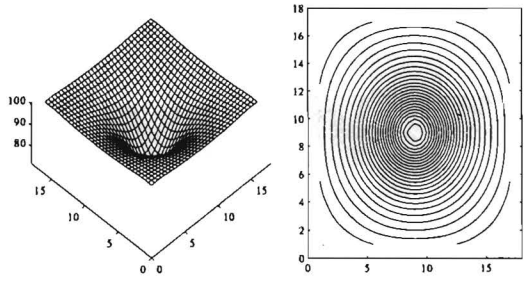

Figure 7.16: Potential field in a three-dimensional configuration space at $q_3 = 3$.

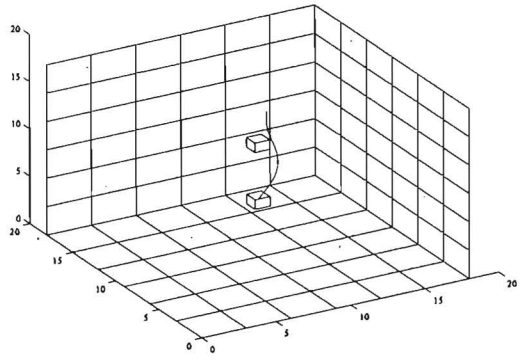

Figure 7.14: Path in a three-dimensional configuration space with a view angle of 30°.

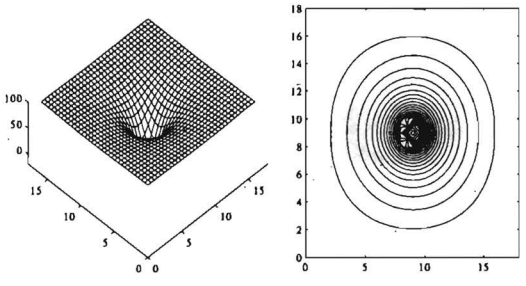

Figure 7.17: Potential field in a three-dimensional configuration space at $q_3 = 5$.

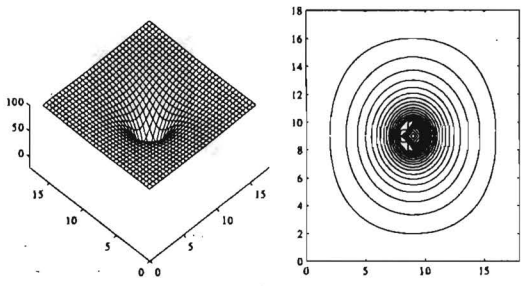

Figure 7.18: Potential field in a three-dimensional configuration space at $q_3 = 7$.

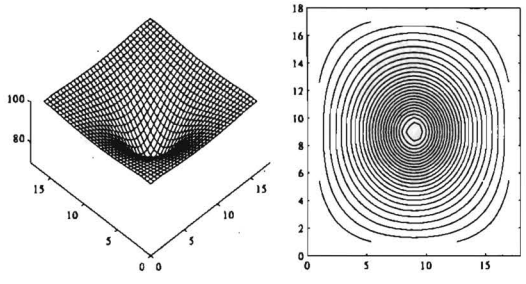

Figure 7.19: Potential field in a three-dimensional configuration space at $q_3 = 9$.

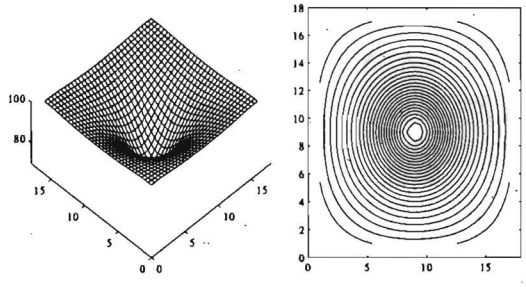

Figure 7.20: Potential field in a three-dimensional configuration space at $q_3 = 11$.

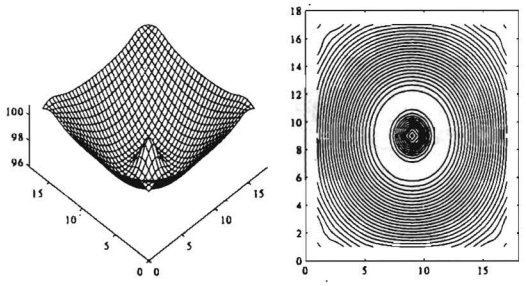

Figure 7.21: Potential field in a three-dimensional configuration space at $q_3 = 13$.

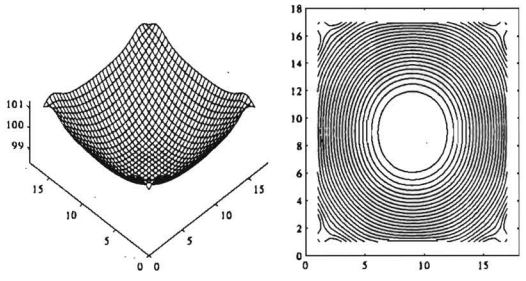

Figure 7.22: Potential field in a three-dimensional configuration space at $q_3 = 15$.

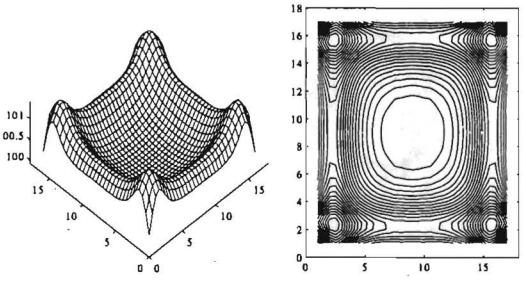

Figure 7.23: Potential field in a three-dimensional configuration space at $q_3 = 17$.

Chapter 7

Conclusions

In this thesis we have considered robot motion planning and control using artificial potential fields (APF). The analysis of this issue has been started giving a control law in the configuration space of a robot which incorporates APF. We have proven that the robotic system reaches asymptotically a given goal configuration under certain conditions stated on the APF. Because the robot motion planning is described in the configuration space of the robot, the transformation of the physical obstacles into the configuration space has been indicated. The main requirement concerning the APF is related to the presence of local minima which has been handled in chapter 5. Finding an APF without any local minima has been achieved using the Boundary Element Method. This method has been theoretically analysed and extended for arbitrary dimensions of the configuration space of a robot. The BEM has been also implemented for a two- and three-dimensional configuration space of a robot where some experiments have been carried out. The main conclusions following from these experiments can be summarised as follows:

- It is possible to find an APF by using the BEM which can be used for robot motion planning and control purposes.
- The usefulness of the potential field obtained for robot motion purposes strongly depends on the size of the boundary elements. However, the smaller the boundary elements the higher the computer storage effort and computational demands.
- It is difficult to apply the method for real-time robot motion planning, due to the time intensive calculations. When real-time applicability is desired, the method requires other than conventional computer platforms or other than conventional computational techniques.

- The performance of the BEM, giving a potential field without local minima either in the interior or on the boundary of the free configuration space, depends on the certain obstacle situation and the goal configurations. That means that we can not give an universal magnitude for the dimensions of the boundary elements which guarantees the absence of local minima of the potential field in the interior and the boundary of the free configuration space of the robot. This problem can be solved by choosing as small as possible boundary elements resulting on the other hand in high memory storage and computation time effort.
- Computer storage space drastically (quadratic) increases when small boundary elements have been chosen to obtain high accuracy of the potential field.

7.1 Contributions

As we have indicated in chapter 2 employing potential fields in robot motion planning has certain bottlenecks, regarding for instance the presence of local minima and the limited degrees of freedom (mostly two) of the robot. The main contributions of the present work are related to these problems, concerning:

- The employment of the Boundary Element Method to solve the problem of finding a potential field used for robot motion planning. The BEM computes a potential field which does not exhibit any local minima in the free configuration space of the robot and in addition it is analytically described. However it is possible depending on the size of the boundary elements that local minima exist at the boundary of the free configuration space which make the APF useless for robot motion purposes.
- The theoretical background concerning the application of potential fields by redundant robots, by introducing the set of goal configurations.
- The extension of the BEM for higher than three-dimensional configuration space of a robot.
- Some practical problems regarding the admissibility of the gradient of the found potential field, and the real-time applicability of the methodology.

Many methodologies have been proposed for robot motion planning. In the case of potential fields the robot motion planning has been described through a mathematical formulation (a spatial control system) in contrast to geometrical formulations commonly used. The potential field contains information about both the *path* and the *trajectory* the robot has to follow. APF's solve at once

different sub-problems in robot motion planning even for redundant robots, i.e. path planning, obstacle avoidance, trajectory generation, robot control. The APF obtained has been analytically given that leads to smooth trajectory generation which is easy and fast to be calculated.

7.2 Future Work

The boundary element method has been implemented but not used in a real robotic cell. We suggest in the first place to apply the method for real robots. We believe that some experiments with a real robot can lead to useful intellectual feedback concerning APF's obtained by the BEM. In our opinion there are three major problems to be solved before the method can be applied.
The first problem concerns the limited computer storage when a conventional computer platform is used. For higher-dimensional (more than three) configuration space of the robot a huge memory capacity is required especially to store the G matrix of the BEM. When the dimensions of the G matrix increase the calculation time also increases, which means that the computation capacity of the computer has to be more appropriate. Anyway we believe that these requirements can already be fulfilled (at certain costs) and perhaps they will be fulfilled in the future for lower costs. Certainly, it should be investigated what the performance of the BEM is when more than one nodes are chosen on a boundary element. A realistic expectation is that on the one hand the size of the boundary elements could be taken larger, but on the other hand the integrals of the elements of the matrix G will more complicated to be calculated.
The second problem is more fundamental and concerns the usefulness of a potential field found by the BEM in robot motion planning. Assuming that we are able to use an arbitrarily small size of the boundary elements, it would then be possible to investigate wether is possible to always find a potential field regardless the obstacles situation for robot motion purposes. Actually what we mean is that the term "close" introduced in chapter 6 is a relative term to the size of the boundary elements and it should be investigated whether there is a minimal dimension of the boundary elements leading to a good potential field.
Even when a potential can be calculated, sometimes it will be too flat to be used in robot motion. Some ideas concerning this problem have been given in this thesis in chapter 6. However, the suggested solution is rather intuitive and merely guarantees that the upper values of the input torques of the robotic system remain within certain limits. Further research could be done concerning the minimum values of the input torques of the robot. The BEM could be considered including for instance other than the Dirichlet conditions on the potential field, which allow no more than a single solution for the potential

field. The Neumann conditions for example described by (5.13) applied on the direction derivative of the potential field along the boundary of the free configuration space can allow more solutions for the potential field as it will briefly be analysed. Obviously for robot motion purposes the Neumann condition do not necessarily have to be formulated as strictly as in (5.13). In fact we want that the gradient along the boundary of the free configuration space point away from the obstacles and point to the goal configurations. That leads to new formulation of the Neumann conditions given by:

$$\frac{\partial \phi(\boldsymbol{x})}{\partial n} = \bar{\nu} > \boldsymbol{c} \tag{7.1}$$

for a given vector $\boldsymbol{c}$. Using these kind of conditions we can derive a similar formulation of the BEM including the direction derivatives of the potential field in the elements of the G matrix (see also (Brebbia et. al. 1984)). The last step of the BEM has been formulated in terms of a system:

$$G\boldsymbol{\sigma} = \bar{\nu} \tag{7.2}$$

where the vector $\boldsymbol{\sigma}$ has to be calculated. The system (7.2) under the conditions of (7.1) transform the problem of a finding a matrix G to an optimization problem. Various techniques exist solving such kind of problems. In that way we are able to formulate some additional requirements on the gradient of the potential field leading to different properties of the potential field.
The last issue that could be investigated is the usage of an APF in a unknown or variable environment of the robot. The behaviour of the robot due to a variable potential field would be a nice experimental feedback concerning the "choices" of an autonomous system which merely obeys a spatial law governed by an **Artificial Potential Field**.

Bibliography

[1] P. Adolphs and R. Hoelper, "Collision-free robot path planning based on local environment information", *International Journal of Robotics and Automation*, vol. 8, pp. 139–150, 1993.

[2] T. M. Apostol, *Calculus*, vol. 2, Xeros College Publishing, 1967.

[3] V. I. Arnold, *Mathematical Methods of Classical Mechanics*, Springer-Verlag, 1978.

[4] P. Bourdon J. Axler and W. Ramey, *Harmonic Function Theory*, Berlin: Springer, 1992.

[5] J. Barraquand and J. C. Latombe, "A monte-carlo algorithm for path planning with many degrees of freedom", in *Proceedings 1990 IEEE International Conference on Robotics and Automation*, 1990, pp. 1712–1717.

[6] B. Barshan and R. Kuc, "A bat-like sonar system for obstacles localization", *Transactions IEEE on Systems, Man, and Cybernetics*, vol. 22, no. 4, pp. 636–646, 1992.

[7] B. I. Becker, *The Boundary Element Method in Engineering*, McGraw-Hill Book Company, 1992.

[8] M. S. Branicky and W. S. Newman, "Rapid computation of configuration space obstacles", in *Proceedings 1990 IEEE International Conference on Robotics and Automation*, 1990, vol. 1, pp. 304–310.

[9] J. C.F. Telles C. A. Brebbia and L. C. Wrobel, *Boundary Element Techniques*, Springer-Verlag, 1984.

[10] C. A. Brebbia and S. Walker, *Boundary Element Techniques in Engineering*, McGraw-Hill Book Company, 1992.

[11] C. A. Brebbia and J. Dominguez, "Boundary element methods for potential problems", *Appl. Math. Modelling*, vol. 1, pp. 372–378, 1977.

[12] R. A. Brooks and T. Lozano-Perez, "A subdivision algorithm in configuration space for find path with rotation", in *Proceedings 8th International Joint Conference on Artificial Intelligence*, 1983, pp. 799–806.

[13] C. Cai and P. P. L. Regtien, "Accurate digital time-of-flight measurement using self-interference", *Transactions IEEE on Instrumentation and Measurement*, vol. 42, no. 6, pp. 990–994, 1993.

[14] J. F. Canny, *The Complexity of Robot Motion Planning*, The MIT Press, Cambridge, Mass, 1988.

[15] J. F. Canny, "A new algebraic method for robot motion planning and real geometry.", in *Proceedings IEEE of the 28th Annual Symposium on Foundations of Computer Science*, 1987, pp. 39–48.

[16] C. I. Connolly, *Harmonic Functions as a Basis for Motion Control and Planning*, PhD thesis, University of Massachusetts, 1994.

[17] C. I. Connolly and R. A. Grupen, "Harmonic control", in *Proceedings 1992 IEEE International Symposium on Intelligent Control*, 1992, pp. 503–506.

[18] C. I. Connolly, J. B. Burns, and R. Weiss, "Path planning using laplace's equation", in *Proceedings 1990 IEEE International Conference on Robotics and Automation*. 1990, vol. 3, pp. 2102–2106, IEEE Comput. Soc. Press.

[19] C. I. Connolly, J. B. Burns, and R. Weiss, "Harmonic functions for robot path construction", in *Proceedings of the SPIE. Intelligent Control and Adaptive Systems*, 1989, pp. 89–98.

[20] M. T. De Pedro and R. G. Rosa, "Robot path planning in the configuration space with automatic obstacle transformation", *Cybernetics and Systems*, vol. 23, pp. 367–378, 1992.

[21] J. Denavit and R. S. Hartenberg, "A kinematic notation for lower-pair mechanisms based on matrices", *Journal of Applied Mechanics*, vol. 22, pp. 215–221, 1955.

[22] B. Faverjon, "Object level programming of industrial robots", in *Proceedings 1986 IEEE International Conference on Robotics and Automation*, 1986, pp. 1406–1412.

[23] J. Graig, *Introduction to Robotics: Mechanics and Control*, Addison-Wesley: Reading, Mass, 1986.

[24] M. H. Overmars D. Halperin and M. Sharir, "Efficient motion planning for l-shaped object", *SIAM Journal on Computing*, vol. 21, pp. 1–23, 1992.

[25] Y. K. Hwang and N. Ahuja, "Gross motion planning - a survey", *ACM Computing Surveys*, vol. 24, pp. 219–291, 1992.

[26] S. Kambhampati and L. S. Davis, "Multiresolution path planning for mobile robots", *Transactions IEEE on Robotics and Automation*, vol. 2, pp. 135–145, 1986.

[27] Y. Ke and J. O'Rourke, "Moving a ladder in three dimensions: upper and lower bounds", in *Proceedings 3rd Ann. ACM Symp. on Computational Geometry*, 1987, pp. 136–145.

[28] J. M. Keil and J. R. Sack, "Minimum decomposition of polygonal objects", *Computational geometry*, pp. 197–216, 1985.

[29] O. Khatib, "A unified approach for motion and force control of robot manipulators: The operational space formulation", *IEEE Journal of Robotics and Automation*, vol. 3, pp. 43–53, 1987.

[30] O. Khatib, "Real-time obstacle avoidance for manipulators and mobile robots", *The International Journal of Robotics Research*, vol. 5, pp. 90–98, 1986.

[31] O. Khatib, "Real-time obstacle avoidance for manipulators and mobile robots", in *International Conference on Robotics and Automation*, 1985, pp. 500–505.

[32] O. Khatib and J. F. Le Maitre, "Dynamic control of manipulators operating in a complex environment", in *Proceedings 3rd International CISM-IFToMM Symposium*, 1978, pp. 267–282.

[33] P. Khosla and R. Volpe, "Superquadric artificial potentials for obstacle avoidance and approach", in *Proceedings 1988 IEEE International Conference on Robotics and Automation*, 1988, pp. 1778–1784.

[34] J. O. Kim and P. K. Khosla, "Real-time obstacle avoidance using harmonic potential functions", *IEEE Transactions on Robotics and Automation*, vol. 8, pp. 338–349, 1992.

[35] J. O. Kim and P. Khosla, "Real-time obstacle avoidance using harmonic potential functions", in *Proceedings 1991 IEEE International Conference on Robotics and Automation*, 1991, pp. 790–796.

[36] D. E. Koditschek, "The control of natural motion in mechanical systems", *Journal of Dynamic Systems, Measurement, and Control*, vol. 113, pp. 547–551, 1991.

[37] D. E. Koditschek, "Some applications of natural motion", *Journal of Dynamic Systems, Measurement, and Control*, vol. 113, pp. 552–557, 1991.

[38] D. E. Koditschek, "Robot planning and control via potential functions", in *Robotics Review*. 1989, vol. 1, MIT Press, Cambridge, Mass.

[39] D. E. Koditschek, "Exact robot navigation by means of potential functions: Some topological considerations", in *Proceedings 1990 IEEE International Conference on Robotics and Automation*. 1989, pp. 1–6, IEEE Comput. Soc. Press.

[40] D. E. Koditschek, "Automatic planning and control of robot natural motion via feedback", *Adaptive and Learning Systems*, pp. 389–402, 1986.

[41] D. E. Koditschek, "Adaptive strategies for the control of natural motion", in *Proceedings 1985 IEEE International Conference on Decision and Control*. 1985, pp. 1405–1409, IEEE Comput. Soc. Press.

[42] D. E. Koditschek, "Natural motion of robot arms", in *Proceedings of 23rd Conference on Decision and Control*. 1984, pp. 733–735, IEEE Comput. Soc. Press.

[43] R. Kuc, "A spatial sampling criterion for sonar obstacles detection", *Transactions IEEE on Pattern Analysis and Machine Intelligence*, vol. 12, no. 7, pp. 686–690, 1990.

[44] J. C. Latombe, *Robot Motion Planning*, Kluwer Academic Publishers, 1991.

[45] D. Leven and M. Sharir, "An efficient and simple motion planning algorithm for a ladder amidst polygonal barriers", *Journal of Algorithms*, vol. 8, pp. 192–215, 1987.

[46] W. Li, B. Zhang, and H. Jaschek, "Real-time collision-free path planning for robots in configuration space", *Journal of Computer Science and Technology (English language edition)*, vol. 9, no. 1, pp. 37–52, 1994.

[47] W. Li, "Fast mapping obstacles in the configuration space", *Robotersysteme*, vol. 7, no. 3, pp. 148–154, 1991.

[48] P. J. McKerrow, *Introduction to Robotics*, Addison-Wesley Publishers Ltd., 1991.

[49] A. Macovski, "Ultrasonic imaging using arrays", *Proceedings IEEE*, vol. 67, pp. 484–495, 1979.

[50] J. A. Marszalec and H. M. Keranen, "A photo electric range scanner using an array of led chips", in *Proceedings IEEE Conference on Robotics and Automation*, 1992, pp. 593–598.

[51] S. A. Masoud A. A. Masoud and M. M. Bayoumi, "Robot navigation using a pressure generated mechanical stress field: 'the biharmonic potential approach"', in *Proceedings IEEE Conference on Robotics and Automation*, 1994, vol. 1, pp. 124–129.

[52] W. Meyer and P. Benedict, "Path planning and geometry of joint space obstacles", in *Proceedings IEEE Conference on Robotics and Automation*, 1988, pp. 215–219.

[53] J. Milner, *Morse Theory*, Princeton University Press, 1963.

[54] B. H. Lee Y. S. Nam and N. Y. Ko, "An analytic approach to moving obstacle avoidance using an artificial potential field", in *Proceedings 1995 IEEE International Conference on Intelligent Robots and Systems. Human Robot Interaction and Cooperative Robots*, 1995, vol. 2, pp. 482–487.

[55] W. S. Newman and M. S. Branicky, "Real-time configuration space transforms for obstacle avoidance", *International Journal of Robotics Research*, vol. 10, pp. 650–667, 1991.

[56] R. P. Paul, *Robot Manipulators: Mathematics, Programming and Control*, Cambridge, MA: MIT Press, 1982.

[57] W. H. Press, S. A. Teukolsky, W. T. Vetterling, and B. P. Flannery, *Numerical Recipes in FORTRAN. The Art of Scientific Computing*, Cambridge University Press, 1992.

[58] E. Ralli and G. Hirzinger, "Fast path planning for robot manipulators using numerical potential fields in the configuration space", in *Proceedings 1995 IEEE International Conference on Intelligent Robots and Systems. Advanced Robotic Systems and the Real World*, 1994, vol. 3, pp. 1922–1929.

[59] S. Ratering and M. Gini, "Robot navigation in a known environment with unknown moving obstacles", *Autonomous Robots*, vol. 1, pp. 149–165, 1995.

[60] S. Ratering, *Goal directed robot navigation in a known indoor environment with unknown stationary and moving obstacles*, PhD thesis, University of Mennesota, 1992.

[61] E. Rimon and D. E. Koditschek, "Exact robot navigation using artificial potential functions", *IEEE Transactions on Robotics and Automation*, vol. 8, pp. 501–518, 1992.

[62] E. Rimon and D. E. Koditschek, "Exact robot navigation in geometrically complicated but topologically simple spaces", in *Proceedings 1990 IEEE International Conference on Robotics and Automation*, 1990, pp. 1937–1942.

[63] E. Rimon and D. E. Koditschek, "The construction of analytic diffeomorphisms for exact robot navigation on star worlds", in *Proceedings 1989 IEEE International Conference on Robotics and Automation*, 1989, pp. 21–26.

[64] K. Sato, "Deadlock-free motion planning using the laplace potential field", *Advanced Robotics*, vol. 7, pp. 449–461, 1993.

[65] R. J. Schilling, *Fundamentals of Robotics: analysis and control*, Prentice-Hall International Editions, 1990.

[66] J. T. Schwartz and M. Sharir, "On the piano mover's problem: I. the case of a two dimensional rigid polygonal body moving amidst polygonal boundaries", *Communications on Pure and Applied Mathematics*, vol. 36, pp. 345–398, 1983.

[67] J. T. Schwartz and M. Sharir, "On the piano mover's problem: Ii. general techniques for computing topological properties of real algebraic manifolds", *Advanced and Applied Mathematics*, vol. 4, pp. 298–351, 1983.

[68] J. T. Schwartz and M. Sharir, "On the piano mover's problem: Iii. coordinating the motion of several independent bodies: the spacial case of circular bodies amidst polygonal barriers", *International Journal of Robotics Research*, vol. 2, pp. 46–75, 1983.

[69] J. T. Schwartz and M. Sharir, "On the piano mover's problem: V. the case of a rod moving in three-dimensional space amidst polyhedral obstacles", *Communications on Pure and Applied Mathematics*, vol. 37, pp. 815–848, 1984.

[70] M. Sharir and E. Ariel-Sheffi, "On the piano mover's problem: Iv. various decomposable two-dimensional motion planning problems", *Communications on Pure and Applied Mathematics*, vol. 37, pp. 479–493, 1984.

[71] Y. Shirai, "Application of laser range finder to robot vision", in *NATO ASI Series: Sensor Devices and Systems for Robotics*, 1989, vol. 52.

[72] S. Sifrony and M. Sharir, "A new efficient motion planning algorithm for a rod in two-dimensional polygonal space", *Algorithmica*, vol. 2, pp. 367–402, 1987.

[73] M. Soumekh, *Synthetic Aperture Echo Imaging*, Plenum Press, 1992.

[74] M. Spivak, *Differential Geometry*, Publish or Perish, Inc., 1979.

[75] O. Takahashi and R. J. Schilling, "Motion planning in a plane using generalized voronoi diagrams", *Transactions IEEE on Robotics and Automation*, vol. 5, no. 2, pp. 143–150, 1989.

[76] M. Takegaki and S. Arimoto, "A new feedback method for dynamic control of manipulators", *Journal Dynanic Systems*, vol. 102, pp. 119–125, 1981.

[77] L. Tarassenko and A. Blake, "Analogue computation of collision-free paths", in *Proceedings 1991 IEEE International Conference on Robotics and Automation.* 1991, pp. 540–545, IEEE Comput. Soc. Press.

[78] R. Volpe and P. Khosla, "Manipulator control with superquadric artificial potential functions:theory and experiments", *IEEE Transactions on Systems, Man and Cybernetics*, vol. 20, pp. 1423–1436, 1990.

[79] R. Volpe and P. Khosla, "Artificial potentials with elliptic isopotential contours for obstacle avoidance", in *Proceedings of the 26th IEEE Conference on Decision and Control*, 1987, pp. 187–185.

[80] J. R. Westlake, *A Handbook of Numerical Matrix Inversion and Solution of Linear Equations*, John Wiley & Sons, 1968.

[81] D. Zhu and J. C. Latombe, "New heuristic algorithms foe efficient hierarchical path planning", *Transactions IEEE on Robotics and Automation*, vol. 7, pp. 9–20, 1991.

Appendix A

Line Integrations of Boundary Elements

The elements of the matrix G are given by:

$$G_{ij} = \frac{1}{2\pi} \int_{-\bar{\xi}}^{\bar{\xi}} \log\left(\frac{1}{|\boldsymbol{x}_i - \boldsymbol{x}_j - \boldsymbol{\xi}|}\right) d\xi \tag{A.1}$$

For the m coordinate of a node $\boldsymbol{x}_{il}$ the notation $x_{il,m}$ will be used.

- For the horizontal boundary elements, holds that $\boldsymbol{\xi} = (\xi, 0)$, then

$$\begin{aligned} G_{ij} = \; & \frac{1}{4\pi}((x_{i,1} - x_{j,1} + \bar{\xi}) \log((x_{i,2} - x_{j,2})^2 + (x_{i,1} - x_{j,1} + \bar{\xi})^2) - \\ & (x_{i,1} - x_{j,1} - \bar{\xi}) \log((x_{i,2} - x_{j,2})^2 + (x_{i,1} - x_{j,1} - \bar{\xi})^2) + \\ & 2(x_{i,2} - x_{j,2}) \arctan\left(\frac{x_{i,1} - x_{j,1} + \bar{\xi}}{x_{i,2} - x_{j,2}}\right) - \\ & 2(x_{i,2} - x_{j,2}) \arctan\left(\frac{x_{i,1} - x_{j,1} - \bar{\xi}}{x_{i,2} - x_{j,2}}\right) + \\ & 4\xi) \end{aligned} \tag{A.2}$$

- And for the vertical boundary elements, holds that $\boldsymbol{\xi} = (0, \xi)$, and G_{ij} is given by:

$$\begin{aligned} G_{ij} = \; & \frac{1}{4\pi}((x_{i,2} - x_{j,2} + \bar{\xi}) \log((x_{i,1} - x_{j,1})^2 + (x_{i,2} - x_{j,2} + \bar{\xi})^2) - \\ & (x_{i,2} - x_{j,2} - \bar{\xi}) \log((x_{i,1} - x_{j,1})^2 + (x_{i,2} - x_{j,2} - \bar{\xi})^2) + \end{aligned}$$

$$2(x_{i,1} - x_{j,1}) \arctan\left(\frac{x_{i,2} - x_{j,2} + \bar{\xi}}{x_{i,1} - x_{j,1}}\right) -$$
$$2(x_{i,1} - x_{j,1}) \arctan\left(\frac{x_{i,2} - x_{j,2} - \bar{\xi}}{x_{i,1} - x_{j,1}}\right) +$$
$$4\xi) \tag{A.3}$$

Appendix B

Surface Integrations of Boundary Elements

This appendix gives the analytic calculation of the integrals (the elements of the matrix G) in the case of a three-dimensional configuration space of a robot. The problem under consideration can generally be formulated as: calculate the following integral

$$G_{ij} = \int_{-\bar{\xi}_1}^{\bar{\xi}_1} \int_{-\bar{\xi}_2}^{\bar{\xi}_2} \frac{1}{|\boldsymbol{x}_i - \boldsymbol{x}_j - \boldsymbol{\xi}|} \, d\xi_2 \, d\xi_1 \tag{B.1}$$

Without loosing the generality of the solution we calculate the following inte-

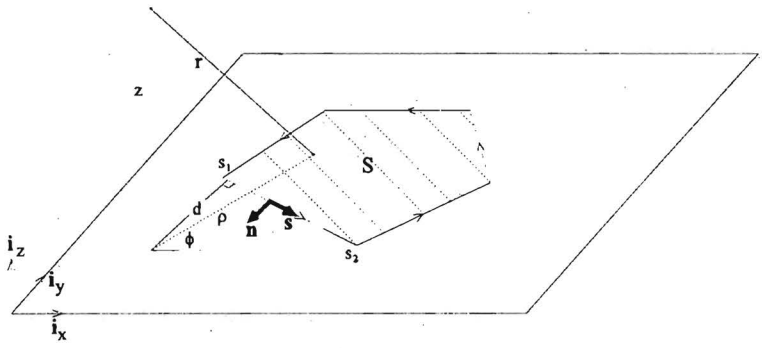

Figure B.1: Boundary element integral calculation in a three-dimensional space

gral where each variable is explained in figure B.1.

$$\int_S\int \frac{1}{r}\,dA = \int_S\int \frac{1}{\sqrt{x^2 + y^2 + z^2}}\,dA \tag{B.2}$$

This surface integral can be calculated by transforming it into a line integral by using the following equation (Stoke's identity):

$$\int_S\int (\boldsymbol{i}_z\,,\,\mathrm{curl}\,\boldsymbol{v})\,dA = \oint (\boldsymbol{v}\,,\,\boldsymbol{s})\,dS \tag{B.3}$$

When we want to apply the above equation in our case, we have to find a vector filed $\boldsymbol{v}$ such that:

$$(\boldsymbol{i}_z\,,\,\mathrm{curl}\,\boldsymbol{v}) = \frac{1}{\sqrt{x^2 + y^2 + z^2}} \tag{B.4}$$

In cylindrical coordinates, it yields:

$$\frac{1}{\rho}\left(\frac{\partial(\rho\, v_\phi)}{\partial\rho} - \frac{\partial v_\rho}{\partial_\phi}\right) = \frac{1}{\sqrt{x^2 + y^2 + z^2}} \tag{B.5}$$

Assuming that:

$$v_\phi \neq 0 \quad \text{and} \quad v_\rho = 0 \tag{B.6}$$

we calculate v_ϕ as follows:

$$\begin{aligned} \frac{\partial(\rho\, v_\phi)}{\partial\rho} &= \frac{\rho}{\sqrt{\rho^2 + z^2}} \Rightarrow \\ \rho\, v_\phi &= \sqrt{\rho^2 + z^2} \Rightarrow \\ v_\phi &= \frac{\sqrt{\rho^2 + z^2}}{\rho} \end{aligned} \tag{B.7}$$

with $\rho = \sqrt{x^2 + y^2}$.
Accordingly, we write $\boldsymbol{v}$ as

$$\boldsymbol{v} = \frac{\sqrt{\rho^2 + z^2}}{\rho}\,\boldsymbol{i}_\phi \tag{B.8}$$

or

$$\boldsymbol{v} = \frac{\sqrt{\rho^2 + z^2}}{\rho^2}\,(\boldsymbol{i}_z \times \boldsymbol{\rho}) \tag{B.9}$$

using the last equation, the initial integral (B.2), using (B.3) becomes:

$$\oint (\boldsymbol{s}\,,\,(\boldsymbol{i}_z \times \boldsymbol{\rho}))\,\frac{\sqrt{\rho^2 + z^2}}{\rho^2}\,dS \tag{B.10}$$

or

$$\oint (\boldsymbol{n}\,,\,\boldsymbol{\rho})\,\frac{\sqrt{\rho^2 + z^2}}{\rho^2}\,dS \tag{B.11}$$

That implies that the integral of (B.2) is the sommation of the line integrals of each line segment of the boundary of the polygon under consideration. We calculate the following line integral of a line segment

$$d\int_{s_1}^{s_2} \frac{\sqrt{s^2 + d^2 + z^2}}{s^2 + d^2}\,ds \tag{B.12}$$

using the following analytical expression:

$$d\ln\left(s + \sqrt{s^2 + d^2 + z^2}\right) + z\arctan\left(\frac{z}{d}\frac{s}{\sqrt{s^2 + d^2 + z^2}}\right)\Bigg|_{s_1}^{s_2} \tag{B.13}$$

where d represents the distance of the line segment to the origin.

List of symbols

Chapter 2

c	a constant scalar
F_{attr}	force induced from an attractive APF
$F_{(O,PSP)}$	force related to the obstacle O and the specific PSP
F_{PSP}	force related to a specific PSP
F_{rep}	force induced from a repulsive APF
k	a constant scalar
n	the dimension of the joint space of a robot
r	length of a vector
U_{art}	an artificial potential field
U_{attr}	an artificial potential field
U_{rep}	an artificial potential field
$\boldsymbol{x}$	an arbitrary vector
η	a constant scalar
λ_i	parameter variable of a panel
ρ	a parameter representing the shortest distance from a robot to an obstacle
ρ_0	a constant scalar
ϕ	an artificial potential field

Chapter 3

a_i	a parameter of the i-th link of the robot
$\boldsymbol{b}(\dot{\boldsymbol{q}})$	the vector representing the friction torques
b_k	the k-th element of the friction torque vector
b_k^d	the dynamic friction coefficient of the k-th joint
b_k^s	the static friction coefficient of the k-th joint
b_k^v	the viscous friction coefficient of the k-th joint
$C(\boldsymbol{q}, \dot{\boldsymbol{q}})$	the matrix representing the Coriolis and centrifugal torques

d_i	a parameter of the i-th link of the robot
$D(\boldsymbol{q})$	the $n \times n$ inertia matrix of the robot
F	skew-symmetric matrix
$\mathcal{G}$	the set of all goal configurations of the motion planning problem
$\boldsymbol{h}(\boldsymbol{q})$	the vector representing the gravitation torques
$\mathcal{J}$	joint or configuration space of a robot
K_2	a positive definite matrix
n	the dimension of the joint space
$\boldsymbol{p}$	the position vector of the TCP of the robot
$\boldsymbol{p}_d$	the goal position vector of the TCP
$\boldsymbol{q}$	the vector of the joint angles of a robot
$\boldsymbol{q}_d$	an element of $\mathcal{G}$
q_i	the i-th joint angle of a robot
$\bar{q}_i$	the maximum limit of the i-th joint angle of a robot
$\underline{q}_i$	the minimum limit of the i-th joint angle of a robot
$\mathcal{Q}$	operational joint or configuration space of a robot
$\boldsymbol{r}$	a constant input of a system S
R	a 3×3 rotation matrix function describing the orientation of the TCP of the robot
R_d	the goal orientation (rotation matrix) of the TCP
S	a nonlinear system
$SO(3)$	the set of all rotation matrices in $\mathcal{R}^3$ with positive orientation
$\mathcal{T}$	operational work space of a robot
$T\mathcal{Q}$	the tangent space of the $\mathcal{Q}$ space
$\boldsymbol{v}$	the vector of the joint angles velocities of a robot
V	a Lyapunov function
V_L	a Lyapunov function
$\boldsymbol{u}$	the input vector of a system S
U	an artificial potential field
$\boldsymbol{w}$	an element of the work space of the robot, describing the position and orientation of the TCP
$\mathcal{W}$	work space of a robot
${}^{i-1}T_i$	a homogeneous transformation matrix
$\boldsymbol{x}$	a vector representing the state of a system S
$\boldsymbol{z}$	an auxiliary joint vector
α_i	a parameter of the i-th link of the robot
$\boldsymbol{\tau}$	the vector of the input torque's of a robot
Ω_ρ	domain of attraction

Chapter 4

d_i	grid size of the i-th coordinate of the physical space of a robot
D_i	grid size of the i-th coordinate of the joint space of a robot
$\boldsymbol{e}_k$	the k-th unit vector of the physical space of a robot
$\boldsymbol{k}$	a grid point of the physical space of a robot
L	dimension of the grid of the physical space of a robot
$\boldsymbol{m}$	a grid point of the joint space of a robot
$\boldsymbol{s}_k$	the kth unit vector of the joint space of a robot
$\mathcal{O}$	set of configuration obstacles
$\boldsymbol{p}$	a point of the physical space of a robot
$\bar{p}_i$	the maximum limit of the i-th coordinate of the physical space of a robot
$\underline{p}_i$	the minimum limit of the i-th coordinate of the physical space of a robot
$\mathcal{P}$	physical space of a robot

Chapter 5

$\boldsymbol{a}$	a point on a level set of a potential field
c	a constant scalar
$\hat{c}$	a constant scalar
$f(\boldsymbol{x})$	an arbitrary scalar function
$\boldsymbol{f}(\boldsymbol{x})$	an arbitrary vector function
$\mathcal{F}$	free joint or configuration space of a robot
G	the dependency matrix of the BEM
G^{ij}	the dependency matrix of the BEM related with the ith and jth boundary elements
G^{ij}_{lk}	the lk element of the dependency matrix G^{ij}
$H(\boldsymbol{x})$	the Hessian matrix of a potential field
j	a scalar
i	a scalar
k	a scalar
l	a scalar
$\mathcal{L}$	the level set of a potential field
m	scalar, denoting the dimension of a domain
M	number of nodes on a boundary element
$\boldsymbol{n}$	outward unit normal vector on the boundary of an arbitrary domain

N	number of boundary elements
$\mathtt{U}$	an artificial potential field
$\mathtt{V}$	an artificial potential field
$\boldsymbol{x}$	an arbitrary vector in Ω
$\boldsymbol{x}_0$	an arbitrary vector in Ω
$\boldsymbol{x}_j$	a point on the jth boundary element of Ω
$\boldsymbol{x}_i$	a point on the ith boundary element of Ω
$\boldsymbol{x}_i^k$	the kth node of the ith boundary element of Ω
Γ	the boundary of an arbitrary domain
Γ_1	a part of the boundary of an arbitrary domain
Γ_2	a part of the boundary of an arbitrary domain
Γ_d	goal boundary
Γ_o	obstacle boundary
Γ_j	the jth boundary element
$\bar{\nu}$	boundary conditions of the directional derivative of a potential field
$\delta(\boldsymbol{x})$	the dirac delta function
$\boldsymbol{\nu}$	outward unit normal vector on the boundary of an arbitrary domain
$\boldsymbol{\xi}^j$	local coordinates of the jth boundary element
$\rho_k^j(\boldsymbol{\xi}^j)$	interpolation function corresponded to the k-th node of the jth boundary element
$\sigma(\boldsymbol{x})$	the unknown density distribution of the potential ψ over the boundary Γ
σ^j	the unknown density of the potential ψ over the boundary element Γ_j
σ_k^j	the unknown density of the potential ψ at the kth node of the jth boundary element
$\boldsymbol{\sigma}$	an $N \cdot M$ vector, containing the variables σ's at each node of each boundary element
$\phi(\boldsymbol{x})$	a potential field in Ω
$\phi'(\boldsymbol{x})$	a potential field in Ω'
$\bar{\phi}$	boundary conditions of the potential field ϕ
$\bar{\phi}_i$	boundary conditions of the potential field ϕ at the point $\boldsymbol{x}_i$
$\bar{\phi}_i^k$	the value of the potential field ϕ at the point $\boldsymbol{x}_i^k$
$\bar{\boldsymbol{\phi}}$	an $N \cdot M$ vector, containing the boundary conditions at each node of each boundary element
$\psi(\boldsymbol{x})$	the fundamental solution in Ω
ψ_i	the value of ψ at the point $\boldsymbol{x}_i$
ψ_{ij}	the value of ψ at the points $\boldsymbol{x}_i$ and $\boldsymbol{x}_j$
Ω	an arbitrary domain, subset of $\mathcal{R}^m$
Ω'	the external domain of the domain Ω

Chapter 6

b_i	upper bound of the gradient of an APF
B_i	upper bound of the gradient of an APF
D_i	an arbitrary matrix
$f(\mathtt{U})$	an arbitrary function of $\mathtt{U}$
G	an arbitrary matrix
G'	an arbitrary matrix
G_i	an arbitrary matrix
k_a	a constant scalar
k_d	a constant scalar
L	an arbitrary matrix
L'	an arbitrary matrix
L_i	an arbitrary matrix
U	an arbitrary matrix
U'	an arbitrary matrix
U_i	an arbitrary matrix
ν_i	parameters of the experimental setup

Samenvatting

In dit proefschrift wordt het onderwerp robot motion planning voor autonome robots behandeld. Kunstmatige potentiaalvelden zijn gebruikt voor het oplossen van het probleem van robot motion planning. Robot motion planning kan beschreven worden als volgt. Genereer een botsingvrije baan naar een gegeven eindpositie beginnend op een willekeurig initiële positie van de robot. Robot motion planning is geformuleerd en opgelost in de configuratieruimte van de robot. Een potentiaalveld is in de configuratieruimte geconstrueerd en representeert een mechanisme voor regeling en planning.
De directe en indirecte kinematika van een robot is in het kort beschreven zodat de transformatie van de obstakels van de werkruimte naar de configuratieruimte van de robot duidelijk kan worden. Die transformatie resulteert in de vrije configuratieruimte. Dat is dat deel van de configuratieruimte waar geen botsing optreedt tussen robot en obstakels.
Berustend op een algemeen dynamisch model van een robot is er een regelstrategie geïntroduceerd die gebruik maakt van potentiaalvelden. Eigenlijk wordt de gradiënt van de potentiaalveld gebruikt bij de ingangskoppel van het robotsysteem waardoor de robot de eindconfiguratie asymptotisch nadert zonder dat er botsingen optreden. Het construeren van de kunstmatige potentiaalvelden is onderzocht onder de eisen omtrent de potentiaalveld die uit de regelstrategie voortkomen. Harmonische functies zijn gebruikt om potentiaalvelden te construeren die hun maximale waarde op de rand van de obstakelconfiguraties bereiken en hun minimale waarde op de rand van de doelconfiguraties bereiken. Het probleem om een harmonische functie te vinden die aan de gestelde voorwaarden voldoet, is geanalyseerd en opgelost. Daarvoor is de Rand-Elementen Methode gebruikt die in een analytische uitdrukking van de potentiaalveld resulteert. Bovendien is die methode uitgebreid voor hogere dimensies van de configuratieruimte van een robot dan drie.
Het robot motion probleem kan opgelost in vier stappen, nl. (1) transformeer de obstakels vanuit de werkruimte naar de configuratieruimte, (2) bereken de doelconfiguraties, (3) bereken een potentiaalveld met de Rand-Elementen Methode,

(4) gebruik de gradiënt van de potentiaalveld in de regelstrategie. Twee praktische problemen die bij real-time toepassingen optreden, worden behandeld en opgelost. Het eerste probleem betreft de boven grenzen van de ingangskoppels van de aktuatoren van een robot. Vervolgens is er een iteratieve algoritme gegeven om rekentijd te winnen voor het uitrekenen van de rand-elementen methode als obstakels worden toegevoegd of verwijderd.
Aan de hand van een aantal experimenten in twee- en driedimensionale configuratieruimten, kunnen we concluderen dat de rand-elementen methode gebruikt kan worden voor robot motion planning. De methode geeft in het algemeen bevredigend resultaten maar gaat gepaard met hoge eisen wat computer geheugencapaciteit en computer rekensnelheid.

STATEMENTS

relating to the dissertation

Autonomous Robots using Artificial Potential Fields

by

Paraskevas Dunias

Eindhoven, 2 December 1996

I

When the boundary element method is used, to find a potential field for robot motion purposes, a size of the boundary elements can always be found which leads to a potential field without local minima, either in the interior of the free configuration space of the robot, or at the boundary of the free configuration space of a robot.

II

Employing harmonic potential fields in robot motion planning has been denoted in the literature by the term *natural* motion planning. We claim that the term may indeed characterise the motion accomplished by this method through which the robot automatically moves carefully in dangerous regions and more freely when no obstacles are present, following the "least energy" surfaces represented by harmonic functions.

- D.E. Koditschek (1991), *Some Applications of Natural Motion*, Journal of Dynamic Systems, Measurement, and Control,vol. 113, pp. 552-557.
- C.I. Connolly (1994), *Harmonic Functions as a Basis for Motion Control and Planning*, University of Massachusetts, chapter 4.

III

Analog, time continuous physical phenomena can be modeled by *digital, time discrete* computers. That modelling process can be reliably achieved up to a certain limit depending on the phenomena under consideration. Potential fields for robot motion planning use the analog machinery of the manipulator itself accomplishing the required motion.

IV

Computation speed and storage capabilities are time- and cost-related issues. Because the main drawbacks using the method introduced in this thesis are related to speed and storage capabilities, it seems a valid expectation that the method can be used in the future for real-time robot motion planning.

V

The present system of higher education is organized on institutionally specialized disciplines resulting in clearly defined mono-disciplinary student independent curricula. It would be more logical to construct the curriculum of the students on individual base according to his/her interests, professional preferences and capacities, market research etc.

VI

The fact that a system is made artificially *intelligent*, does not also imply *autonomous* behaviour. However, an *autonomous* system can be a useful tool in discovering *artificial intelligence*.

VII

Life looks like a theatre play. Some people think that they are still busy with the rehearsals. Some think that they are the scenario-writers, and some think that they do not need any scenario-writers.

VIII

Engineers are assumed to use *deductive reasoning* in solving problems, in contrast to *creative thinking* used by artists for depicting problems. However, sometimes it is indirectly required that an engineer possesses creativity which in turn creates problems.

IX

Unpredictability is usually the annoying element in human behaviour but is nevertheless the inevitable result of the crucial element in our life, *the right to choose*.

X

Responsible fatherhood is the best training in practical intelligence, social skills and emotional talents.